TECHNICAL REPORT STANDARD TITLE PAGE

1. REPORT NO.	2. GOVERNMENT ACCESSION NO.	3. RECIPIENT'S CATALOG NO.
WA-RD 384.1		

4. TITLE AND SUBTITLE	5. REPORT DATE
VEHICLE/PAVEMENT INTERACTION AT THE PACCAR TEST SITE	November 1995
	6. PERFORMING ORGANIZATION CODE
7. AUTHOR(S)	8. PERFORMING ORGANIZATION REPORT NO.
Joe P. Mahoney, Brian C. Winters, Karim Chatti, Thomas J. Moran, Carl L. Monismith, Steven L. Kramer	
9. PERFORMING ORGANIZATION NAME AND ADDRESS	10. WORK UNIT NO.
Washington State Transportation Center (TRAC) University of Washington, Box 354802 University District Building; 1107 NE 45th Street, Suite 535 Seattle, Washington 98105-4631	11. CONTRACT OR GRANT NO. GC8719, Task 42
12. SPONSORING AGENCY NAME AND ADDRESS	13. TYPE OF REPORT AND PERIOD COVERED
Washington State Department of Transportation Transportation Building, MS 7370 Olympia, Washington 98504-7370	Final report
	14. SPONSORING AGENCY CODE

15. SUPPLEMENTARY NOTES

This study was conducted in cooperation with the U.S. Department of Transportation, Federal Highway Administration.

16. ABSTRACT

The condition of the U.S. highway system has been and continues to be a major concern of both the highway and trucking communities. This is understandable given the fact that in 1990, combination vehicles with five or more axles accounted for 91 percent of the 18,000 pound equivalent axle loads (ESALs) on rural Interstate highways. This heavy vehicle traffic and the pavement system it travels on combine to generate a perpetual cycle of pavement deterioration and rehabilitation. Increasing truck traffic leads to predictable pavement damage that in turn contributes to potentially increasing dynamic loading of the pavement. This cycle continues until some form of pavement rehabilitation is undertaken. The trucking community alters the design and operation of their vehicles largely due to economic considerations (profit) but also in response to the ride quality (or lack thereof) of the infrastructure to which they are bound. On the other hand, the pavement community is constantly updating design and construction practice to improve pavement performance. Unfortunately, both parties develop a form of "technical tunnel vision" and work to resolve some of the same concerns without the benefit of a possible mutual effort. As such it was recognized that there was a need to improve our mutual understanding of truck pavement interaction. Often, but not always, a beneficial change in one community (such as smoother pavements) benefits the other (less truck/cargo damage).

This report is part of a multiphased research project entitled "Truck/Pavement Interaction" conducted jointly by the University of Washington, University of California-Berkeley, Washington State Department of Transportation (WSDOT), California Department of Transportation (Caltrans), and PACCAR, Inc. This is an attempt to promulgate a mutually beneficial dialog between the pavement and trucking communities. The objective of the research is to investigate how different truck suspensions, tire/axle combinations, tire loads, and tire pressures affect pavement response and conversely how pavement condition affects truck performance and damage. These objectives will be accomplished by operating instrumented trucks over an instrumented pavement section.

17. KEY WORDS	18. DISTRIBUTION STATEMENT
Truck/pavement interaction, pavement strains, falling weight deflectometer, truck speed, tire pressure, spatial repeatability, backcalculation, moduli	No restrictions. This document is available to the public through the National Technical Information Service, Springfield, VA 22616

19. SECURITY CLASSIF. (of this report)	20. SECURITY CLASSIF. (of this page)	21. NO. OF PAGES	22. PRICE
None	None	160	

Final Report
Research Project GC87195, Task 42
Truck/Pavement Interaction

VEHICLE/PAVEMENT INTERACTION AT THE PACCAR TEST SITE

by

Joe P. Mahoney
Professor of Civil Engineering
University of Washington

Brian C. Winters
Captain
U.S. Army

Karim Chatti
Assistant Professor
Michigan State University

Thomas J. Moran
Project Engineer
PACCAR Technical Center

Carl L. Monismith
Professor of Civil Engineering
University of California, Berkeley

Steven L. Kramer
Associate Professor of Civil Engineering
University of Washington

Washington State Transportation Center (TRAC)
University of Washington, Box 354802
University District Building, 1107 NE 45th Street, Suite 535
Seattle, Washington 98105-4631

Washington State Department of Transportation
Technical Monitor
Robyn Moore, Pavement and Soils Engineer

Prepared for

Washington State Transportation Commission
Department of Transportation
and in cooperation with
U.S. Department of Transportation
Federal Highway Administration

November 1995

DISCLAIMER

The contents of this report reflect the views of the authors, who are responsible for the facts and the accuracy of the data presented herein. The contents do not necessarily reflect the official views or policies of the Washington State Transportation Commission, Department of Transportation, or the Federal Highway Administration. This report does not constitute a standard, specification, or regulation.

TABLE OF CONTENTS

Section			Page
1. INTRODUCTION			**1**
1. THE PROBLEM			1
2. BACKGROUND AND OBJECTIVES			1
3. REPORT SCOPE			2
2. LITERATURE REVIEW			**3**
1. INTRODUCTION			3
2. FLEXIBLE PAVEMENT TEST FACILITIES			3
2.1 Types of Test Facilities			3
2.2 Comparisons of Measured and Calculated Strains from Various Flexible Pavement Experiments			4
2.2 Comparisons of Measured and Calculated Strains from Various Flexible Pavement Experiments			4
3. ANALYSIS APPROACHES FOR PAVEMENT AND TRUCK MODELING			8
3.1 Pavement Models			8
	3.1.1 Static Methods		8
	3.1.2 Quasi-Static Methods		10
	3.1.3 Dynamic Models		10
3.2 Truck Models			12
3. EVALUATION AND INSTRUMENTATION OF THE PACCAR TEST PAVEMENT			**13**
1. INTRODUCTION			13
2. DESCRIPTION OF THE PACCAR TEST SECTION			13
3. BACKCALCULATION OF TEST SECTION LAYER MODULI			18
3.1 PACCAR Test Section			18
3.2 SR 525 Pavement Section			25
3.3 Backcalculation Observations			28
4. INSTRUMENTATION			28
4.1 Introduction			28
4.2 Acquisition			28
4.3 Layout			29
4.4 Installation			35
	4.4.1 Axial Strain Cores		35
	4.4.2 Shear Strain Cores		37
	4.4.3 Shear Slot		37
	4.4.4 Surface Gauges		37
	4.4.5 Temperature Compensation Gauges		37
	4.4.6 Other Instruments		39
	4.4.7 Wiring Slots and Electrical Panel		39
	4.4.8 Epoxy		41
	4.4.9 Data Acquisition and Signal Conditioning		43

TABLE OF CONTENTS (Continued)

Section		Page
5.	INSTRUMENTATION VERIFICATION	45
5.1	Introduction	45
5.2	General Procedure for Reduction and Conversion of Measured Strain Responses	45
5.3	FWD—Testing October 10, 1991	47
5.3.1	Effective Layer Thicknesses	48
5.3.2	Calculated Strains	49
5.3.3	Comparison of Measured and Calculated Strains	50
5.4	FWD Testing—February 3, 1993	52
5.4.1	Backcalculation of Layer Moduli	52
5.4.2	Effective Layer Thicknesses	58
5.4.3	Calculated Strains	60
5.4.4	Comparison of Measured and Calculated Strains	61
5.5	Comparison of October 1991 and February 1993 FWD Testing	69
4.	**PACCAR TRUCK TESTS**	**72**
1.	INTRODUCTION	72
2.	INSTRUMENTED TEST SECTION	72
3.	TEST TRUCKS	72
3.1	Primary Test Truck	73
3.2	Spatial Repeatability Test Vehicles	73
4.	SEPTEMBER 28-29, 1993, TRUCK TEST RESULTS	77
4.1	Test Procedure	77
4.2	Test Results	77
4.2.1	Load Measurements	78
4.2.2	Strain Measurements	78
4.3	Spatial Repeatability Tests	92
4.3.1	Test Procedure	92
4.3.2	Test Results	93
5.	**SUMMARY AND CONCLUSIONS**	**100**
1.	SUMMARY	100
2.	IMPLICATIONS FOR WSDOT	102
2.1	Fundamental Pavement Response	102
2.2	Truck/Pavement Interaction	102
2.2.1	Truck Speed	102
2.2.2	Tire Pressures	103
2.2.3	Pavement Temperature	103
2.2.4	Spatial Repeatability	103
2.2.5	Axle Loads	103
2.2.6	Vehicle Suspensions	104
REFERENCES		**105**

TABLE OF CONTENTS (Continued)

Section	Page
APPENDIX A. SUMMARY OF MEASURED AND CALCULATED STRAINS FROM VARIOUS FLEXIBLE PAVEMENT EXPERIMENTS.....	**A-1**
1. INTRODUCTION	A-1
2. NIJBOER	A-1
3. DEMPWOLFF AND SOMMER	A-1
4. HALIM	A-4
5. OECD/NARDÒ TEST	A-8
6. DOHMEN AND MOLENAAR	A-16
7. SEBAALY	A-20
8. LENNGREN	A-22
9. COMPARISON OF STRAIN GAUGE TYPES	A-28
REFERENCES	A-36

LIST OF FIGURES

Figure		Page
3.1	Cross Section of the PACCAR Test Section	14
3.2	PACCAR Technical Center—Plan View	17
3.3	Calculated Horizontal Tensile Strain vs. FWD Load at Varying Stiff Layer Moduli—PACCAR Test Section	21
3.4	AC Modulus vs. FWD Load—PACCAR Test Section	22
3.5	Base Modulus vs. FWD Load—PACCAR Test Section	23
3.6	Subgrade Modulus vs. FWD Load—PACCAR Test Section	24
3.7	Cross-sections for SR 525 Pavement Sections, MP 1.70 and 2.45 [17]	26
3.8	PACCAR Pavement Test Track Layout	34
3.9	Saw Cutting Details for Axial Strain Cores	36
3.10	Saw Cutting Details for Shear Strain Cores	36
3.11	Shear Gauge Slot Dimensions	38
3.12	Surface Gauge Slot Dimensions	38
3.13	Plan View of Lead Wire Slots Bisecting Core Holes	40
3.14	Electrical Panel Layout	42
3.15	Measured vs. Calculated Strain for Axial Core Surface Longitudinal Gauges—October 1991 FWD Testing	51
3.16	Measured vs. Calculated Strain for Axial Core Surface Transverse Gauges—October 1991 FWD Testing	54
3.17	Measured vs. Calculated Strain for Axial Core Bottom Longitudinal Gauges—October 1991 FWD Testing	55
3.18	Measured vs. Calculated Strain for Axial Core Bottom Transverse Gauges—October 1991 FWD Testing	56
3.19	Measured vs. Calculated Strain for Axial Core Surface Longitudinal Gauges—February 1993 FWD Testing	64
3.20	Measured vs. Calculated Strain for Axial Core Surface Transverse Gauges—February 1993 FWD Testing	65
3.21	Measured vs. Calculated Strain for Axial Core Bottom Longitudinal Gauges—February 1993 FWD Testing	66
3.22	Measured vs. Calculated Strain for Axial Core Bottom Transverse Gauges—February 1993 FWD Testing	67
4.1	Elevation View of Peterbilt B359 Truck	74
4.2	Plan View of Peterbilt B359 Truck	74
4.3	PACCAR Test Vehicles	76
4.4	Typical Wheel Load Variability with Triplicate Runs (Steer is single tire and drive is dual tires)	79
4.5	Typical Time Histories of Measured Strain in the AC Layer from Peterbilt 359 Truck Tests	80
4.6	Effect of Truck Speed on Longitudinal Strain at the bottom of AC Layer—Core 1	82
4.7	Effect of Truck Speed on Longitudinal Strain at the bottom of AC Layer—Core 3	83
4.8	Effect of Truck Speed on Longitudinal Strain at the surface of AC Layer—Core 4	84
4.9	Effect of Truck Speed on Transverse Train at the bottom of AC Layer—Core 4	85
4.10	Comparison of Longitudinal and Transverse Strain Distributions	86

LIST OF FIGURES (Continued)

Figure		Page
4.11	Comparison of Surface and Bottom Longitudinal Strain—Core 4 in Block 1	87
4.12	Effect of Tire Pressure on Longitudinal Strain at the bottom of AC Layer—Core 1	89
4.13	Effect of Tire Pressure on Longitudinal Strain at the bottom of AC Layer—Core 3	90
4.14	Effect of Tire Pressure on Longitudinal Strain at the bottom of AC Layer—Core 4	91
4.15	Measured Axle Load Variatoins as a Function of Distance for Triplicate Runs—Peterbilt 359—Smooth Pavement	94
4.16	Comparison of Axle Loads for the Peterbilt 359 Generated by Pavement Profile with and without Ramp (Distance = 0 at end of roughness event)	95
4.17	Average Load and Surface Strain Variations with Distance for Peterbilt 359 Ramp Tests	97
4.18	Pavement Surface Strain Variation with Distance for All Test Vehicles (Distance = 0 at end of roughness event)	98
4.19	Variations of Peak Surface Strain with Distance—Grouped by Axle Type and Vehicle Type (Distance = 0 at end of roughness event)	99

LIST OF FIGURES (Continued)

Figure		Page
A.1	Classification of Gauges Installed at the Nardò Test Facility [A5]	A-9
A.2	Thickness and Voids Content of the AC Layer—Nardò Test Facility [A5]	A-11
A.3	Mean and Standard Deviation of Strain Measurement Results at 75° F, All Gauges, By Day of Measurement, Team and Gauge Category—Nardò Test Facility [A5]	A-13
A.4	Mean and Standard Deviation of Maximum Strains at 75° F, All Gauges, By Day of Measurement, Team and Gauge Category —Nardò Test Facility [A5]	A-13
A.5	Ratio of Measured to Calculated Strain from FWD Testing—Nardò Test Facility [A5]	A-14
A.6	Comparison of Measured and Calculated Strains Adjusted for AC Temperature, AC Thickness, and Gauge Location—Nardò Test Facility [A5]	A-15
A.7	Comparison of Measured and Calculated Strains Due to a FWD Load —Section 01, FORCE Project [A6]	A-18
A.8	Comparison of Measured and Calculated Strains Due to a FWD Load —Section 02, FORCE Project [A6]	A-18
A.9	Comparison of Measured and Calculated Longitudinal Strains Due to a FWD Load—RRRL, Delft University of Technology [A6]	A-19
A.10	Comparison of Measured and Calculated Transverse Strains Due to a FWD Load—RRRL, Delft University of Technology [A6]	A-19
A.11	Comparison of Measured and Calculated Longitudinal Strains Due to a FWD Load for Gauge IVDL1—RRRL, Delft University of Technology [A6]	A-21
A.12	Comparison of Measured and Calculated Strains under a Drive Single Axle Load of 12,000 Pounds—Thin Section	A-23
A.13	Comparison of Measured and Calculated Strains under a Drive Single Axle Load of 20,000 Pounds—Thin Section [A7]	A-24
A.14	Comparison of Measured and Calculated Strains under a Drive Single Axle Load of 12,000 Pounds—Thick Section [A7]	A-25
A.15	Comparison of Measured and Calculated Strains under a Drive Single Axle Load of 20,000 Pounds—Thick Section [A7]	A-26

LIST OF TABLES

Table		Page
2.1	Summary of Various Instrumented Flexible Pavement Tests	5
2.2	Range of Experimental Conditions from Various Instrumented Flexible Pavement Tests	9
3.1	Results of Thickness and Density Evaluation of AC Surfacing—PACCAR Test Section	15
3.2	Results of Extraction and Gradation of Cores 1 through 5—PACCAR Test Section	16
3.3	Calculated (EVERCALC 3.3) Depth to Stiff Layer Based on October 1991 FWD Testing—PACCAR Test Section	19
3.4	Sensitivity of Layer Moduli as a Function of the Stiff Layer Modulus—PACCAR Test Section, October 1991 FWD Testing	19
3.5	Sensitivity of RMS Values as a Function of the Stiff Layer Modulus—PACCAR Test Section, October 1991 FWD Testing	19
3.6	Sensitivity of Layer Moduli as a Function of Stiff Layer Modulus—SR 525 Pavement Section, MP 1.70	27
3.7	Sensitivity of Layer Moduli as a Function of Stiff Layer Modulus—SR 525 Pavement Section, MP 2.45	27
3.8	Distribution of Strain Gauges—PACCAR Test Section	30
3.9	Description of Gauge Destinations—PACCAR Test Section	31
3.10	Summary of Data Acquisition Parameters	44
3.11	Descriptive Statistics for Backcalculated Layer Moduli—October 1991 FWD Testing	47
3.12	Effective Pavement Layer Thicknesses Based on October 1991 FWD Data—Axial Cores 1, 3, 4, and 5	49
3.13	Summary of Calculated Depths to Stiff Layer Based on October 1991 WSDOT FWD Data—Axial Cores 1, 3, 4, and 5	49
3.14	Summary of Layer Characteristics Used as Input to CHEVPC—I October 1991 FWD Testing	50
3.15	Comparison of Measured and Calculated Strains from 1991 FWD Testing—PACCAR Test Station	51
3.16	Summary of Layer Characteristics Used as Input to CHEVPC—October 1991 FWD Testing	57
3.17	Descriptive Statistics for Measured to Calculated Strain Ratios by Drop Height—October 1991 FWD Testing	57
3.18	Descriptive Statistics for Measured to Calculated Strain Ratios by Core—October 1991 FWD Testing	57
3.19	Sensitivity of Layer Moduli as a Function of the Stiff Layer Modulus—PACCAR Test Section, February 1993 FWD Testing	59
3.20	Sensitivity of RMS Values as a Function of the Stiff Layer Modulus—PACCAR Test Section, February 1993 FWD Testing	59
3.21	Descriptive Statistics for Backcalculated Layer Moduli—February 1993 FWD Testing	59
3.22	Summary of Calculated Depths to Stiff Layer Based on February 1993 FWD Data—Axial Cores 1, 3, 4, and 5	60
3.23	Summary of Layer Characteristics Used as Input to CHEVPC—February 1993 FWD Testing	60
3.24	Comparison of Measured and Calculated Strains from February 1993 WSDOT FWD Testing—PACCAR Test Section	62

LIST OF TABLES (Continued)

Table		Page
3.25	Descriptive Statistics for Measured to Calculated Strain Ratios by Gauge Type—February 1993 FWD Testing	68
3.26	Descriptive Statistics for Measured to Calculated Strain Ratios by Drop Height—February 1993 FWD Testing	68
3.27	Descriptive Statistics for Measured to Calculated Strain Ratios by Core—February 1993 FWD Testing	68
3.28	Comparison of Measured to Calculated Strain Ratios from February 1993 and October 1993 FWD Testing—PACCAR Test Section	70
3.29	Descriptive Statistics for Measured to Calculated Ratios for Selected Gauges—October 1991 and February 1993 FWD Testing	71
4.1	Static Wheel Loads of Test Vehicles	75
4.2	Tire Geometry of Test Vehicles	75
A.1	Comparison of Measured and Calculated Surface Radial Strains—State Highway 1, The Netherlands (after Nijboer [A1])	A-2
A.2	Comparison of Measured and Calculated Radial Strains at the Bottom of the AC Layer—State Highway 1, The Netherlands (after Nijboer [A1])	A-3
A.3	Comparison of Measured and Calculated Strains at the Bottom of the AC Layer—Shell Laboratory Test Track, Hamburg (after Dempwolff and Sommer [A2])	A-4
A.4	Comparison of Measured and Calculated Strains at the Bottom of the AC Layer—RMC Test Pit (after Halim et al. [A4])	A-6
A.5	Composition of OECD Group RTR 12 "Full Scale Pavement Tests" (after Scazziga [A5])	A-7
A.6	Comparison of Measured and Calculated Strains—Delft University Test Facility (after Dohmen and Molenaar [37])	A-17
A.7	Comparison of Measured and Calculated Strains at the Bottom AC Layer—3.1 inch Section: Road and Traffic Laboratory, Finland (after Lenngren [A8])	A-27
A.8	Comparisons of Measured and Calculated Strains at the Bottom of the AC Layer—5.9 inch Section: Road and Traffic Laboratory, Finland (after Lenngren [A8])	A-27
A.9	Strain Gauges Evaluated During Field Performance Testing (after Sebaaly [A7])	A-30
A.10	Survivability of Gauges Installed in the Thin Section (after Sebaaly [A7])	A-30
A.11	Survivability of Gauges Installed in the Thick Section (after Sebaaly [A7])	A-32
A.12	Survivability of Gauges—Both Pavement Sections (after Sebaaly [A7])	A-32
A.13	Statistical Summary of the Regression Analysis of All Measured Strain Responses (after Sebaaly et al. [A7])	A-34

ACKNOWLEDGMENTS

This multiyear effort has required a good measure of patience and assistance on the part of many. Some of these important individuals include Newton Jackson, formerly with the WSDOT Materials, Keith Anderson and Martin Pietz of the WSDOT Research Office, Bill Nokes at Caltrans who was the contract monitor for the work funded at UCB, and certainly all of our past and current associates at the PACCAR Technical Center. These included Margaret Sullivan (now with the Kenworth Truck Division), Garrick Hu (now with Navistar), Lori Baker (formerly General Manager at the Technical Center), and the current General Manager, Jim Bechtol.

A special thanks goes to Derald Christensen who worked so diligently to install the instrumentation. It is clear that his efforts worked! Finally, the agencies and cooperation which supported this effort must be noted. First, PACCAR Inc. had the vision to work with the infrastructure community. Their support for this effort cannot be measured. Hopefully, the collective results will eventually validate that support. Second, WSDOT and Caltrans provided direct financial support. Further, WSDOT provided the FWD equipment and crew as well as coring and lab testing services. The authors sincerely thank them all. They deserve it.

This report was largely prepared from two significant documents. These are

- "The PACCAR Pavement Test Section—Instrumentation and Validation," a thesis prepared by Brian C. Winters, University of Washington, March 1993.
- "PACCAR Full-Scale Pavement Tests," a report prepared by Karim Chatti, Kyong Ku Yun, Hyung Bae Kim, and Roshan Utamsingh at Michigan State University for the University of California at Berkeley, and the California Department of Transportation, April 1995.

SECTION 1

INTRODUCTION

1. THE PROBLEM

The condition of the U.S. highway system has been and continues to be a major concern of both the highway and trucking communities. [1] This is understandable given the fact that in 1990, combination vehicles with five or more axles accounted for 91 percent of the 18,000 pound equivalent axle loads (ESALs) on rural Interstate highways. [2] This heavy vehicle traffic and the pavement system it travels on combine to generate a perpetual cycle of pavement deterioration and rehabilitation. Increasing truck traffic leads to predictable pavement damage that in turn contributes to potentially increasing dynamic loading of the pavement. This cycle continues until some form of pavement rehabilitation is undertaken. The trucking community alters the design and operation of their vehicles largely due to economic considerations (profit) but also in response to the ride quality (or lack thereof) of the infrastructure to which they are bound. On the other hand, the pavement community is constantly updating design and construction practice to improve pavement performance. Unfortunately, both parties develop a form of "technical tunnel vision" and work to resolve some of the same concerns without the benefit of a possible mutual effort. As such it was recognized that there was a need to improve our mutual understanding of truck pavement interaction. [3] Often, but not always, a beneficial change in one community (such as smoother pavements) benefits the other (less truck/cargo damage).

2. BACKGROUND AND OBJECTIVES

This report is part of a multiphased research project entitled "Truck/Pavement Interaction" conducted jointly by the University of Washington, University of California-Berkeley, Washington State Department of Transportation (WSDOT), California

Department of Transportation (Caltrans), and PACCAR, Inc. This is an attempt to promulgate a mutually beneficial dialog between the pavement and trucking communities. The objective of the research is to investigate how different truck suspensions, tire/axle combinations, tire loads, and tire pressures affect pavement response and conversely how pavement condition affects truck performance and damage. These objectives will be accomplished by operating instrumented trucks over an instrumented pavement section. [1]

3. REPORT SCOPE

The report scope includes the following:

- analysis of material properties of the flexible pavement test section
- validation of instrumented pavement responses
- analyses of the truck and pavement responses.

The report is divided into five sections. Section 1 contains an introduction to the study. Section 2 provides a brief review of some of the relevant literature. Section 3 overviews the evaluation and characterization of the pavement test section built for this study at the PACCAR Technical Center. Included is a discussion of the installed instrumentation along with an analysis of the various strain measurements collected during the FWD verification phase. Section 4 presents an overview of the instrumented truck and pavement analyses conducted during September 1993. Section 5 is used to summarize the study findings.

SECTION 2

LITERATURE REVIEW

1. INTRODUCTION

This section will be used to focus on previous flexible pavement test facilities and analysis of pavement responses due to truck loads.

2. FLEXIBLE PAVEMENT TEST FACILITIES

Wester [25] noted that L.W. Nijboer performed the first comparison of calculated and measured strain values in AC pavements in the Netherlands in 1955.

> "This very promising first experiment was the start in developing techniques to measure, under actual conditions, the strain at various levels in a bituminous bound layer and at the interface between the bituminous layer and the unbound base or sub-base."

In Nijboer's study the surface strains were measured using elastic resistance strain gauges mounted on the pavement surface. The results showed "relatively good agreement" between the measured and calculated strain values.

Over the past 40 years since Nijboer's work there have been numerous other attempts to design, construct, operate, and validate other AC pavement test facilities. In general, the purpose of these facilities is to examine the correlation between theory and what happens in real pavements under actual loads. [26]

2.1 Types of Test Facilities

Test facilities with controlled construction and some form of accelerated loading provide several advantages. Specifically, they allow relatively complete control over test parameters, repeatability of testing conditions, and the ability to apply a large number of loads in a relatively short period of time. [27] Of course, test roads with retrofitted instrumentation and actual vehicular loading provide the opposite scenario. They provide

an environment closer to in-service conditions but they sacrifice the experimental control found in controlled test tracks.

The various test facilities can be divided into three basic groups:

- linear test tracks
- circular test tracks
- test roads with controlled or uncontrolled loading.

Sebaaly et al. [27] provided a thorough description of the prominent test facilities in each of the three groups.

Most of the test facilities have been designed and built as true "test" sections where the construction was controlled to allow instrumentation to be installed during the construction phase. Only a small number of experiments have been conducted using instrumentation retrofitted into an existing pavement and applying actual truck loads. The loading was usually applied by some form of accelerated loading device. Accelerated loading devices (ALD's) are of basically two types: circular and linear. Generally speaking, circular ALD's are restricted to operation at only one pavement facility and linear ALD's are capable of being transported to various test locations including in-service pavements. This is not to say that circular ALD's can not be moved. Some of the circular ALD's can be moved from one test pavement to another at the same facility to allow testing and construction to occur simultaneously.

2.2 Comparisons of Measured and Calculated Strains from Various Flexible Pavement Experiments

A review of the research from flexible pavement test facilities shows numerous examples of acceptable agreement between measured and calculated strains in bituminous layers. A summary of these tests is contained in Table 2.1, which is not a complete list but rather a representative sample. The number of tests conducted that result in unacceptable agreement between measured and calculated strains is unknown. A discussion of the specific results from a sample of the tests in Table 2.1 is contained in Appendix A.

Table 2.1 Summary of Various Instrumented Flexible Pavement Tests

Reporting Agency (Reference)	Test Location	Type of Facility	Type of Strain Instrumentation	Strain Responses Measured	Pavement Structure (inches)	Type of Loading for Testing	Load Magnitude (pounds)	Source of Theoretical Computation	Year of Testing	Exposed to Normal Traffic
California Division of Highways (Zube [4])	Northern California	Linear Test Track and Test Road	SR-4 strain gauges glued to surface or placed in carrier block	Transverse at surface and bottom of AC	Six Total Sections 1: AC 3.75, BS 8.0 (CTB) 2: AC 6.75, BS 6.0 3: AC 3.75, BS 12.0 4: AC 3.0, BS 9.0 5: AC 3.0 New plus 2.0 Old, BS Variable 6: AC 2.0, BS 4.0	Duals and super single - 2 axle truck	5000 to 9000 per wheel	Boussinesq equations	1963	Yes
Dutch Road Research Centre (Nijboer [26])	Highway 1	Test Road	Strain gauge attached to a thin slab of sand asphalt	Radial at surface and bottom of AC	AC: 7.5 BS: None	Single wheel loads	2804 to 4847	Burmister 2 - layer	1967*	Yes
Shell Laboratory (Gusfeldt [29])	Hamburg, Germany	Linear Test Track	Gauge stuck to asphalt carrier block	Radial strain at various depths in AC	AC: 5.5 BS: 33.9	Linear test apparatus (single tire)	880 to 4400 per wheel	Jones' tables of stresses in 3 layer elastic system	1967*	No
Shell Research N.V. (Klomp [30])	Highway 1	Test Road	600 ohm electrical resistance	Horizontal at surface and various depths in AC (0-5.5 in.)	AC: 1.2 BS: 6.7 (ATB)	Single front wheel of a loaded truck	2818 to 4862 per wheel	Jones' tables of stresses in 3 layer elastic system	1967*	Yes
Shell Laboratory (Dempwolff [28])	Hamburg, Germany	Linear Test Track	Wire gauges glued into asphalt carrier blocks	Transverse and Longitudinal at various depths in the AC	AC: 8.7 Section I (Dense) Section II(Open) BS: 11.8	Linear test apparatus (single tire)	1100 to 4400 per wheel	BISTRO	1967-69 1972*	No
Nihon Univ, Japan (Miura [31])	Tomei Highway (between Tokoyo and Nagoya)	In service pavement	Electric resistance gauges molded by epoxy and polyester resin	Transverse and Longitudinal at various depths in the AC	AC: 3.9 BS: 7.1 (ATB) SB: 6.7 (CTB)	Dual wheel loads	6600 to 15,400 per wheel	Burmister (single and dual circular loading)	1972*	Yes
National Institute for Road Research, South Africa (Freeme [11])	Special Road 12/2, South Africa	In service pavement	Strain meters developed by Road Research Lab in the UK	Tensile strain at the bottom of the AC	AC: 1.0, 2.0, 3.9 (Dense and Open Grade) BS: 11.8 SB: 3.9 (LTB)	2 axle single wheel truck	2565 to 8370 per wheel	Chevron computer program	1972*	Yes

Table 2.1 Summary of Various Instrumented Flexible Pavement Tests (continued)

Reporting Agency (Reference)	Test Location	Type of Facility	Type of Strain Instrumentation	Strain Responses Measured	Pavement Structure (inches)	Type of Loading for Testing	Load Magnitude (pounds)	Source of Theoretical Computation	Year of Testing	Exposed to Normal Traffic
Koninklijke/Shell -Laboratorium (Valkering [32])	E8 Motorway, Netherlands	Trial Section	Strain gauge type not reported	Longitudinal and transverse at surface and transverse at 2.8 in depth	Section I AC: 8.3 BS: 7.1 (CTS) Section II AC: 11.0 BS: None	Wheel of a skid measurement system	450	BISAR	1972*	Yes
Royal Military College; Ontario Ministry of Transportation and Communication; Gulf Canada, Ltd.; Univ of Waterloo (Halim [33])	Royal Military College, Kingston	Test Pit	Foil type gauges bonded to top and bottom of plastic mesh; Mastic strain carriers (ARC) with two 120 ohm gauges embedded in mastic plate	Horizontal tensile strains at mesh and bottom of AC	AC: 4.5 to 9.8 (with and without plastic mesh) BS: None SG: Dry and saturated	12 in. diameter rigid circular plate	2250 to 9000	BISAR	1983*	No
Laboratoire Central des Ponts et Chaussées (LCPC) (Autret [34])	Nantes, France	Circular test track	H-gauges glued to aluminum or plexiglass backing	Horizontal strain at bottom of AC and vertical strain at top of SG	Ring B_0, Section 1 AC: 2.0 BS: 17.7	Accelerated loading device (ALD) with 4 half axles	22,500 and 29,250 per axle	ALIZE III computer program	1984	No
Organization for Economic Cooperation and Development (OECD) (Scazziga [35])	Nardò, Italy	Linear test track	H-gauges, gauges glued into carrier blocks, core gauges	Horizontal strain at a depth of 2.0 in. and at bottom of AC	AC: 5.1 BS: 6.7	2 axle truck	Front axle: 12,155 Rear axle: 25,636	Method of Equivalent Thickness (MET)	1984	No
FHWA (Bonaquist [36])	Turner-Fairbank Highway Research Facility	Linear test track	Gauge type not reported	Surface and bottom of AC	Lane 1 AC: 5.0 BS: 5.0 Lane 2 AC: 7.0 BS: 12.0	Linear ALF (one half of a dual tire single axle)	9400, 14,100 and 19,000 per half axle	ELSYM5	1988*	No
Ministry of Transport, The Netherlands (Dohmen [37])	Road and Railroad Research Laboratory	Linear test track	Dynatest strain transducer and TML embedment gauges	.3 inches above bottom of AC	AC: 4.7, 7.1, and 9.4 BS: None	FWD	11,250	BISAR	1992*	No
Dutch Team, FORCE Project, OECD [38]	LCPC, Nantes, France	Circular test track	TML embedment strain gauges	Radial strain at bottom of AC	AC: 5.5 BS: 11.0	ALD (half axle)	12,938 per half axle	BISAR	1989 1991*	No

Table 2.1 Summary of Various Instrumented Flexible Pavement Tests (continued)

Reporting Agency (Reference)	Test Location	Type of Facility	Type of Strain Instrumentation	Strain Responses Measured	Pavement Structure (Inches)	Type of Loading for Testing	Load Magnitude (pounds)	Source of Theoretical Computation	Year of Testing	Exposed to Normal Traffic
Ministry of Transport, The Netherlands (Dohmen [37])	LCPC, Nantes, France	Circular test track	TML embedment gauges	Bottom of AC	Section 01 AC: 4.8 BS: 11.0 Section 02 AC: 5.5 BS: 11.0	FWD	13,500 and 16,875	BISAR	1989 1992*	No
Ministry of Transport, The Netherlands (Dohmen [37])	Road and Railroad Research Laboratory	Linear test track	Gauge type not reported	Longitudinal and transverse at bottom of AC	AC: 5.9 BS: None	FWD	Not reported	3 layer system	1992*	No
Ministry of Transport, The Netherlands (Dohmen [37])	Road and Railroad Research Laboratory	Linear test track	Gauge type not reported	Longitudinal and transverse at bottom of AC	AC: 5.9 BS: None	LINTRACK Super singles and duals (half axle)	11,250 per half axle	BISAR	1992*	No
FHWA (Sebaaly [39])	Pennsylvania Transportation Institute	Linear test track	Dynatest H-gauge Kyowa gauge ARC gauge Core gauge	Bottom of the AC	Thin AC: 6.0 BS: 8.0 Thick AC: 10.0 BS: 10.0	Single drive axle tractor with a tandem axle semitrailer	3760 to 20,820 per axle	PENMOD	1989 1992*	No
Royal Institute of Technology, Sweden (Lenngren[24])	Road and Traffic Laboratory, Finland	Linear test pavement	Core gauges	Horizontal at bottom of AC	Thin Section AC: 3.1 BS/SB: 24.4 Thick Section AC: 5.9 BS/SB: 21.7	FWD	2813, 5626, and 11,250	BISAR and CLEVERCALC	1989 1991*	No
Cambridge Univ. (Hardy [40])	Transport and Road Research Lab	Test section	Metal foil gauges	Transverse at bottom of AC	AC: 7.9 BS: 11.8	Four - axle articulated vehicle	Not reported (based on dynamic load)	Convolution Theory	1992*	No

Notes:

AC = Asphalt Concrete
BS = Base Course
SB = Subbase
CTB = Cement treated base
ATB = Asphalt treated base
CTS = Cement treated sand
SG = Subgrade
LTB = Lime treated base
* = Year reported in literature

The information contained in Appendix A demonstrates that reasonable comparisons between measured and calculated strains can be achieved under a variety of experimental conditions which include

- pavement loading
  - magnitude of load
  - source of load
    - plate loading
    - truck axle
    - accelerated loading device
    - falling weight deflectometer
- pavement structures
- theoretical computational techniques
- strain measurement techniques (gauge type).

The range of these conditions sorted by pavement load type are summarized in Table 2.2.

One observation from this summary is that a range of about 20 percent is regarded as a reasonable expectation when comparing measured to calculated strains.

3. ANALYSIS APPROACHES FOR PAVEMENT AND TRUCK MODELING

3.1 Pavement Models

The currently available methods of pavement analysis are mostly based on static analysis and may be subdivided into two main groups: Continuum methods and finite-element and finite-difference methods. A few analytical methods for solving dynamic problems in pavements are now available.

3.1.1 Static Methods

Elastic layer theory has been used successfully for the analysis of flexible pavements since the 1940s, when it was introduced by Burmister [56]. Initially, the use of the method was restricted to systems with two or three layers that extend to infinity in the horizontal directions. More recently, a number of computer models, which can handle more layers, have been developed (53, 64, 75). The finite-element method has also been used for both flexible and jointed rigid pavements (63, 70, 71, 72, 74, 77, 79, 80, 82, 83,

Table 2.2 Range of Experimental Conditions From Various Instrumented Flexible Pavement Tests

Source of Load [Reference(s)]	Load Magnitude (pounds)	Pavement Structure (inches)	Gauge Type	Theoretical Comparison
Plate Loading from a Hydraulic Actuator [33]	2250 to 9000	AC: 4.5 to 9.8 BS: None	Foil gauges and mastic carriers	BISAR
FWD [24, 37]	2813 to 16,875	AC: 3.1 to 9.4 BS: 0 to 11.0	Core, TML, Dynatest	BISAR, CLEVERCALC
Single Wheel Loads (vehicular) [4, 11, 26, 30, 32, 35,]	450 to 9000 per wheel	AC: 1.0 to 11.0 BS: 0 to 33.9 CTB, ATB, CTS SB: 0 to 3.9 (LTB)	SR4, SR4 in carrier blocks, gauges attached to sand asphalt, electric resistance, UK strain meters	Boussinesq, Burmister 2-layer, Jones' Tables, Chevron, BISAR
Dual Wheel Loads (vehicular) [4, 31, 35]	5000 to 15,400 per wheel	AC: 2.0 to 10.0 BS: 4.0 to 12.0 CTB, ATB SB: 0 to 6.7	SR4, SR4 in carrier blocks, electric resistance molded by epoxy and polyester resin, H-gauges, gauges in carrier blocks, core, Kyowa, ARC	Boussinesq, Burmister, MET, BISAR, PENMOD
Single Wheel ALF [28, 29, 37]	880 to 11,250 per wheel	AC: 5.5 to 8.7 Open, Dense BS: 0 to 33.9	Gauges in carrier blocks	Jones' Tables, BISTRO, BISAR
Dual Wheel ALF [34, 36, 37, 38]	9400 to 19,000 per set of duals	AC: 2.0 to 7.0 BS: 0 to 17.7	H-gauges glued to aluminum or plexiglass backing, TML	ALIZE III, ELSYM5, BISAR

85, 91, 93). Surprisingly, there is only a small number of studies which have considered the validation of these models by comparison with field measurements (54, 72, 81, 92).

3.1.2 Quasi-Static Methods

Quasi-static methods are based on the idea of positioning the load at subsequent positions along the pavement for each new time step, and assuming the load to be static at each position. These methods use static analysis to compute the loading position which will give the most severe effect. This is done via the concept of influence lines or functions. The influence line determines the (static) effect of a unit load, acting at various positions, on the magnitude and sign of the primary response of the pavement structure (i.e. stresses, strains, and deflections). An influence line thus gives the variation in the static response at one (fixed) point due to a unit load traversing the pavement. The concept of using the influence line of a moving unit load to determine the critical positions of actual loads which give a maximum or minimum effect in a pavement structure was published by Winkler in 1868.

A recent study has applied this concept with a static finite-element computer program to study the contribution of dynamic truck loading to rigid pavement performance [51]. Another study has compared strain time histories obtained in a field experiment with predictions made using a quasi-static application with a static finite element computer program [81]. The justification for using a quasi-static method has been based on the fact that traffic velocities are less than 10 percent of the critical velocity of typical pavements. This velocity is defined as the propagation velocity of a transverse deflection wave through the pavement.

3.1.3 Dynamic Methods

Dynamic models that have been developed for the analysis of pavements can be largely classified into two main categories:

- A beam or plate supported by massless springs (Winkler foundation) [55, 57, 58, 60, 69, 73, 76, 78, 95] or supported by a half-space [52, 60]. The foundation may be modified to include inertial effects [69, 87].
- A layered structure of elastic or visco-elastic solids [62, 88].

A new prismatic model combining the finite element method and visco-elastic layer theory has been published very recently [67]. The finite element formulation is used to model an irregular region which includes the pavement structure and the soils underneath it. The visco-elastic layer theory is used to model the far-field region via semi-infinite thin-layered elements. The two regions are joined by energy-transmitting boundaries. This model applies only to continuous flexible pavements because of its prismatic nature and its inability to handle discontinuities.

Dynamic models vary in complexity according to the structure analyzed (finite or infinite beam/plate; elastic or visco-elastic Winkler foundation, or visco-elastic layers) and the loading (stationary, moving, constant, harmonic, random). The solutions vary from closed-form expressions using Fourier and Laplace transforms to numerical algorithms using direct time integration methods, numerical convolution, and the method of complex response. A number of methods have been used to account for the moving effect of the load. They range from using the Dirac function or the Kronecker delta operator to pre-multiplying the load by time dependent deflection shape functions or applying a pulse load with a duration equal to the time taken to travel one tire contact length.

Research conducted in the late eighties and early nineties at the University of California at Berkeley led to the development of two finite layer/element computer programs for the dynamic analysis of "flexible" and "rigid" pavements:

- SAPSI Computer Program

  SAPSI is a PC-based FORTRAN computer program which calculates the dynamic response of a n-layered viscoelastic system to multiple surface loads. Material properties for each layer may be varied with frequency. Chen verified the program against analytical solutions [61], and Tabatabaie validated it by comparison with field measurements [92].

- DYNA-SLAB Computer Program

  DYNA-SLAB is a PC-based FORTRAN computer program which calculates the dynamic response of a concrete slab system to moving fluctuating loads using the finite-element method of analysis. The underlying soils can be modeled either as a damped Winkler foundation or as a layered viscoelastic system. Chatti validated the model by comparison with theoretical results as well as with field measurements [60].

3.2 TRUCK MODELS

As seen by pavements, a truck is a set of moving, time-varying surface stresses. These stresses represent the static load carried by each axle as well as the dynamic fluctuations generated by the roughness of the pavement surface profile.

A number of truck simulation models for predicting dynamic wheel loads have been developed by several research organizations, including MIT [68], UMTRI [65] and the University of Cambridge. These models are planar, with pitch being the only form of rotation allowed. Key factors affecting the accuracy of these models include the proper modeling of non-linear properties of the suspension springs, kinematics of tandem axles and the sequential input of the road profile into the different axles. Truck simulation models have by-in-large been validated by comparison with full-scale tests.

SECTION 3

EVALUATION AND INSTRUMENTATION OF THE PACCAR TEST PAVEMENT

1. INTRODUCTION

This section will be used to describe the PACCAR test pavement, its evaluation, and the instrumentation including the installation and verification process.

2. DESCRIPTION OF THE PACCAR TEST SECTION

The test pavement is located at the PACCAR Technical Center at Mount Vernon, Washington (about 60 miles north of Seattle). It is a flexible pavement surfaced with 5.4 inches (mean value) of dense graded AC (WSDOT Class B) over a 13.0 inch crushed stone base. The subgrade is a sandy clay. A cross section of the pavement structure is shown in Figure 3.1. The water table was measured at a depth of 66 inches during installation of the instrumentation.

Fifteen AC core samples were taken from the section for installation of the instrumentation. These cores were used to conduct various tests of the materials. The coring and materials testing were conducted by WSDOT. The results are contained in Tables 3.1 and 3.2. Table 3.1 shows that based on the 15 samples taken, the AC layer is relatively homogeneous and of a generally uniform thickness. Table 3.2 compares the gradation of axial Cores 1 through 5 to the gradation band for WSDOT Class B ACP. The PACCAR mix mostly falls within the Class B band except for the No. 200 sieve.

The instrumented section is approximately 14 feet wide and 40 feet long. It is located along a section of the durability track at the Technical Center (see Figure 3.2). It was closed to vehicular traffic except during scheduled pavement testing. There was standing water virtually year round in the infield adjacent to the test section.

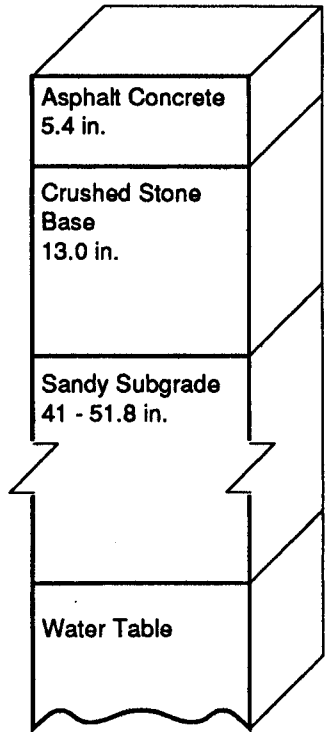

Figure 3.1 Cross Section of the PACCAR Test Section

Table 3.1. Results of Thickness and Density Evaluation of AC Surfacing—PACCAR Test Section

Core Number	AC Thickness (in.)	Bulk Density	Rice Density	Percent Voids
1	5.16	2.300	2.503*	8.1
2	5.16	2.326	2.503*	7.1
3	5.16	2.387	2.503*	4.6
4	5.28	2.368	2.503*	5.4
5	5.16	2.347	2.503*	6.2
6	5.40	2.289	2.505	8.6
7	5.16	2.349	2.502	6.1
8	5.40	2.369	2.503*	5.4
9	5.28	2.326	2.503*	7.1
10	5.76	2.297	2.503*	8.2
11	5.52	2.315	2.503*	7.5
12	5.64	2.301	2.503*	8.1
13	5.76	2.285	2.503*	8.7
14	5.64	2.278	2.503*	9.0
15	5.52	2.313	2.503*	7.6
Mean	5.40	2.323	N/A	7.2
Standard Deviation	0.23	0.034	N/A	1.4
Minimum	5.16	2.278	N/A	4.6
Maximum	5.76	2.387	N/A	9.0
Count	15	15	N/A	15

Notes: Rice densities performed on cores 6 and 7 only.

* Average of Rice densities from cores 6 and 7 used to determine air voids.

Table 3.2. Results of Extraction and Gradation of Cores 1 through 5—PACCAR Test Section

Sieve Size	Percent Passing					
	Core Number					WSDOT
	1	2	3	4	5	Class B
5/8	100	100	100	100	100	100
1/2	98	98	98	99	99	90-100
3/8	89	89	90	92	89	75-90
1/4	68	67	71	74	69	55-75
10	36	37	37	39	37	32-48
40	17	18	18	19	18	11-24
80	11	12	12	12	12	6-14
200	7.4	8.3	8.0	8.4	8.1	3-7
% Asphalt	5.4	5.1	5.1	5.5	5.0	

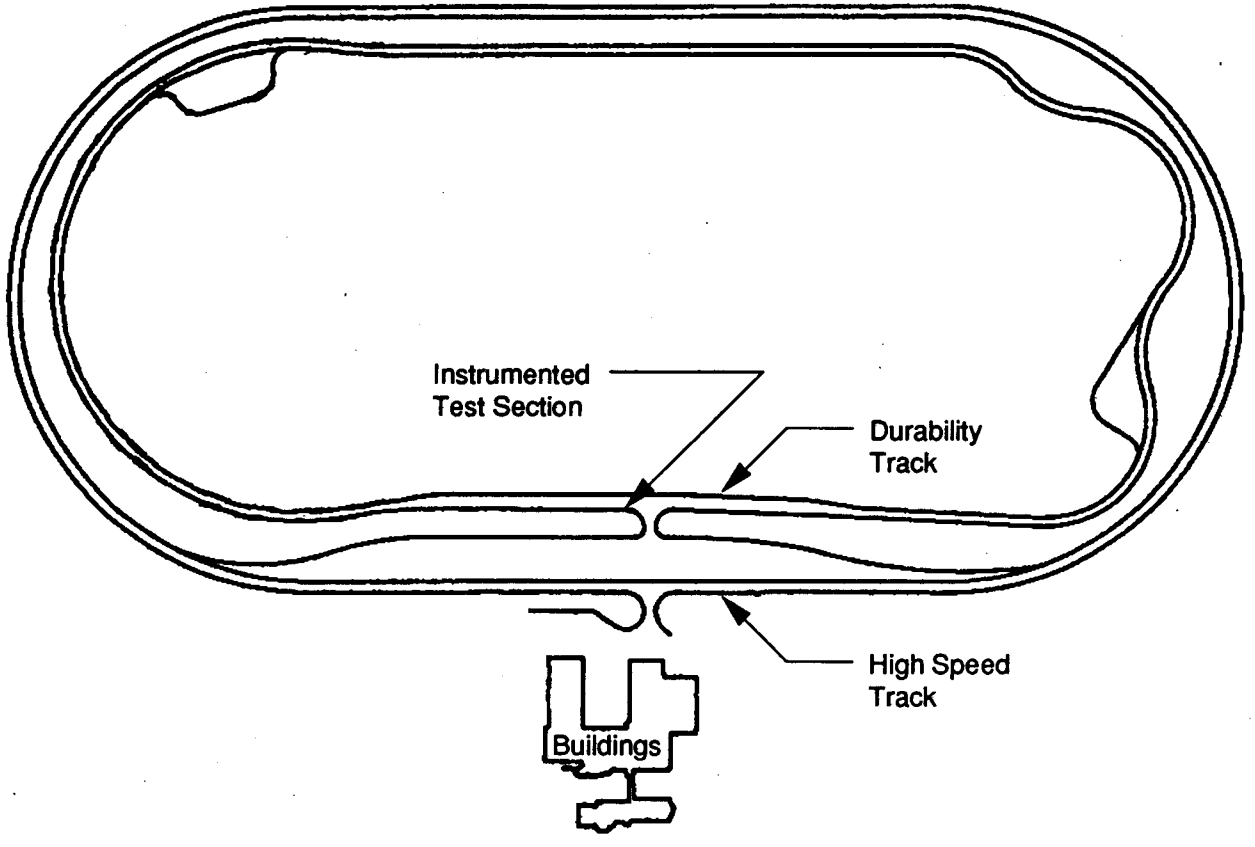

Figure 3.2 PACCAR Technical Center—Plan View

3. BACKCALCULATION OF TEST SECTION LAYER MODULI

The first step in evaluating a test section is to establish the material properties for each of the layers in the pavement structure. There are two basic methods: laboratory testing and field testing. For this test section, a combination of both methods was used. Cores and laboratory tests were used to verify AC layer thickness and evaluate the asphalt concrete mixture that was discussed above. Backcalculation of FWD deflection data was used to establish appropriate layer moduli.

Subsequently, due to insight gained during the estimation of layer moduli for this test section, an additional examination of available data from SR 525 was made. This was done to verify or confirm the significant impact of the water table on the backcalculated layer moduli.

3.1 PACCAR Test Section

During October 1991, the WSDOT Dynatest 8000 FWD was used to obtain deflection measurements at 61 separate locations (130 drops). One basin was deleted due to a faulty sensor reading at the 8 inch offset. The applied loads varied from 4,874 to 14,527 pounds. Sensor spacings for the FWD were set at 0, 8, 12, 24, 36, and 48 inches. During testing, the measured average mid-depth temperature of the AC layer was 68° F. By use of EVERCALC 3.3, the layer moduli were estimated for various conditions using the previously mentioned layer thicknesses (surface and base) and Poisson's ratios of 0.35 (AC) and 0.40 (base). The pavement structure was modeled as a four layer system by inclusion of the stiff layer option in EVERCALC.

Initially, the stiff layer was fixed with a modulus of 1,000 ksi with the depth to stiff layer estimated by use of the software algorithm. This estimated depth from the top of the pavement surface ranged between 60 and 70 in. and was extremely close to the measured depth of water table (see Table 3.3). Further, there are no known rock or other major layer transitions within several feet of the surface at this site. Using the 1,000 ksi

Table 3.3. Calculated (EVERCALC 3.3) Depth to Stiff Layer Based on October 1991 FWD Testing—PACCAR Test Section

DEPTH TO STIFF LAYER	(inches)
Mean	64.9
Standard Deviation	2.9
Minimum	59.4
Maximum	70.2
Number of Drop Locations (n)	61

Table 3.4. Sensitivity of Layer Moduli as a Function of the Stiff Layer Modulus — PACCAR Test Section, October 1991 FWD Testing

Pavement Layers	E_{stiff}						
	10 ksi	25 ksi	40 ksi	50 ksi	75 ksi	100 ksi	1000 ksi
Asphalt Concrete* (ksi)	884	828	563	476	405	368	284
Crushed Stone Base* (ksi)	2.5	4.2	15	20	27	30	42
Fine-grained Subgrade* (ksi)	1436	43	10	8.5	7	7	5.3
Total Runs with RMS% <=2.5*	22	113	120	118	80	77	31

*Calculated from runs with a RMS% <=2.5%.

Table 3.5. Sensitivity of RMS Values as a Function of the Stiff Layer Modulus — PACCAR Test Section, October 1991 FWD Testing

RMS (%)	E_{stiff}						
	10 ksi	25 ksi	40 ksi	50 ksi	75 ksi	100 ksi	1000 ksi
Mean*	3.0	1.4	1.3	1.7	2.3	2.6	3.8
Standard Deviation*	0.7	0.8	0.9	1.0	1.2	1.3	1.6
Minimum*	1.4	0.4	0.2	0.2	0.6	0.8	1.4
Maximum*	5.6	5.2	6.9	7.5	8.2	8.5	9.4
Total Runs with RMS% <=2.5*	22	113	120	118	80	77	31

*Calculated for 129 deflection basins.

modulus for the stiff layer, only 31 of the 130 deflection basins resulted in an RMS error convergence of 2.5 percent or less (2.5 percent was used as an acceptable upper limit). Thus, it was decided to try various values for the stiff layer modulus ranging from a low of 10 ksi to a high of 1,000 ksi. The resulting layer moduli are shown in Table 3.4 and associated RMS statistics in Table 3.5.

The results suggest that the stiff layer was "triggered" by the saturated conditions below the water table and, for this condition, a stiff layer modulus of about 40 ksi is more appropriate than the traditional value of 1,000 ksi. This observation is based on the RMS and AC modulus values. For example, the AC modulus of 563 ksi corresponds to an expected value of about 600 ksi based on previously conducted laboratory tests for WSDOT Class B mixes — a rather close agreement. The base modulus of 15 ksi might be a bit low but the subgrade modulus of 10 ksi appears to be reasonable (based on soil type).

The effect of using various stiff layer stiffnesses can be illustrated by use of one of the critical pavement response parameters (horizontal tensile strain at the bottom of the AC) used in mechanistic-empirical pavement design (new or rehabilitation). Figure 3.3 shows the strain backcalculated from the October 1991 deflection data versus FWD load using all deflection basins that converged with a RMS error percentage at or below 2.5 percent at each of the three stiff layer conditions. Clearly, the estimated strain levels are significantly influenced by the stiff layer modulus condition.

Layer moduli backcalculated from the October 1991 FWD deflection data were plotted as a function of FWD load to examine the suitability of using layered elastic analysis to determine the layer moduli for the PACCAR section. The layer moduli were backcalculated from the 122 deflection basins that converged with a RMS error percentage at or below 2.5 percent. The stiff layer modulus was set at 40 ksi and the FWD load ranged from 4874 to 14,527 pounds. The results of this analysis are shown in Figures 3.4 to 3.6. Even though there is considerable variability in the layer moduli for

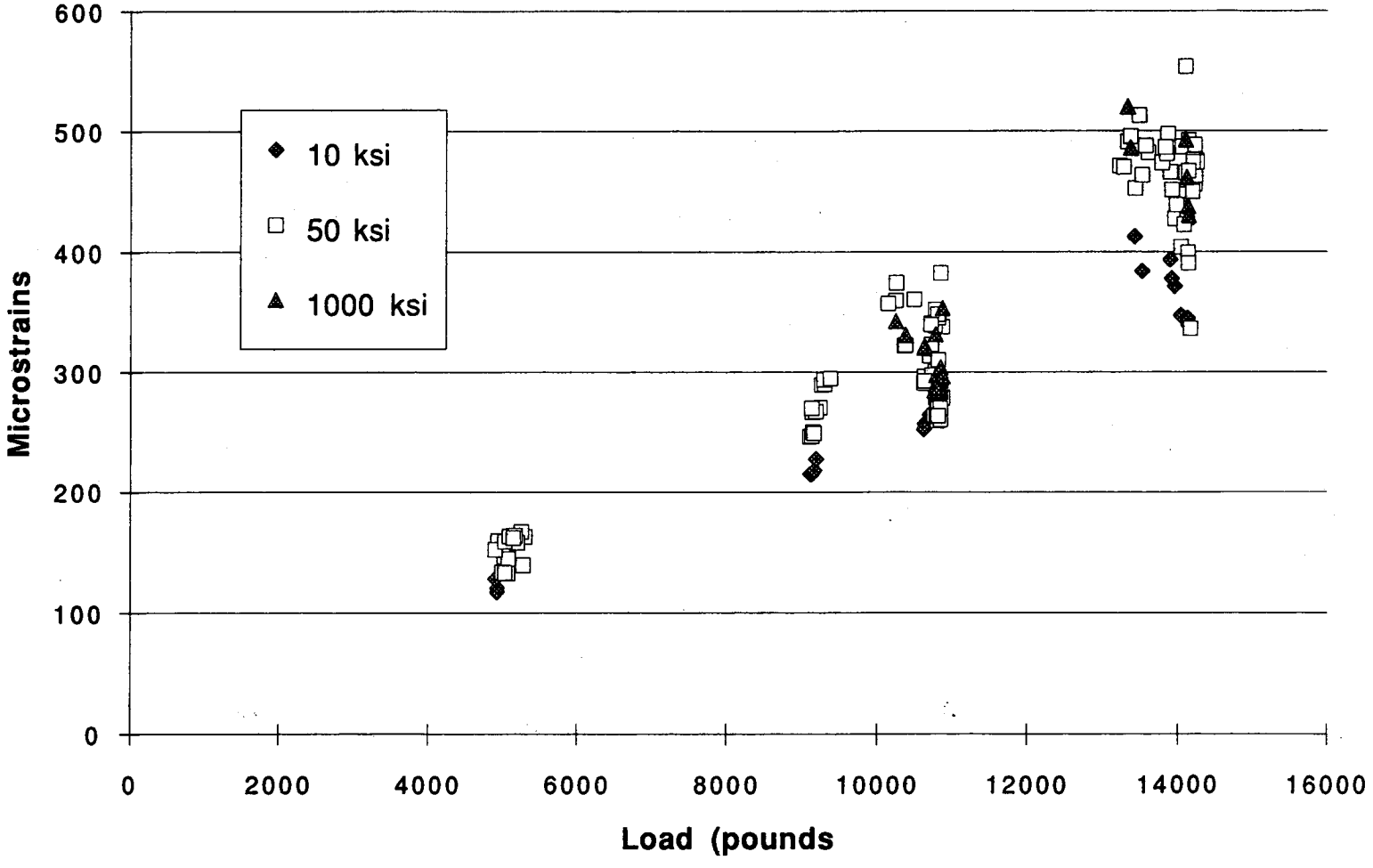

Figure 3.3 Calculated Horizontal Tensile Strain vs. FWD Load at Varying Stiff Layer Moduli—PACCAR Test Section

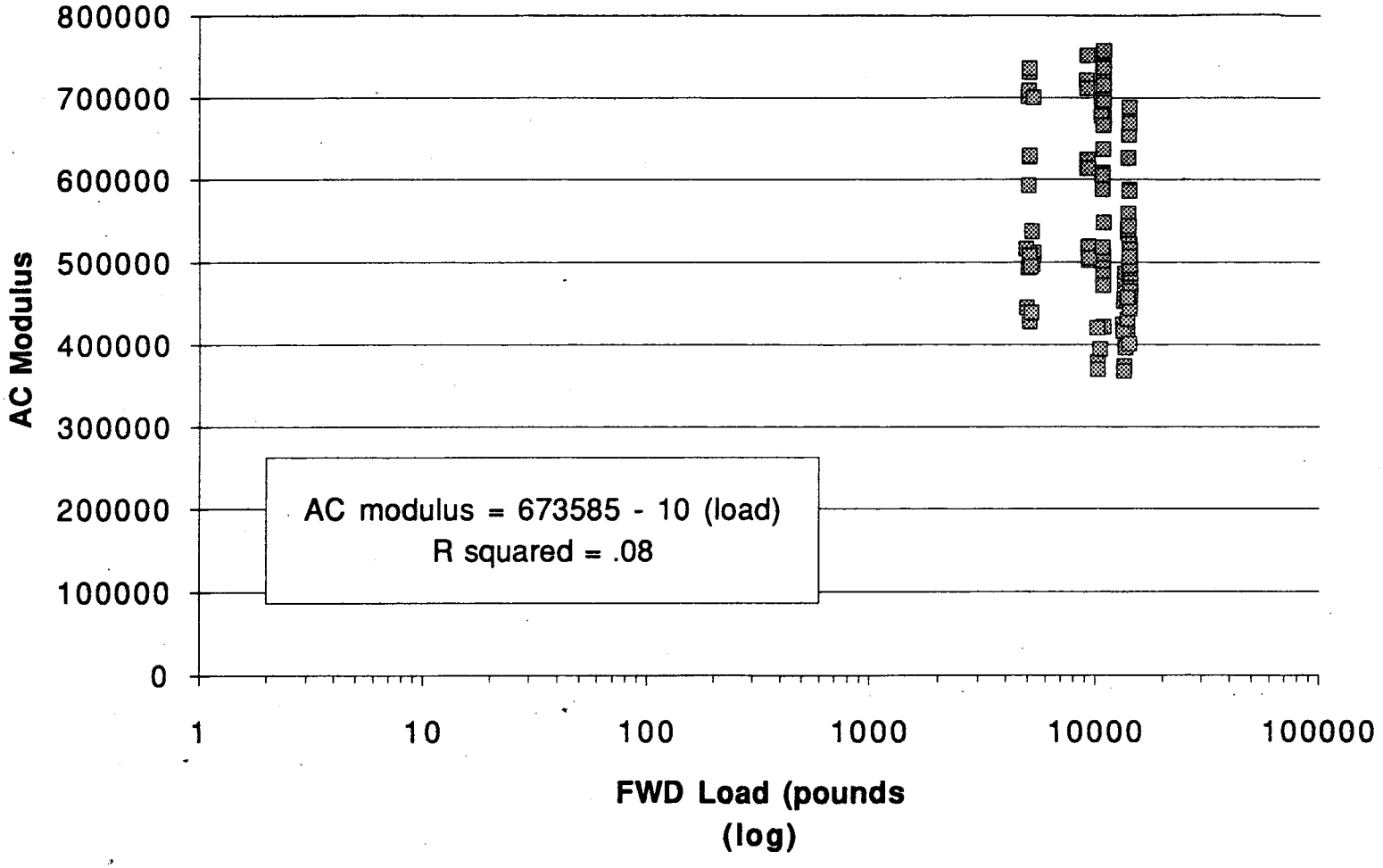

Figure 3.4 AC Modulus vs. FWD Load—PACCAR Test Section

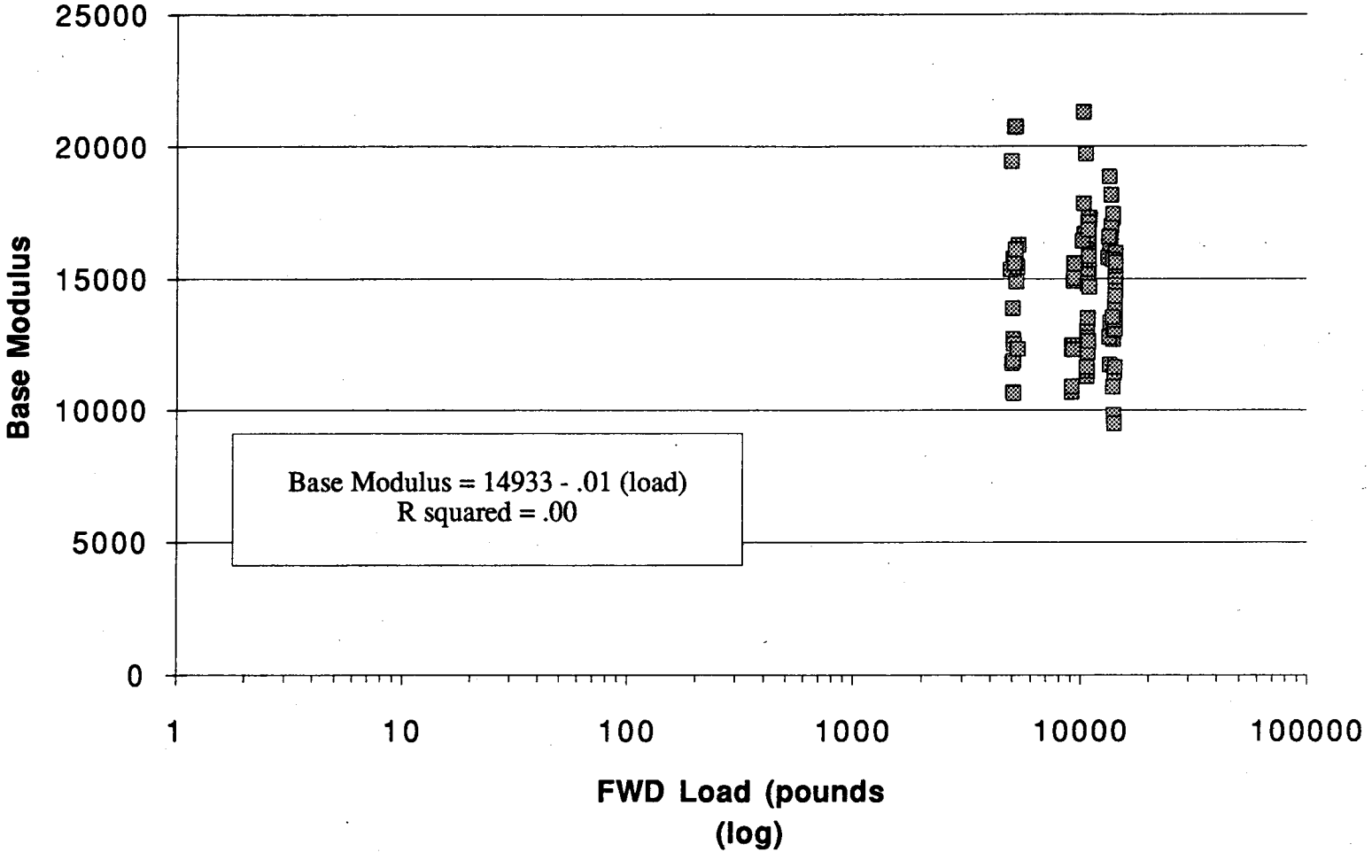

Figure 3.5 Base Modulus vs. FWD Load—PACCAR Test Section

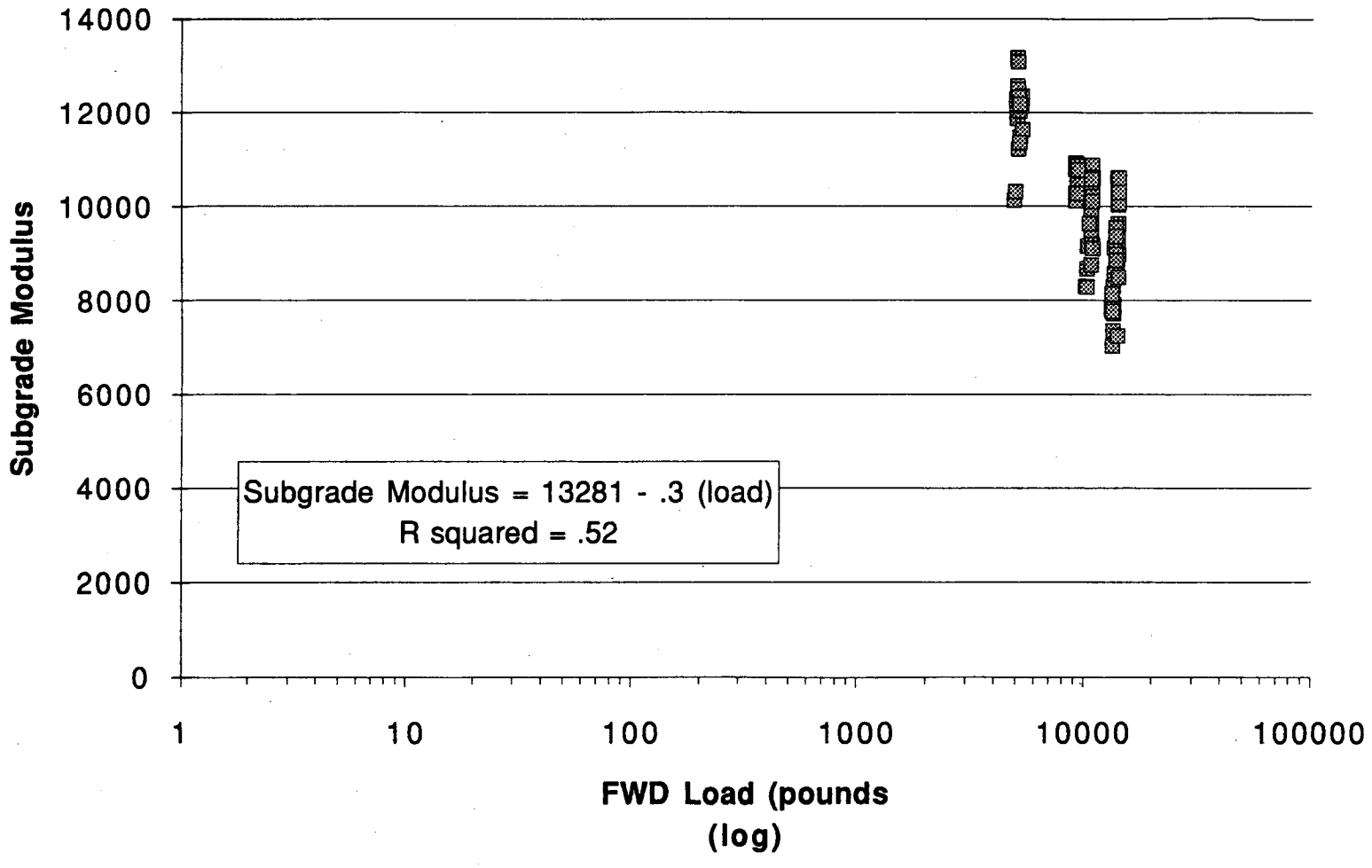

Figure 3.6 Subgrade Modulus vs. FWD Load—PACCAR Test Section

the AC and base layers at a given load, the regression fit can be regarded as horizontal (based on the coefficient of determination). This implies that the two variables (layer modulus and FWD load) are independent of each other. The subgrade modulus does show more sensitivity to load than the other two layers but not significantly.

In order to conduct further analysis of this potential influence of saturated soil conditions on backcalculated layer moduli, data from a pavement section with a known or suspected saturated subgrade condition was requested from the Washington State DOT (SR 525).

3.2 SR 525 Pavement Section

Since both the depth and stiffness of the "stiff layer" can strongly influence the backcalculated layer moduli (hence backcalculated strains in the pavement structure), further verification was sought that saturated conditions are significant. To do this, existing information on the SR 525 pavement section was used.

The field data for this pavement section consisted of FWD (Dynatest 8000) deflection basins and boring logs at Mileposts 1.70 and 2.45 (the location is near the Alderwood Mall in Lynnwood, Washington). This information was obtained from WSDOT production data associated with the normal pavement design process. The FWD testing was done on April 15, 1992, with a measured mid-depth AC temperature of 45° F. The condition of the AC layer was quite variable with various amounts of fatigue and longitudinal cracking, patching, and minor rutting. The boring logs (summaries of which are shown as Figure 3.7) indicated no specific water table but moist/wet conditions were encountered at about 3 feet (MP 1.70) and 2 feet (MP 2.45).

The stiff layer algorithm in EVERCALC estimated a stiff layer condition at a depth of 5.9 ft for MP 1.70. This depth coincides with a transition point from a medium dense sand (22 blows per ft measured by standard penetration test (SPT)) to a very dense sand (51 blows per ft). The calculated stiff layer for MP 2.45 was 5.0 ft which coincides

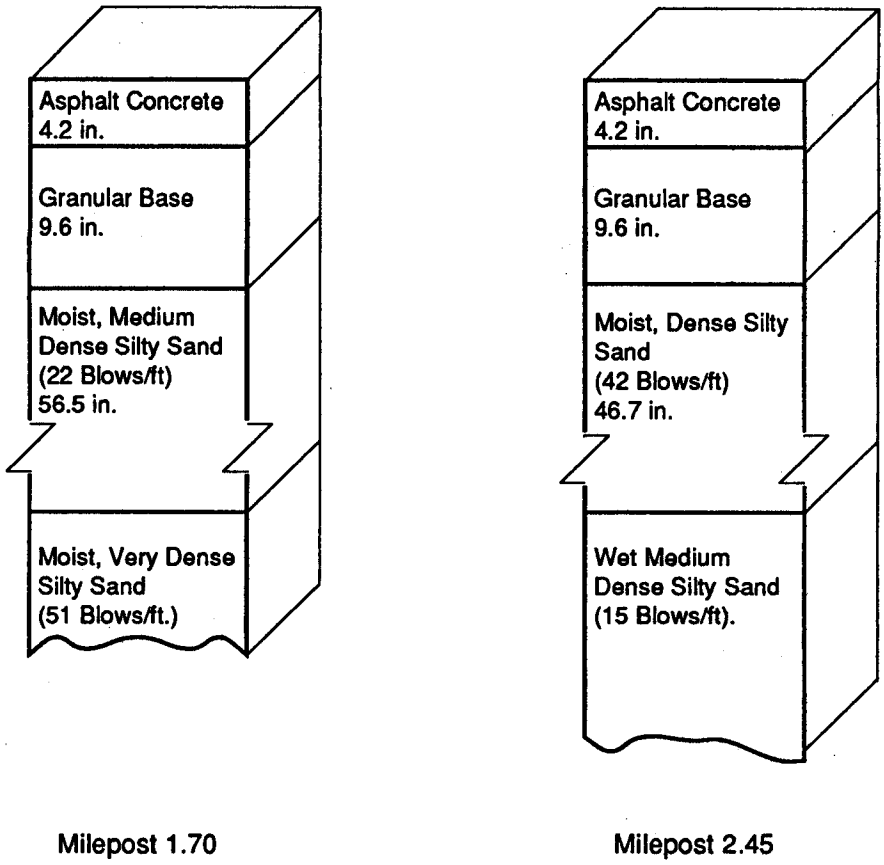

Figure 3.7 Cross-sections for SR 525 Pavement Sections, MP 1.70 and 2.45 [17]

with a transition from a moist, dense sand (42 blows per ft) to a wet, medium dense sand (15 blows per ft).

The backcalculated layer moduli, stiff layer moduli, and associated RMS values are shown in Table 3.6 for MP 1.70 and Table 3.7 for MP 2.45. The results for MP 1.70 appear to best match with the lower stiff layer modulus (50 ksi). An AC modulus of about 1500 ksi would be expected based on uncracked laboratory test conditions. The backcalculated AC modulus is within this range. Further, a visual inspection of the AC condition showed no cracking or rutting at this specific milepost. The base and subgrade moduli are reasonable with a low RMS level (1.0 percent average based on four deflection basins). The MP 2.45 section was quite different. The AC layer exhibited fatigue cracking and rutting, resulting in lower AC moduli. Overall, the lower stiff layer stiffness is preferred; however, the average RMS values (again, based on four deflection basins) are all rather high at this milepost.

Table 3.6. Sensitivity of Layer Moduli as a Function of Stiff Layer Modulus — SR 525 Pavement Section, MP 1.70

Pavement Layers	E_{stiff}	
	50 ksi	1000 ksi
Asphalt Concrete* (4.2 in)	1765 ksi	503 ksi
Crushed Stone Base* (9.6 in)	34 ksi	109 ksi
Subgrade* (56.5 in)	12.9 ksi	7.6 ksi
RMS(%)*	1.0	2.7

*Average of all runs

Table 3.7. Sensitivity of Layer Moduli as a Function of Stiff Layer Modulus — SR 525 Pavement Section, MP 2.45

Pavement LAYERS	E_{stiff}	
	50 ksi	1000 ksi
Asphalt Concrete* (4.2 in)	378 ksi	234 ksi
Crushed Stone Base* (9.6 in)	28 ksi	41 ksi
Subgrade* (46.7 in)	3.9 ksi	3.0 ksi
RMS(%)*	3.7	5.4

*Average of all runs

Only 50 ksi and 1000 ksi were used as stiff layer moduli for this pavement section. While 50 ksi provides much better results than 1000 ksi, 50 ksi may not be the optimal value for the stiff layer modulus. These two moduli values were selected only to demonstrate the potential importance of the influence of saturated soil conditions.

3.3 Backcalculation Observations

The analysis of these two sections (PACCAR and SR 525) illustrates and supports the following points:

- The stiff layer is important.
- The Rhode and Scullion [20] algorithm contained within the EVERCALC software provides a reasonable estimate of the depth to the stiff layer.
- The stiffness of the stiff layer appears to be influenced by saturated soil conditions as well as the more obvious reasons (such as rock, and stress sensitivity of the subgrade soils).

4. INSTRUMENTATION

4.1 Introduction

The following overviews the pavement instrumentation. Topics include the types of instruments acquired, their location in the test section, installation techniques, and the procedures used in data collection and reduction. A brief discussion of the initial validation testing is also presented.

4.2 Acquisition

The types of instruments acquired for installation in the test section were selected based on two parameters:

1. the data required to achieve the objectives of the research
2. installation requirements.

Because the instruments were to be installed in an existing pavement structure, this dictated that the instruments must be suitable for such an application.

Information was obtained from three sources:

- review of literature
- dialog with other pavement researchers
- staff of the PACCAR Technical Center.

Instruments were needed to measure the following pavement responses:

- longitudinal and transverse strain at the pavement surface
- longitudinal and transverse strain at the bottom of the AC layer
- shear strain at the pavement surface
- shear strain at the mid-depth of the AC layer
- deflection at the pavement surface
- deflection at the bottom of the AC layer
- deflection two inches below the top of the aggregate base
- deflection two inches below the top of the subgrade
- pavement temperature at various depths throughout the structure.

A foil-type gauge manufactured by Micro-Measurement was chosen to measure the various strain responses. An Australian-made Multidepth Deflectometer (MDD), used extensively by the Australian Road Research Board, with four linear variable differential transformers (LVDTs) and a piezoresistive accelerometer, was selected to measure pavement layer deflections. For temperature data, a multi-sensor thermistor-based temperature probe manufactured by Measurement Research Corporation was chosen.

4.3 Layout

A total of 102 (excluding temperature compensation gauges) of the foil-type strain gauges (hereafter referred to as strain gauges) and one MDD were installed in the pavement section. The measurement applications for the strain gauges are shown in Table 3.8. Each axial strain gauge is designated by a three element name. The first element represents the gauge number in the series of gauges at the same location in the AC layer and oriented in the same direction. The second element represents the gauge's location in the AC layer. An "S" represents the surface of the AC layer; a "B" the bottom of the AC layer. The third element identifies the orientation of the measurement

Table 3.8. Distribution of Strain Gauges—PACCAR Test Section

Type of Installation	Number of Locations	Number of Longitudinal Gauges per Location		Number of Transverse Gauges per Location		Number of Shear Gauges per Location	Total
		At Surface	At Bottom	At Surface	At Bottom		
Axial Core	5	1	1	1	1		20
Shear Core	10					2	20
Shear Slot	1					20	20
Independent Surface	4			1			4
Independent Surface	38	1					38
Totals	67						102

direction. An "L" represents the longitudinal direction; a "T" the transverse. An example is the gauge 3BL. This gauge is the third gauge which measures longitudinal strain at the bottom of the AC layer.

The shear slot gauges are also identified by a three element name. The first element represents the gauge number. The second and third elements for all these gauges are the letters "SS" which stand for "shear slot."

The shear core gauges have a two element name. The first element is the gauge number. The second element is an "S" for "shear". A complete list of all the gauge designations and their appropriate gauge location and measurement orientation is contained in Table 3.9.

The physical layout of these gauges at the test section is shown at Figure 3.8. The layout was designed to ensure the collection of critical pavement responses for both layer elastic and finite element analysis methods. The axial cores were displaced laterally to

Table 3.9. Description of Gauge Designations—PACCAR Test Section

Gauge Destination	Core Number	Gauge Location	Measurement Dimension
3ST	Axial Core 1	Surface of the AC	Transverse
3SL	Axial Core 1	Surface of the AC	Longitudinal
1BT	Axial Core 1	Bottom of the AC	Transverse
1BL	Axial Core 1	Bottom of the AC	Longitudinal
1ST	N/A	Surface of the AC	Transverse
1SL	N/A	Surface of the AC	Longitudinal
2ST	N/A	Surface of the AC	Transverse
2SL	N/A	Surface of the AC	Longitudinal
4ST	N/A	Surface of the AC	Transverse
4SL	N/A	Surface of the AC	Longitudinal
5ST	Axial Core 2	Surface of the AC	Transverse
5SL	Axial Core 2	Surface of the AC	Longitudinal
2BT	Axial Core 2	Bottom of the AC	Transverse
2BL	Axial Core 2	Bottom of the AC	Longitudinal
6ST	N/A	Surface of the AC	Transverse
6SL	N/A	Surface of the AC	Longitudinal
7ST	Axial Core 3	Surface of the AC	Transverse
7SL	Axial Core 3	Surface of the AC	Longitudinal
3BT	Axial Core 3	Bottom of the AC	Transverse
3BL	Axial Core 3	Bottom of the AC	Longitudinal
8SL	N/A	Surface of the AC	Longitudinal
9SL	N/A	Surface of the AC	Longitudinal
8ST	Axial Core 4	Surface of the AC	Transverse
10SL	Axial Core 4	Surface of the AC	Longitudinal
4BT	Axial Core 4	Bottom of the AC	Transverse
4BL	Axial Core 4	Bottom of the AC	Longitudinal
11SL	N/A	Surface of the AC	Longitudinal
12SL	N/A	Surface of the AC	Longitudinal
13SL	N/A	Surface of the AC	Longitudinal
14SL	N/A	Surface of the AC	Longitudinal
15SL	N/A	Surface of the AC	Longitudinal

Table 3.9. Description of Gauge Designations—PACCAR Test Section (Continued)

Gauge Destination	Core Number	Gauge Location	Measurement Dimension
16SL	N/A	Surface of the AC	Longitudinal
9ST	Axial Core 5	Surface of the AC	Transverse
17SL	Axial Core 5	Surface of the AC	Longitudinal
5BT	Axial Core 5	Bottom of the AC	Transverse
5BL	Axial Core 5	Bottom of the AC	Longitudinal
18SL	N/A	Surface of the AC	Longitudinal
19SL	N/A	Surface of the AC	Longitudinal
20SL	N/A	Surface of the AC	Longitudinal
21SL	N/A	Surface of the AC	Longitudinal
22SL	N/A	Surface of the AC	Longitudinal
23SL	N/A	Surface of the AC	Longitudinal
24SL	N/A	Surface of the AC	Longitudinal
25SL	N/A	Surface of the AC	Longitudinal
26SL	N/A	Surface of the AC	Longitudinal
27SL	N/A	Surface of the AC	Longitudinal
28SL	N/A	Surface of the AC	Longitudinal
29SL	N/A	Surface of the AC	Longitudinal
30SL	N/A	Surface of the AC	Longitudinal
31SL	N/A	Surface of the AC	Longitudinal
32SL	N/A	Surface of the AC	Longitudinal
33SL	N/A	Surface of the AC	Longitudinal
34SL	N/A	Surface of the AC	Longitudinal
35SL	N/A	Surface of the AC	Longitudinal
36SL	N/A	Surface of the AC	Longitudinal
37SL	N/A	Surface of the AC	Longitudinal
38SL	N/A	Surface of the AC	Longitudinal
39SL	N/A	Surface of the AC	Longitudinal
40SL	N/A	Surface of the AC	Longitudinal
41SL	N/A	Surface of the AC	Longitudinal
42SL	N/A	Surface of the AC	Longitudinal
43SL	N/A	Surface of the AC	Longitudinal

Table 3.9. Description of Gauge Designations—PACCAR Test Section (Continued)

Gauge Destination	Core Number	Gauge Location	Measurement Dimension
1S	Shear Core 1	Just Below Surface	Shear
2S	Shear Core 2	Just Below Surface	Shear
3S	Shear Core 3	Just Below Surface	Shear
4S	Shear Core 4	Just Below Surface	Shear
5S	Shear Core 5	Just Below Surface	Shear
6S	Shear Core 6	Just Below Surface	Shear
7S	Shear Core 7	Just Below Surface	Shear
8S	Shear Core 8	Just Below Surface	Shear
9S	Shear Core 9	Just Below Surface	Shear
10S	Shear Core 10	Just Below Surface	Shear
1SS	Shear Slot	Just Below Surface	Shear
2SS	Shear Slot	Just Below Surface	Shear
3SS	Shear Slot	Just Below Surface	Shear
4SS	Shear Slot	Just Below Surface	Shear
5SS	Shear Slot	Just Below Surface	Shear
6SS	Shear Slot	Just Below Surface	Shear
7SS	Shear Slot	Just Below Surface	Shear
8SS	Shear Slot	Just Below Surface	Shear
9SS	Shear Slot	Just Below Surface	Shear
10SS	Shear Slot	Just Below Surface	Shear

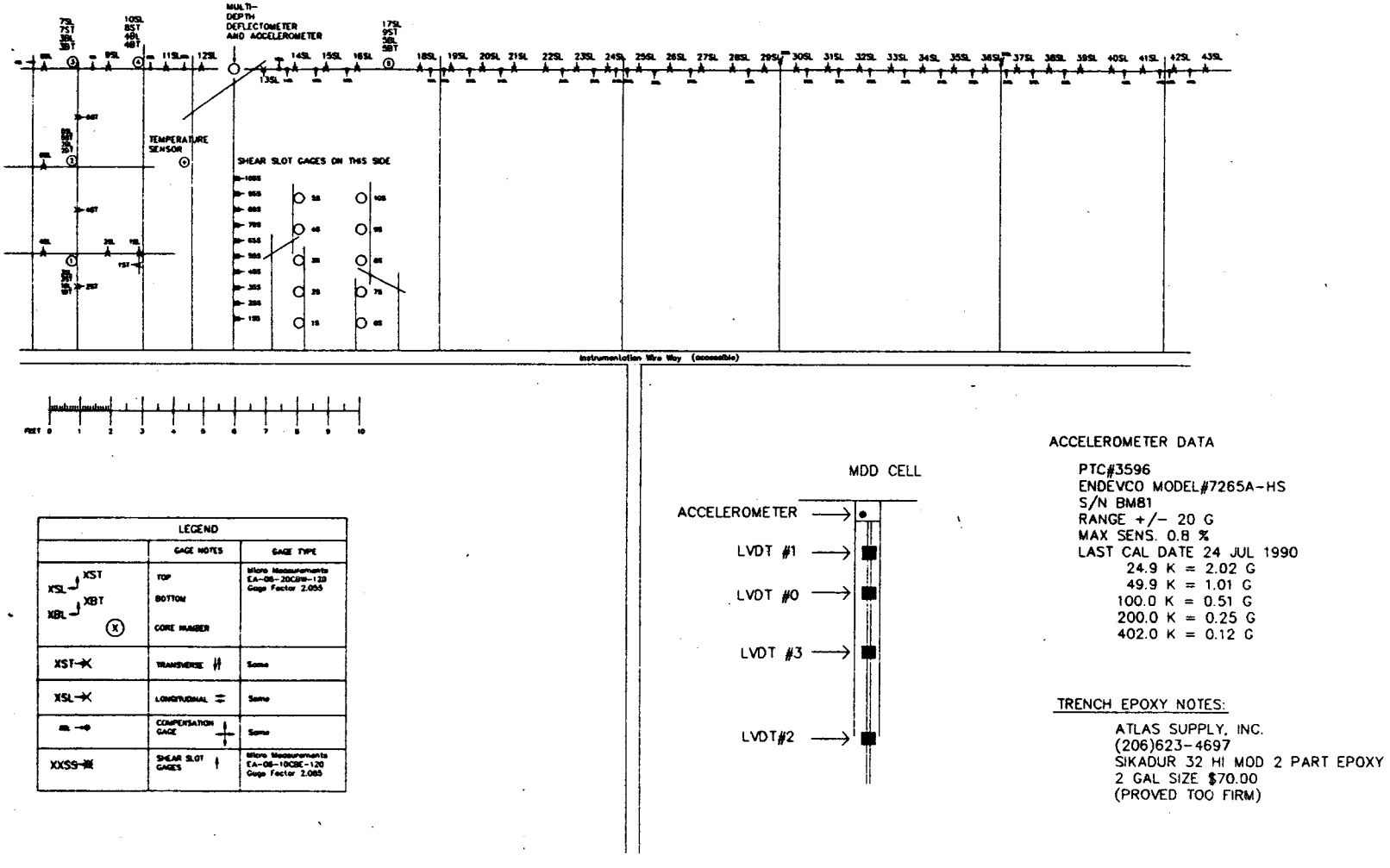

Figure 3.8 PACCAR Pavement Test Track Layout

allow collection of strain measurements from both wheel paths and the approximate centerline of the wheel base. The longitudinally oriented surface strain gauges were specifically designed to evaluate the dynamic response of a truck as it travels down the pavement section.

4.4 Installation

A four inch diameter core barrel was used to cut the 15 cores (5 axial, 10 shear) from the pavement section. These 15 core samples were used to perform the materials testing discussed earlier. The strain gauges were mounted on cores that were removed from the adjacent lane of the pavement section using a 4.5 inch core barrel. This procedure resulted in a clearance of only 1/16 of an inch between the sides of the core and the hole in the pavement. One quarter of an inch was cut off the top and bottom of the cores to provide a smooth surface for mounting the gauges. All pavement coring and cutting was performed by WSDOT.

4.4.1 Axial Strain Cores

A slot 1/8 inch wide by 1/4 inch deep was cut along the length of the core as a path for the necessary wiring (see Figure 3.9). Two gauges were glued to each end of the core using a thin layer of epoxy. These two gauges were in the same perpendicular plane and mounted at a 90 degree angle to each other forming an "L". One gauge measured transverse strain, the other longitudinal strain. Coring resulted in varying amounts of aggregate loss from the base course. The void resulting from this aggregate loss and reduced core thickness was filled with the same epoxy used to bond the core back to the pavement section. To ensure the epoxy completely filled the gap between the sides of the core and the hole in the pavement, the core was pushed into the hole until epoxy oozed up along the sides of the core. In most cases this caused the top of the core to be below the surface of the pavement and epoxy was also used to fill this void. As a result, the gauges mounted on the surface of the cores were actually underneath the epoxy layer on top of the core.

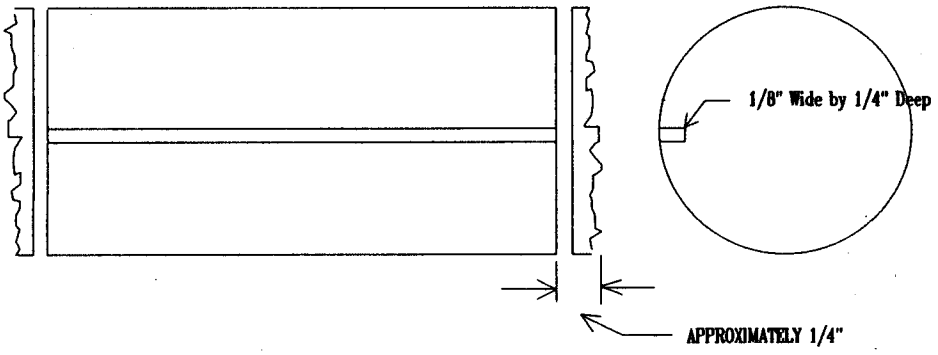

Figure 3.9 Saw Cutting Details for Axial Strain Cores

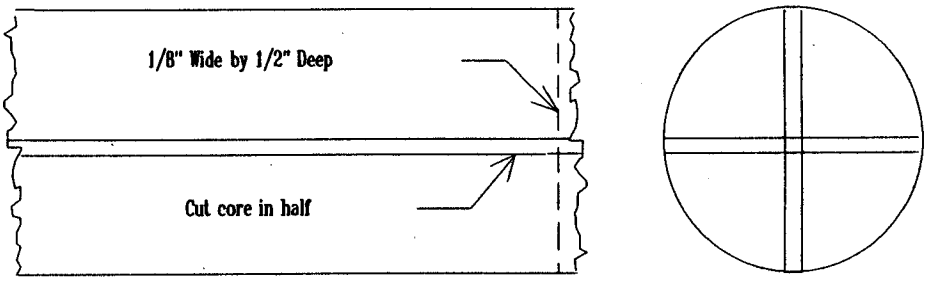

Figure 3.10 Saw Cutting Details for Shear Strain Cores

4.4.2 Shear Strain Cores

The cores were cut in half lengthwise to provide a mounting surface for the shear gauges. A slot 1/8 of an inch wide by 1/2 inch deep was cut across the diameter of the top of the core to provide a path for the lead wires (see Figure 3.10). The procedures used for gauge mounting and core installation were the same as those used for the axial cores. The only difference was that a layer of epoxy was placed between the two core halves just prior to their insertion into the hole in the pavement to bond them back together.

4.4.3 Shear Slot

A long slot shaped like an inverted "L" was cut perpendicular to the section from about the centerline to the shoulder of the pavement. The slot dimensions are shown in Figure 3.11. Epoxy was used to glue the shear gauges along the vertical face of the cut at six inch spacing. The lead wires were laid in the bottom of the slot and it was filled with epoxy.

4.4.4 Surface Gauges

A series of inverted "L" shaped slots were cut into the section for mounting the longitudinal and transverse surface gauges. The slot was formed by two cuts made side by side. One was 0.25 inch deep and 0.5 inch wide. The other was 0.5 inch wide by 1 inch deep (see Figure 3.12). The gauges were glued in a horizon position on the ledge formed by the width of the shallower cut. As in the shear slot, the lead wires were laid at the bottom of the slot and the slot was filled with epoxy.

4.4.5 Temperature Compensation Gauges

Temperature compensation gauges were installed in both axial strain cores and independent surface strain gauge applications. A separate strain gauge was embedded in a layer of room temperature vulcanization (RTV) silicon sealant and mounted on a strip of asphalt concrete. The RTV isolates the temperature compensation gauge from the bending in the AC caused by temperature. The active gauge and the temperature

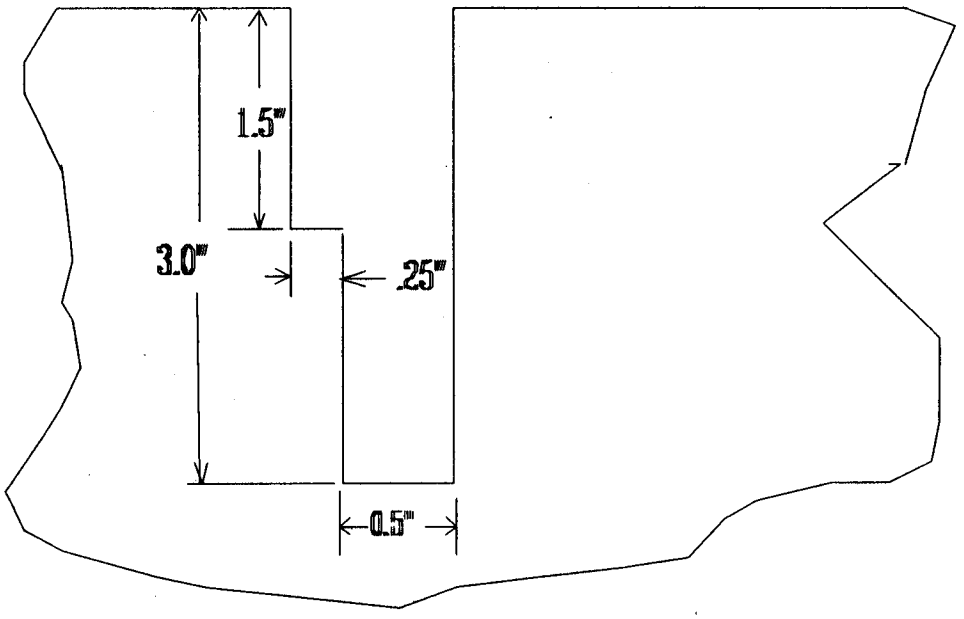

Figure 3.11 Shear Gauge Slot Dimensions

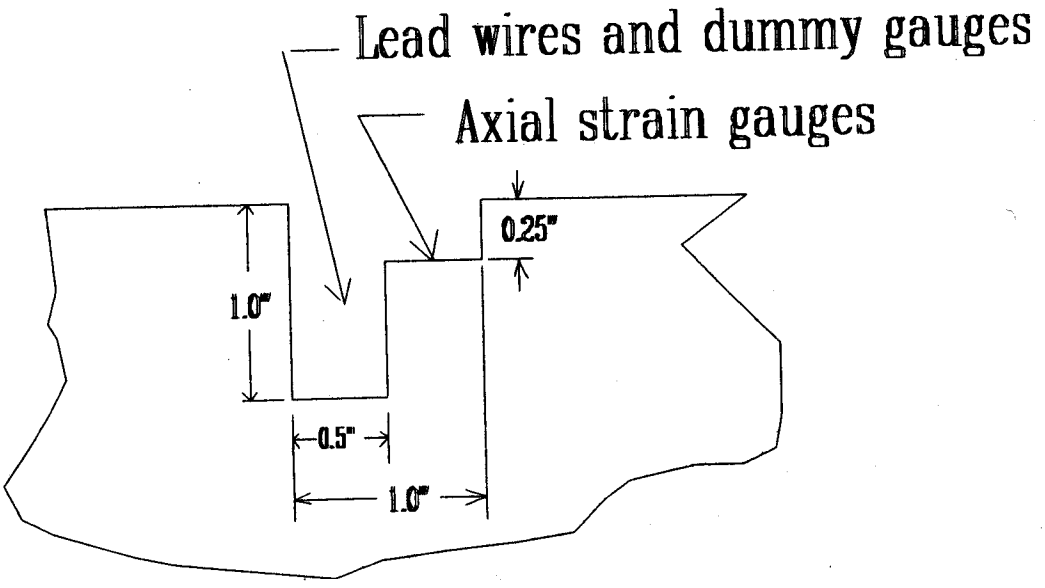

Figure 3.12 Surface Gauge Slot Dimensions

compensation gauge were connected to adjacent arms of the Wheatstone bridge circuit. Use of the two gauges cancels the voltage output from the active gauge due to bending caused by a temperature change in the AC. [43] One of these gauges was placed in the 1 inch slot parallel to each surface strain gauge. A temperature compensation gauge was also mounted in series with each of the four active gauges per axial strain core. This resulted in a total of eight gauges installed at each axial core (four active gauges, four temperature compensation gauges). The shear gauges used in both the shear slots and the shear cores were self compensating and did not require a temperature compensation gauge. The temperature compensation gauges also eliminated the non-linearity problems associated with completing only one arm of a Wheatstone bridge circuit.

4.4.6 Other Instruments

A temperature probe and multidepth deflectometer were also installed in the test section; however, due to data acquisition difficulties, this data was not collected. The thesis by Winters [5] contains installation details.

4.4.7 Wiring Slots and Electrical Panel

Numerous slots (0.5 inch wide by 1 inch deep) were cut parallel and perpendicular to the test section to accommodate the enormous amount of lead wires from all the gauges. At least one, and in some cases two, lead wire slots bisected the hole in the pavement formed by the core (see Figure 3.13). The slots must be cut after the cores are removed to prevent deformation of the core and to ensure proper alignment of the cut. These slots allowed all the wiring to be channeled into a metal conduit (6 inches wide x 2 inches deep x 40 inches long) running parallel to the section just inside the shoulder lane. The conduit is rectangular in shape and has a removable cover. From the conduit, all the lead wires terminate in an electrical panel mounted just off the shoulder of the section. The panel is inside a standard electrical cabinet mounted approximately 5 feet above the ground. All Wheatstone bridge circuits were completed at the panel. The panel also

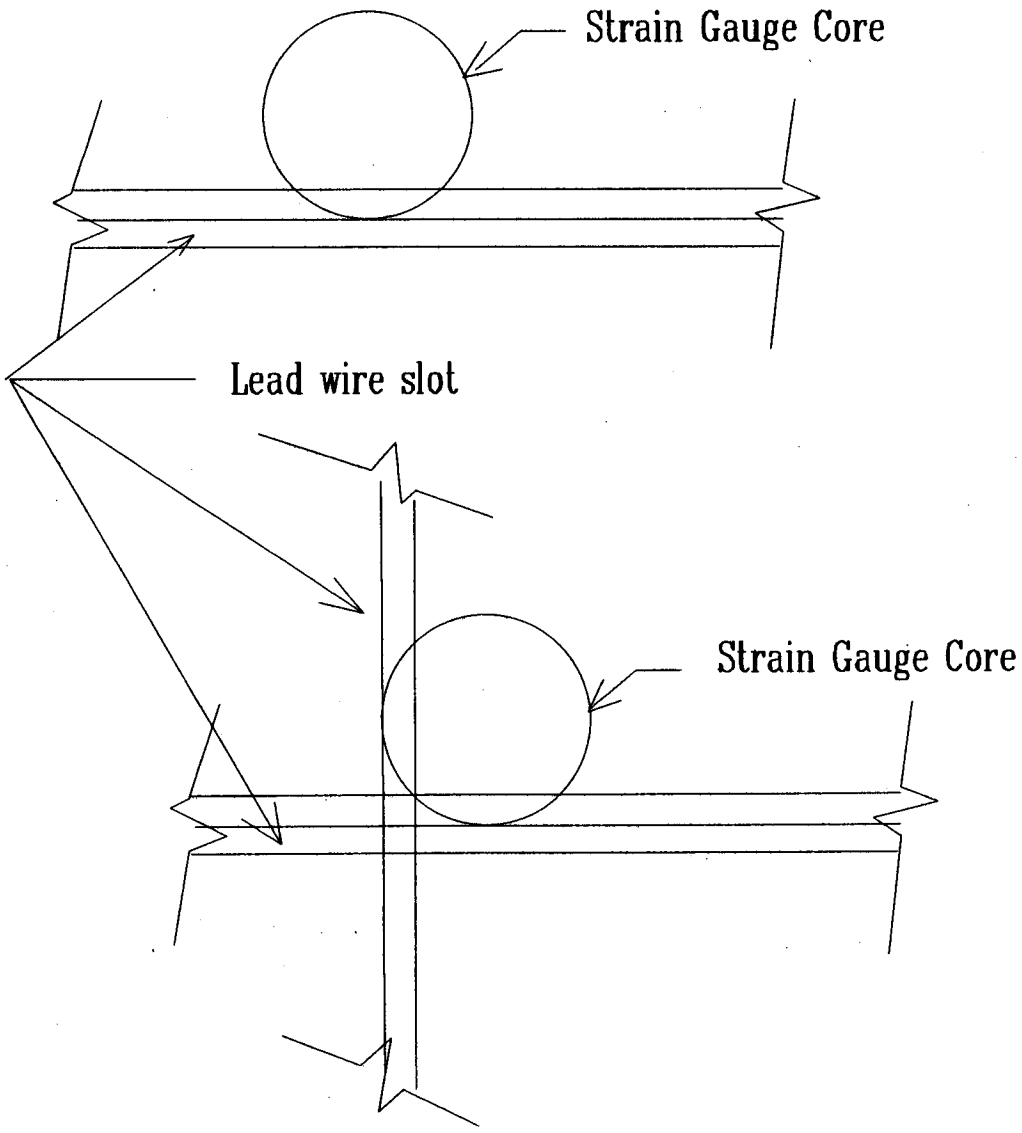

Figure 3.13 Plan View of Lead Wire Slots Bisecting Core Holes

provides the connectors for data collection instrumentation. The electrical panel layout is shown in Figure 3.14.

4.4.8 Epoxy

There were two types of epoxy used in gauge installation. One type was used to mount the gauges to the asphalt concrete, whether it was cores or slots, and the other was used to bond cores to the pavement or fill in slots cut in the pavement.

4.4.8.1 Gauge Epoxy. The epoxy used to glue the strain gauges to the AC was Micro-Measurement M-Bond AE-10. This epoxy system is designed for strain gauge applications [46]; however, the product manufacturer does not publish a modulus of elasticity for this adhesive. [47] The layer of epoxy between the gauge and AC surface is so thin that its effect on measured strain is probably insignificant, particularly in view of the other uncertainties in this measurement environment. The sensitivity of epoxy modulus to temperature is also unknown. Should these uncertainties become more important, laboratory testing could be used to establish the epoxy stiffness and temperature sensitivity.

4.4.8.2 Pavement Epoxy. The selection of this epoxy was critical. As mentioned earlier, the modulus of the epoxy should match that of the AC as closely as possible. Unfortunately, technical and research reports describing previous use of epoxy in instrumented pavement core applications did not provide any details on the specific type or material properties of the epoxy used. From discussions with the Turner-Fairbank Highway Research Center, they have recently used a 3M® Structural Epoxy; however, the modulus of this product is unknown.

After further research, Sikadur® 32 Hi Mod 2 part epoxy was chosen. Originally, it was understood that the modulus of this epoxy was 500 ksi (approximately the same modulus for Class B ACP at 72°F) and that value was used when calculating theoretical strain responses due to pavement loading. Near the end of this research, it was discovered that the actual modulus of this epoxy is 440 ksi under ideal mixing and curing

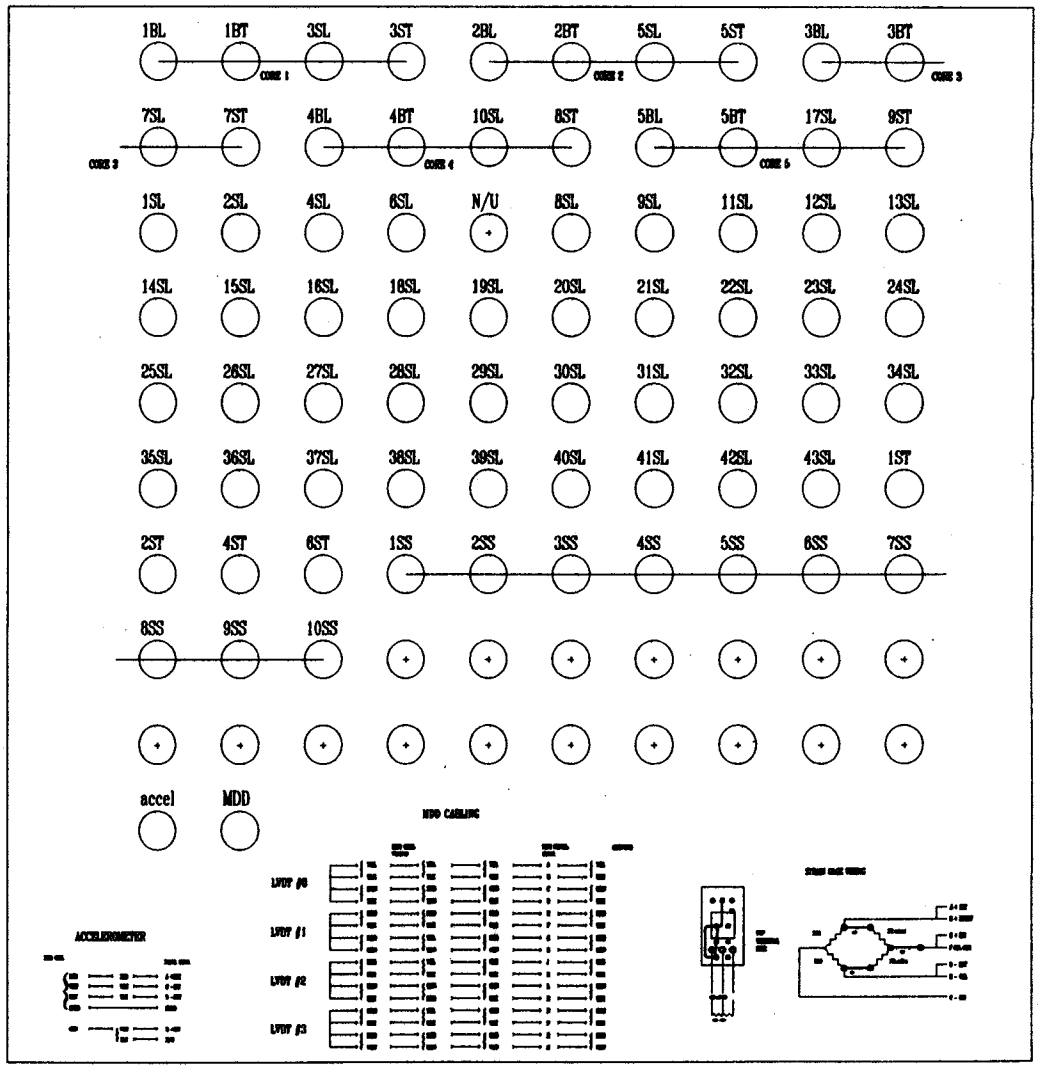

Figure 3.14 Electrical Panel Layout

conditions (73° F and 50 percent relative humidity). [48] It is known that the curing temperature ranged from 80 to 90°F; however, the relative humidity was unknown. The effect of these less than ideal conditions on the modulus of the epoxy is unknown. The modulus could be determined under laboratory testing but a comparison of the results to the in situ material would be uncertain. In order to duplicate the stiffness of the in situ material, the same proportions of the two components (as originally mixed) would have to be mixed under the same curing conditions. It is believed that this is both impractical and unnecessary. This will be discussed further. There was some minor cracking in the epoxy within the first few weeks of installation. This cracking was caused by an excessive volume of epoxy being used to fill the 4 inch diameter of the space above and below the core. [49] When the epoxy is used to anchor cylindrical objects, the hole diameter can not exceed .25 inch. [48] Exceeding this diameter causes "creep" which results in cracking. [49] The cracking stabilized almost immediately and no further problems have been experienced. Approximately 10 gallons of this epoxy were used throughout the section.

4.4.9 Data Acquisition and Signal Conditioning

The proper data acquisition system is the key to obtaining meaningful data. [39] Data acquisition and conditioning consist of three major components: hardware, software, and acquisition parameters.

Hardware consisted of various computers and signal conditioners. The following hardware was used during testing:

- Microcomputer (IBM compatible)
  - 80286 microprocessor
  - data acquisition board
  - fixed disk
  - serial/parallel port
  - multichannel analog-to-digital interface boards
  - color monitor

- Signal Conditioner
  - Signal conditioner mainframe
    Pacific Industries, PN # R16DC
  - Signal conditioner modules
    Pacific Industries, PN # 3210 (1 per channel)

The signal conditioner provides the excitation voltage for the gauge circuitry and amplifies the millivolt signal from the transducers to a voltage that can be more easily recorded and analyzed. A low pass (20 Hertz) filter was used in all data acquisition except during the February 1993 FWD testing. It was found that this filtering was a desirable method to reduce electrical noise.

The HEM Snapshot software package was used to control the hardware and acquire the data from the strain gauges. The software stores the data in a binary format but can be used to convert the binary format to ASCII. The signal from any gauge can also be displayed on the monitor immediately after collection. This very useful capability provides for immediate verification of signal quality and can help prevent acquisition of "problem" data. The software also appends appropriate "header" information (date, time, testing parameters) to the data file before writing to the fixed disk.

There are five basic parameters for data acquisition. The parameters and the associated values used in data collection are shown in Table 3.10.

Table 3.10. Summary of Data Acquisition Parameters

	Test Series			
Data Acquisition Parameter	October 1991 FWD Testing	May 1992 Truck Testing	June 1992 FWD Testing	February 1993 FWD Testing
Sample Rate (Hertz)	512	128, 256	512	512
Sweep Time (seconds)	4	10, 5	10	4
Voltage Range	± 1	± 1	± 1	± 1
Gain	1	5	5	5
Shunt Resistance (ohms)	100k	200k	200k	200k

5. INSTRUMENTATION VERIFICATION

5.1 Introduction

The following provides an overview of the extensive effort made to verify the accuracy of the installed instrumentation. Data collected during two series of FWD testing is analyzed and a comparison of measured to calculated strains is presented. A comparison is also made between measured longitudinal and transverse strains at the surface and bottom of the AC layer for one of the FWD tests. Because of their importance to mechanistic-empirical design, only strains measured by the axial cores in the wheel paths (Cores 1, 3, 4, and 5) will be presented. Core 2 is omitted due to its location (centerline of the section) and the inability to establish realistic effective layer thicknesses for the epoxy above and below the core.

5.2 General Procedure for Reduction and Conversion of Measured Strain Responses

When a load is applied to the pavement surface directly above a strain gauge, the pavement deflects under the load. This deflection causes the AC layer to bend which in turn causes the strain gauge to elongate and thus induces a change in its resistance. A Wheatstone bridge circuit is used to convert the change in resistance to a voltage signal that can be measured by the instrumentation discussed previously. The voltage is then converted to engineering units (microstrains) through the following steps.

1. A system calibration factor is determined by dividing the calibration strain value of the shunt resistor used to calibrate the measurement system by the voltage used to calibrate the system (shunt voltage).

2. A channel calibration factor for each channel is determined by taking the system calibration factor from Step 1 and dividing it by the calibration voltage of the bridge produced when the shunt resistance is applied to that channel.

3. The data series collected during a load application is then zeroed by subtracting a zero offset for each channel representing an average of the first forty data points from each individual data point. This type of zero procedure accounts for any "zero shift" in the data between initial system calibration and actual data collection.

4. Microstrains are then computed by multiplying the result of Step 3 by the channel calibration factor computed in Step 2. The resulting data series

can be plotted for a strain-time trace or the maximum strain value can be determined.

An example of this procedure for one channel is shown below where:

- calibration strain value of shunt resistor = 291.1 microstrains,
- system calibration voltage (shunt voltage) = .727 volts,
- channel calibration voltage = .772 volts,
- channel zero offset = .08 volts, and
- maximum voltage recorded under a 10k (pound) FWD load = .27 volts.

Step 1

$$\text{system calibration factor} = \frac{\text{calibration strain value of shunt resistor}}{\text{shunt voltage}}$$

$$= \frac{291.1 \text{ microstrains}}{.727 \text{ volts}}$$

$$\approx 400 \text{ microstrains / volt}$$

Step 2

$$\text{channel calibration factor} = \frac{\text{system calibration factor}}{\text{channel calibration voltage}}$$

$$= \frac{400 \text{ microstrains / volt}}{.772 \text{ volts}}$$

$$\approx 518 \text{ microstrains / volt}$$

Step 3

zeroed voltage = measured voltage channel zero offset
= .27 volts -.08 volts
= .19 volts

Step 4

measured strain under the FWD load channel calibration factor (zeroed voltage)

= 518 microstrains volt (.19 volts)
= 98 microstrains

The raw data was recorded in a binary format. Because Microsoft® Excel was used to perform the data reduction, the HEM Snapshot software was used to convert the data to an ASCII format so it could be read by Excel. Some of the data was also converted to ASCII using a basic program.

As noted by Sebaaly et al. [39], data conversion and reduction was a time consuming process. This is mainly due to the volume of data. Four seconds of data

collected during one FWD drop at one gauge represents 2000 data points. One data file consists of 16 times (16 channels) this amount of data (about 600k bytes).

While this data reduction and conversion process was automated, visual inspection and engineering judgment were used at critical stages of the analysis to ensure that the reduction and conversion process did not introduce any inaccuracies in the output.

5.3 FWD Testing—October 10, 1991

The WSDOT Dynatest FWD was used to conduct deflection testing over the entire test section. Testing was performed in a grid of 61 drop locations totaling 130 drops with more extensive testing on the five instrumented axial cores. As discussed previously, EVERCALC 3.3 was used to backcalculate layer moduli from the deflection data. It was decided that a stiff layer modulus of 40 ksi best represented the in situ conditions and as such was used in the backcalculation procedure. The layer moduli (mean values) presented earlier were used as representative of any location in the section (descriptive statistics are contained in Table 3.11).

Table 3.11. Descriptive Statistics for Backcalculated Layer Moduli—October 1991 FWD Testing

	Layer Modulus (psi)		
Pavement Layers	AC	Base	Subgrade
Mean*	562,800	14,800	10,200
Standard Deviation*	113,700	2,400	1,200
Minimum*	368,100	9,500	7,000
Maximum*	757,800	21,300	13,200
Number of Drops*	120	120	120

Notes:

* RMS <= 2.5%

Stiff Layer Modulus set at 40 ksi.

5.3.1 Effective Layer Thicknesses

The first step in analyzing the strain data collected during this testing was to model the effect that the epoxy above and below each core would have on the measured strains. It was determined that the most practical method to accomplish this would be to determine an effective thickness for each pavement layer based on the strains measured under FWD loading.

The original AC and base course thicknesses were accurately measured during coring and installation of the MDD. The approximate thicknesses of the epoxy on top of and below each core were also known, but needed to be refined because of the inability to physically measure the epoxy thicknesses. The effective layer thicknesses for axial Cores 1, 3, 4, and 5 are shown in Table 3.12. In all cases, the effective thickness of the AC layer is 4.9 inches. This was calculated by subtracting the 0.5 inch (0.25 removed from each end) trimmed from each core for gauge installation. The effective thicknesses of each epoxy layer were determined by varying the thickness of the epoxy on top of and below each core until the theoretical strain calculated from linear elastic theory (CHEVPC) was similar to the strain measured by the gauges installed in the pavement section. At Core 2, measured strains were only half of the calculated values with epoxy thicknesses modeled at 1.5 inches on top of the core and none below the core. These theoretical thicknesses are unrealistic given the known approximate thicknesses and as a result, no further analysis of Core 2 was conducted. The effective thickness of the base course was computed by subtracting the combined thicknesses of the AC and epoxy layers from the original thickness (13 inches). The total thickness of the top four layers was subtracted from the average depth to stiff layer for each core as predicted by EVERCALC to determine the subgrade thickness. A summary of the stiff layer depths for each axial core is contained in Table 3.13. It should be stressed that these are effective layer thicknesses for their respective location along the test section. It was not possible to physically validate these thicknesses without destroying the strain gauges.

Table 3.12. Effective Pavement Layer Thicknesses Based on October 1991 FWD Data—Axial Cores 1, 3, 4, and 5

Pavement Layers	Axial Core			
	1	3	4	5
Epoxy	0.4 in.	0.25 in.	0 in.	0.6 in.
AC	4.9 in.	4.9 in.	4.9 in.	4.9 in.
Epoxy	0.4 in.	1.25 in.	0.5 in.	0.6 in.
Base	12.7 in.	12.0 in.	13.0 in.	12.3 in.
Subgrade	42.7 in.	46.0 in.	46.1 in.	43.8 in.
Stiff Layer	Semi-Infinite	Semi-Infinite	Semi-Infinite	Semi-Infinite

Table 3.13. Summary of Calculated Depths to Stiff Layer Based on October 1991 WSDOT FWD Data—Axial Cores 1, 3, 4, and 5

Axial Core Number	Number of Drops at the Core	Average Depth to Stiff Layer ($\bar{x}$) (inches)	Standard Deviation (s) (inches)	Resulting Subgrade Thickness (inches)
1	10	61.1	1.2	42.7
3	5	64.4	1.1	46.0
4	2	64.5	1.9	46.1
5	4	62.2	1.8	43.8

5.3.2 Calculated Strains

As mentioned previously, the linear elastic program, CHEVPC, was used to calculate the theoretical strains under the various FWD loading conditions. The AC, base, and subgrade layer moduli (mean values) backcalculated by EVERCALC with a stiff layer modulus of 40 ksi were used as input to CHEVPC. The modulus of the Sikadur® epoxy was set at 500 ksi. While the exact modulus of the Sikadur® epoxy is unknown, 500 ksi is a reasonable assumption based on nondestructive test results and manufacturer's information. Strain calculated at the surface and bottom of the AC layer is a result of the compensating effect of the effective thickness and modulus of the epoxy. Given the procedure used to calculate the effective thickness of the epoxy, reducing the

modulus of the epoxy to 440 ksi (based on manufacturer's representation [48]) would only result in a potential increase in effective thickness. The computational assumptions of layered elastic analysis also contribute to the approximate nature of the calculation. Layered elastic analysis assumes that all pavement layers (including the epoxy layers above and below each core) extend laterally over the entire pavement section. The effect of this assumption should be minimal since the only calculated strains being evaluated are those actually above and below the layers of epoxy. Given these and other uncertainties in the measurement environment, it is believed that this difference in epoxy modulus is of minor concern. A summary of the layer characteristics used as input to CHEVPC is presented in Table 3.14.

5.3.3 Comparison of Measured and Calculated Strains

A comparative sample of the measured and calculated strains is shown in Table 3.15. Strains were measured at only three of the four gauges at each core. Due to the difficulty in matching the load data from each FWD drop to the corresponding measured strain data (these are two different data files from two different computer systems) the average load of all the same drop heights at each core was used to calculate the theoretical strain. A loss of measured strain data for Core 3 resulted in a comparison at drop height one only. As can be seen from the ratio of measured to calculated strains, the agreement is reasonable.

Table 3.14. Summary of Layer Characteristics Used as Input to CHEVPC—October 1991 FWD Testing

Pavement Layer	Layer Modulus (psi)	Poisson's Ratio
Epoxy	500,000	0.35
AC	562,800	0.35
Base	14,800	0.40
Subgrade	10,200	0.45
Stiff Layer	40,000	0.35

Table 3.15. Comparison of Measured and Calculated Strains from 1991 FWD Testing—PACCAR Test Station

AXIAL CORE	GAUGE	DROP HEIGHT	AVERAGED LOAD	MICROSTRAIN		RATIO (MEAS/CALC)
				MEASURED	CALCULATED	
1	1BL*	1	5109	130	120	1.08
1	1BL*	2	10785	240	253	0.95
1	1BL	3	14196	324	333	0.97
1	1BT	1	5109	120	120	1.00
1	1BT	2	10785	267	253	1.06
1	1BT*	3	14196	383	333	1.15
1	3ST	1	5109	-108	-109	0.99
1	3ST	2	10785	-202	-231	0.87
1	3ST	3	14196	-222	-303	0.73
3	3BL	1	5110	76	76	1.00
3	7SL	1	5110	-118	-101	1.17
3	7ST	1	5110	-71	-101	0.70
4	10SL	1	5268	-148	-142	1.04
4	10SL	2	10849	-304	-293	1.04
4	10SL	3	14099	-449	-381	1.18
4	4BL	1	5268	125	125	1.00
4	4BL	2	10849	256	257	1.00
4	4BL	3	14099	381	334	1.14
4	4BT	1	5268	122	125	0.98
4	4BT	2	10849	249	257	0.97
4	4BT	3	14099	348	334	1.04
5	17SL	1	5204	-82	-95	0.86
5	17SL	2	10718	-172	-196	0.88
5	17SL	3	13479	-231	-246	0.94
5	5BL	1	5204	104	106	0.98
5	5BL	2	10718	226	217	1.04
5	5BL	3	13479	276	274	1.01
5	5BT	1	5204	86	106	0.81
5	5BT	2	10718	172	217	0.79
5	5BT	3	13479	224	274	0.82

* The measured strain was extrapolated from a plot of strain vs. time.

Mean	0.97
Standard Dev.	0.12
n	30

A more detailed analysis is provided in Figures 3.15 through 3.18. These figures plot the calculated versus measured strains for the axial core surface longitudinal, surface transverse, bottom longitudinal, and bottom transverse gauges, respectively. These plots indicate that, in general, the best agreement between measured and calculated strains is found with the longitudinal gauges (surface and bottom). The surface transverse gauges show the least satisfactory agreement (although acceptable). The descriptive statistics representing the measured to calculated ratio for each gauge category (top or bottom of AC, longitudinal or transverse orientation) are shown in Table 3.16. The dispersion about the mean is relatively consistent across gauge type. Since horizontal tensile strain at the bottom of the AC layer (as measured by the BL gauges) is a critical pavement response for mechanistic-empirical design, the performance of the BL gauge type is particularly noteworthy.

Measured to calculated ratios were also grouped for all gauges by drop height (Table 3.17) and core number (Table 3.18) for analysis. A review of these statistics shows relatively consistent performance across all drop heights and all cores.

5.4 FWD Testing—February 3, 1993

5.4.1 Backcalculation of Layer Moduli

The deflection data collected by the WSDOT FWD was used to backcalculate layer moduli using EVERCALC 3.3. This series of tests was only conducted over axial Cores 1, 3, 4, and 5. There were three drops at each of three drop heights (1, 2, and 4) per core. The intent was to backcalculate a set of layer moduli for each of the cores tested. Unfortunately, the deflection data for Cores 3 and 4 was lost due to a computer file problem. The resulting data base consisted of 18 deflection basins. To make maximum use of the measured strain data, the layer moduli backcalculated for Core 5 were used for analysis of Cores 3 and 4. The decision was based on the fact that Cores 3, 4, and 5 are on the same longitudinal line in the section and realistic moduli were calculated for the entire section from the October 1991 data based on a 61 location grid.

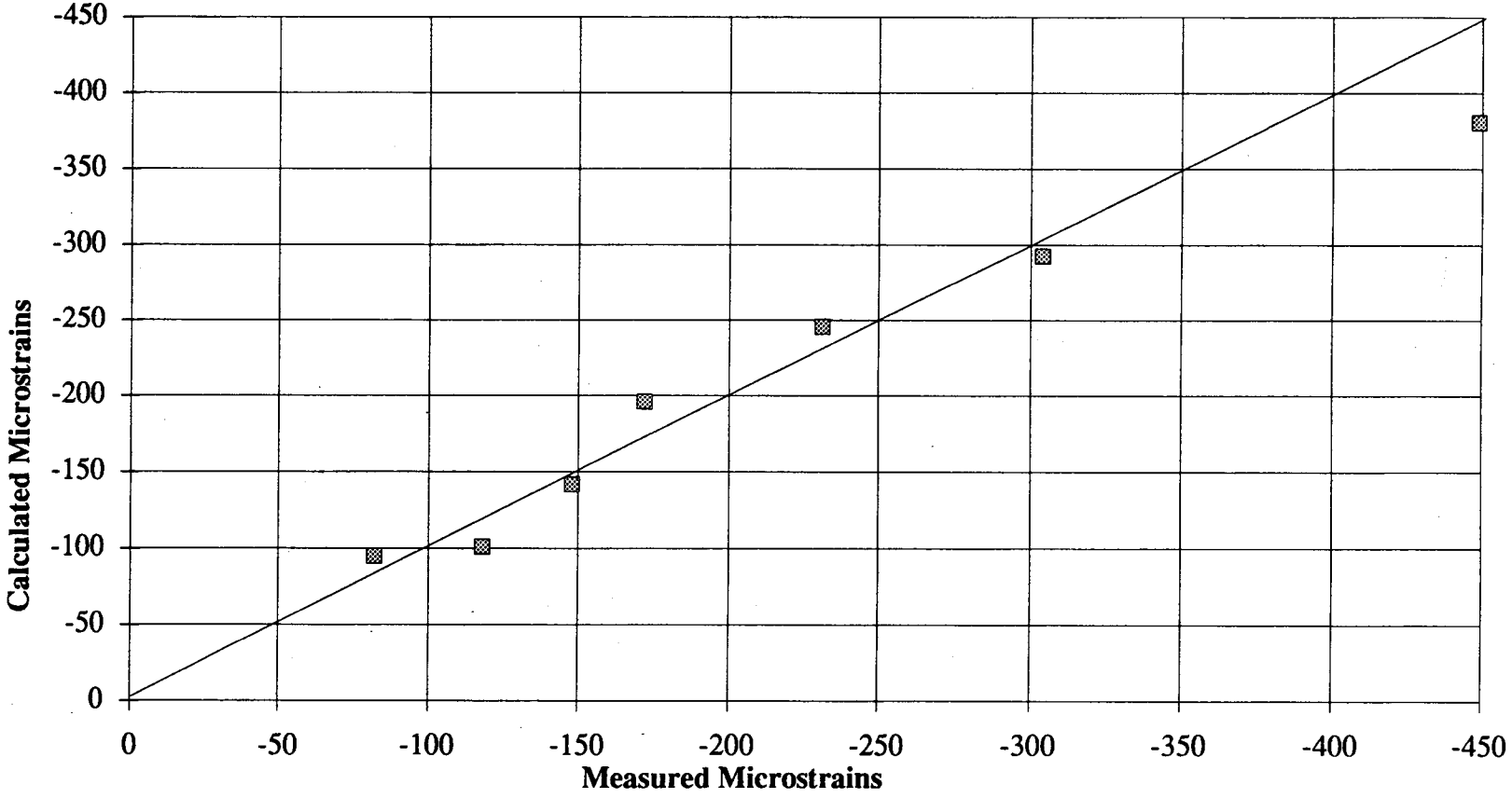

Figure 3.15 Measured vs. Calculated Strain For Axial Core Surface Longitudinal Gauges—October 1991 FWD Testing

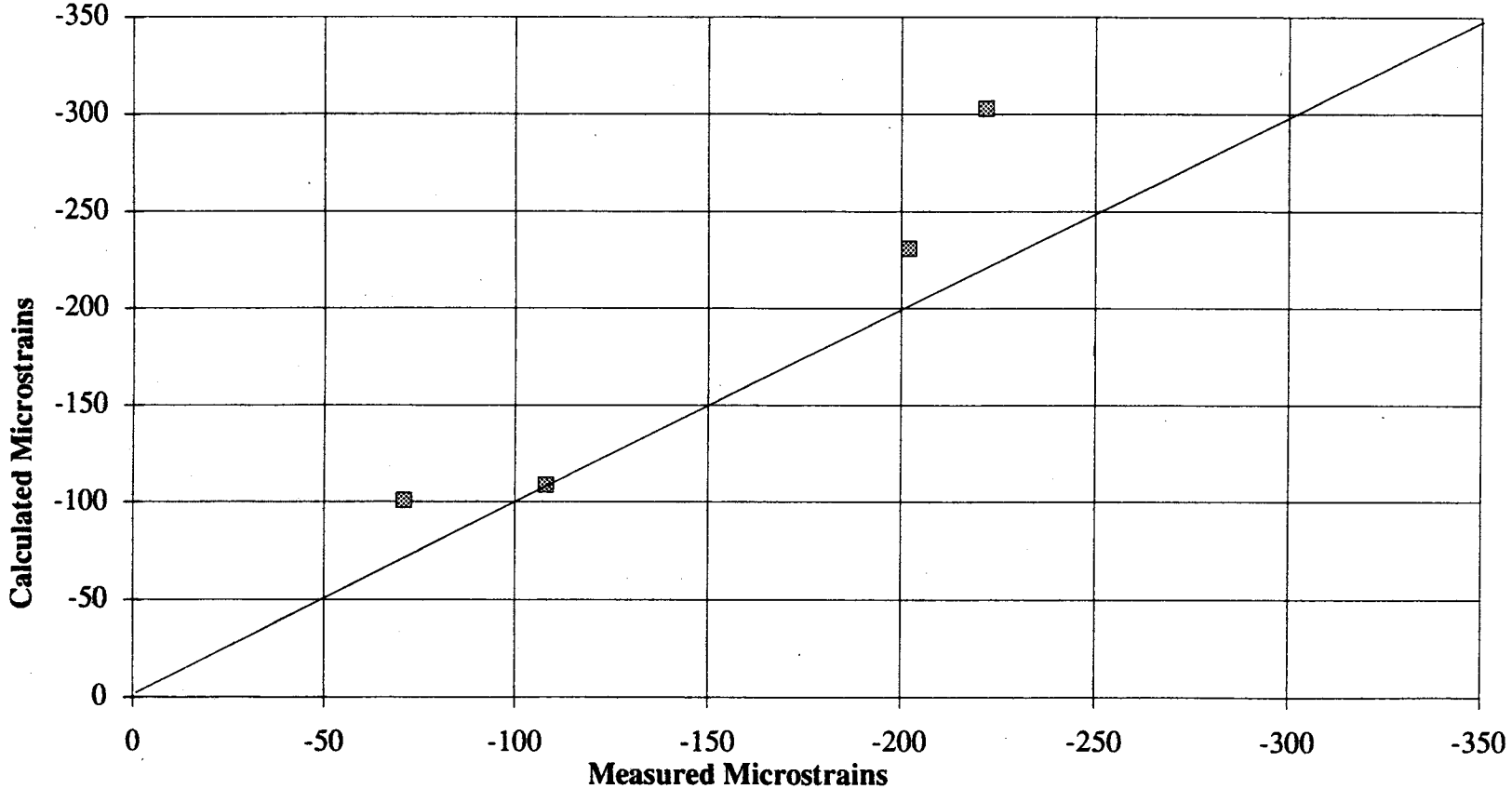

Figure 3.16 Measured vs. Calculated Strain For Axial Core Surface Transverse Gauges—October 1991 FWD Testing

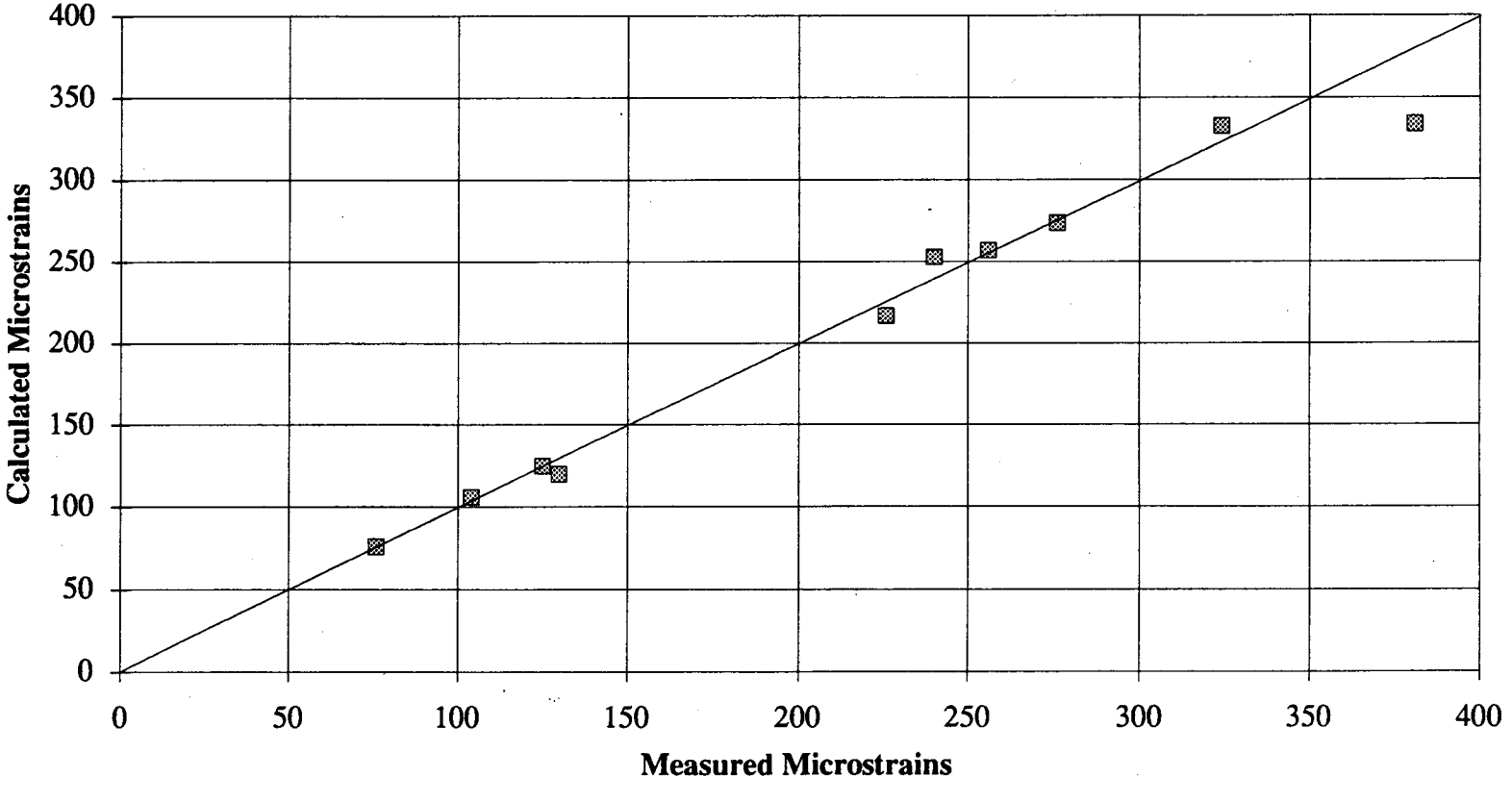

Figure 3.17 Measured vs. Calculated Strain For Axial Core Bottom Longitudinal Gauges—October 1991 FWD Testing

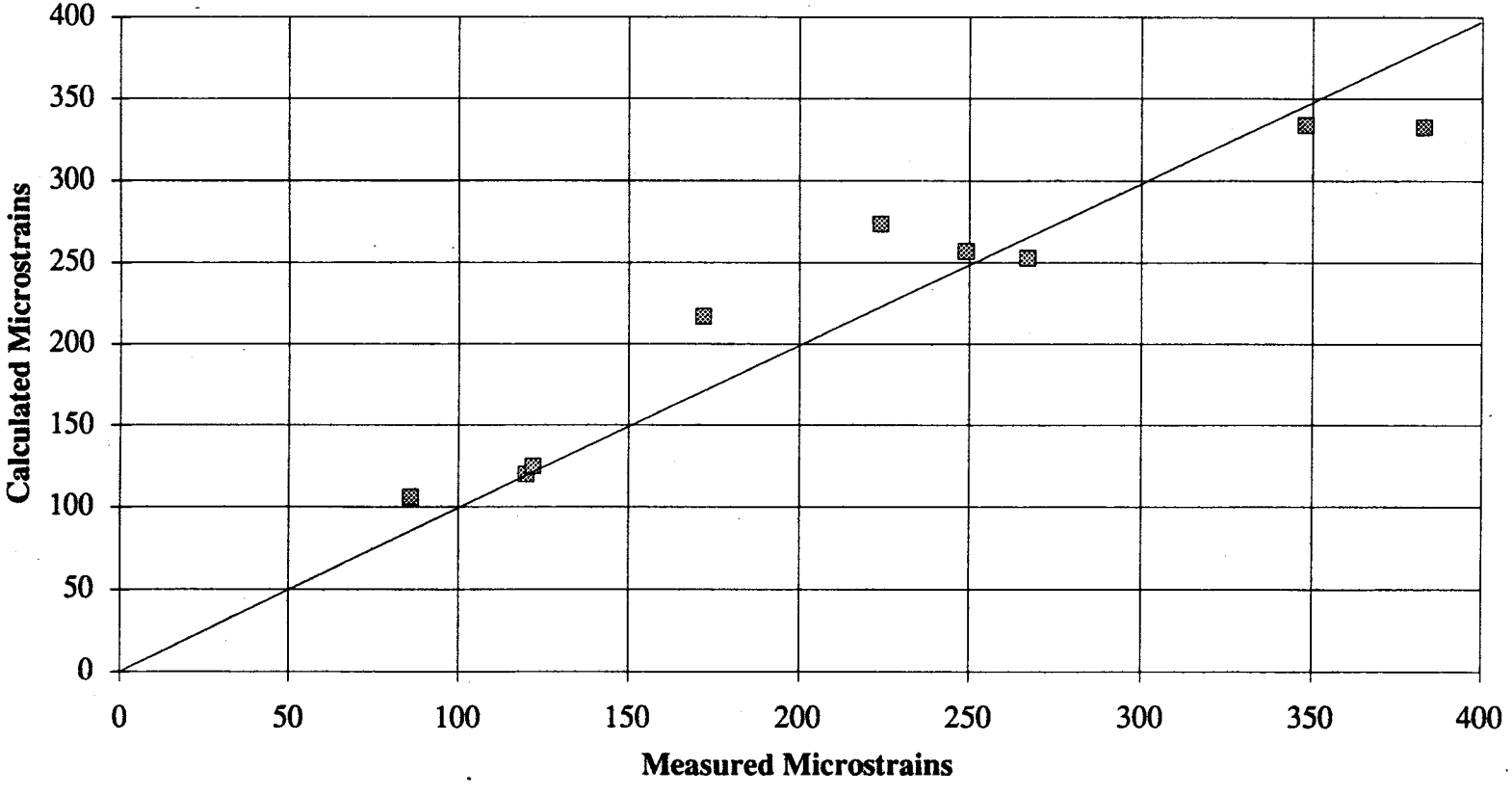

Figure 3.18 Measured vs. Calculated Strain For Axial Core Bottom Transverse Gauges—October 1991 FWD Testing

Table 3.16. Summary of Layer Characteristics Used as Input to CHEVPC—October 1991 FWD Testing

Measured to Calculated Ratio	Gauge Type			
	SL	ST	BL	BT
Mean	1.02	0.83	1.02	0.96
Standard Deviation	0.13	0.13	0.06	0.12
Minimum	0.86	0.70	0.95	0.79
Maximum	1.18	0.99	1.14	1.15
Sample Size	7	4	10	9

Table 3.17. Descriptive Statistics for Measured to Calculated Strain Ratios by Drop Height—October 1991 FWD Testing

Measured to Calculated Ratio	FWD Drop Height		
	1 (5 ksi)	2 (10 ksi)	3 (14 ksi)
Mean	0.97	0.95	1.00
Standard Deviation	0.12	0.09	0.15
Minimum	0.70	0.79	0.73
Maximum	1.17	1.06	1.18
Sample Size	12	9	9

Table 3.18. Descriptive Statistics for Measured to Calculated Strain Ratios by Core—October 1991 FWD Testing

Measured to Calculated Ratio	Axial Core			
	Core 1	Core 3	Core 4	Core 5
Mean	0.98	0.96	1.04	0.90
Standard Deviation	0.12	0.24	0.07	0.09
Minimum	0.73	0.7	0.97	0.79
Maximum	1.15	1.17	1.18	1.04
Sample Size	9*	3**	9*	9*

Notes:
* Based on 3 drops at 3 gauges.
** Based on 1 drop at 3 gauges.

The applied load varied from 6050 to 17,880 pounds. Sensor spacings, layer thicknesses, and Poisson's ratios were the same as those used when backcalculating the October 1991 data. The measured temperature of the AC layer at a depth of 2 inches was 46° F at the start of testing and 43° F at the conclusion of testing (air temperatures were 47° F and 44° F, respectively).

Initially, the stiff layer modulus was set at 40 ksi. The resulting layer moduli were unsatisfactory in that the AC and base moduli were too high and low, respectively (refer to Table 3.19.). A value of 50 ksi resulted in more realistic layer moduli with similar RMS error convergence. All the deflection basins (40 and 50 ksi stiff layer) resulted in an RMS error convergence of 1.7 percent or less. The mean values for the AC modulus were 1,575 ksi for Core 1 and 1,510 ksi for Core 5. This is remarkably close to the laboratory value of 1,490 ksi for Class B ACP at 45° F. A summary of the resulting layer moduli and RMS statistics is shown in Tables 3.19 to 3.21.

5.4.2 Effective Layer Thicknesses

The only layer thicknesses that were changed for analysis of this data were the subgrade thicknesses. The subgrade thickness was determined by evaluating the calculated depth to stiff layer in the same manner as was done for the October 1991 data. Since there was no available information to determine the subgrade thickness for Cores 3 and 4, and the difference between the calculated depth for Cores 1 and 5 was generally the same for both testing periods (1.1 inches in October; 1.3 inches in February), the subgrade thicknesses for Cores 3 and 4 were based on this same relationship. A summary of the stiff layer depths (and resulting subgrade thicknesses) is contained in Table 3.22. It is interesting to note that the calculated depth to stiff layer is about 14 inches deeper in February 1993 than calculated in October 1991 (as calculated by EVERCALC). This is indirectly supported by the fact that rainfall in the 13 months preceding the February testing was approximately 7 inches below normal. [50]

Table 3.19. Sensitivity of Layer Moduli as a Function of the Stiff Layer Modulus — PACCAR Test Section, February 1993 FWD Testing

Pavement Layers	E_{stiff}			
	Core 1		Core 5	
	40 ksi	50 ksi	40 ksi	50 ksi
Asphalt Concrete* (ksi)	1,874	1,576	1,949	1,510
Crushed Stone Base* (ksi)	11	20	13	27
Fine-grained Subgrade* (ksi)	14	11	18	13

*All runs resulted in a RMS% <=1.7%.

Table 3.20. Sensitivity of RMS Values as a Function of the Stiff Layer Modulus — PACCAR Test Section, February 1993 FWD Testing

RMS (%)	E_{stiff}	
	40 ksi	50 ksi
Mean*	1.1	1.2
Standard Deviation*	0.3	0.3
Minimum*	0.6	0.7
Maximum*	1.5	1.7
Total Runs with RMS% <=1.7*	18	18

*Calculated for 18 deflection basins.

Table 3.21. Descriptive Statistics for Backcalculated Layer Moduli—February 1993 FWD Testing

Pavement Layer Moduli (psi)	Axial Core Number					
	Core 1			Core 5		
	AC	Base	Subgrade	AC	Base	Subgrade
Mean	1,575,700	20,300	10,700	1,510,300	27,500	13,400
Standard Deviation	197,300	4,000	400	128,600	1,800	501
Minimum	1,351,800	14,800	10,200	1,339,500	24,900	12,601
Maximum	1,832,300	25,600	11,000	1,679,000	30,200	13,742
Number of Drops	9	9	9	9	9	9

Note: Stiff Layer Modulus set at 50 ksi.

Table 3.22. Summary of Calculated Depths to Stiff Layer Based on February 1993 FWD Data — Axial Cores 1, 3, 4, and 5

Axial Core Number	Depth to Stiff Layer ($\bar{x}$) (inches)	Resulting Subgrade Thickness (inches)
1	75.5	57.1
3	78.8*	60.4
4	78.9*	60.5
5	76.8	58.4

* Based on relationship established between Cores 1 and 5 from October 199 FWD Data.

Table 3.23. Summary of Layer Characteristics Used as Input to CHEVPC— February 1993 FWD Testing

Pavement Layer	Core 1		Cores 3, 4, and 5	
	Layer Modulus (psi)	Poisson's Ratio	Layer Modulus (psi)	Poisson's Ratio
Epoxy	500,000	0.35	500,000	0.35
AC	1,575,700	0.35	1,510,300	0.35
Base	20,300	0.40	27,500	0.40
Subgrade	10,700	0.45	13,400	0.45
Stiff Layer	50,000	0.35	50,000	0.35

The epoxy thicknesses were not changed for two reasons. First, it was felt that the data collected in October 1991 matched the in situ relationship between gauge, epoxy, and AC more closely—at least chronologically. Second, this allows for a more direct comparison between the two tests.

5.4.3 Calculated Strains

The theoretical strains were calculated using the same procedure as for the October 1991 data. Table 3.23 summarizes the layer characteristics used as input to

CHEVPC. The stiff layer modulus of 50 ksi was used due to the resulting AC modulus, even though the RMS error was slightly larger (0.1 percent).

5.4.4 Comparison of Measured and Calculated Strains

In this test series, strains were measured at all four gauges at each core. The averaged FWD loads for each drop height at each core were used for Cores 1 and 5. Since this data was missing for Cores 3 and 4, the average of the loads used for Cores 1 and 5 was used for Cores 3 and 4. A comparison of the measured and calculated strains is shown in Table 3.24. With a few exceptions, the agreement is within reasonable limits.

A plot of the calculated versus measured strain for the surface longitudinal, surface transverse, bottom longitudinal, and bottom transverse gauges is contained in Figures 3.19 to 3.22, respectively. In general, the best agreement is found with the bottom gauges (longitudinal and transverse). The descriptive statistics representing the measured to calculated ratio for each gauge type are shown in Table 3.25. Dispersion about the mean is generally consistent excluding the BT gauges which show more variability. The agreement between measured and calculated strains is acceptable for all gauge types except the ST gauges. While the standard deviation is modest, the mean value is too low. A possible explanation for this poor agreement is the misalignment of the FWD load plate over the cores. If the load plate was not centered over the cores one would expect the effect of this misalignment to dissipate with depth. In fact, the mean value of the measured to calculated ratio for both surface gauges is substantially lower than that of the bottom gauges.

Table 3.26 shows relatively consistent agreement across all three drop heights. When the measured to calculated ratios are compared across cores (Table 3.27), Core 4 indicates poor agreement. The reason for this is unknown. It is unlikely that any of the assumptions made regarding depth to stiff layer or layer moduli could have affected the agreement. The assumptions appear reasonable for Core 3, and Cores 3 and 4 are only 2 feet apart.

Table 3.24. Comparison of Measured and Calculated Strains from February 1993 WSDOT FWD Testing—PACCAR Test Section

GAUGE	DROP HEIGHT	AVERAGED LOAD	MICROSTRAIN		RATIO (MEAS/CALC)
			MEASURED	CALCULATED	
1BL	1	6205	71	79	0.90
1BL	2	10753	99	138	0.72
1BL	4	17614	171	226	0.76
1BT	1	6205	91	79	1.15
1BT	2	10753	162	138	1.17
1BT	4	17614	253	226	1.12
3SL	1	6205	-46	-73	0.63
3SL	2	10753	-81	-126	0.64
3SL	4	17614	-122	-208	0.59
3ST	1	6205	-62	-73	0.85
3ST	2	10753	-100	-126	0.79
3ST	4	17614	-153	-208	0.74
3BL	1	6160	68	60	1.13
3BL	2	10660	125	105	1.19
3BL	4	17730	205	175	1.17
3BT	1	6160	70	60	1.17
3BT	2	10660	131	105	1.25
3BT	4	17730	212	175	1.21
7SL	1	6160	-63	-66	0.95
7SL	2	10660	-90	-114	0.79
7SL	4	17730	-164	-190	0.86
7ST	1	6160	-35	-66	0.53
7ST	2	10660	-44	-114	0.39
7ST	4	17730	-85	-190	0.45
4BT	1	6160	61	76	0.80
4BT	2	10660	106	131	0.81
4BT	4	17730	151	218	0.69
10SL	1	6160	-53	-77	0.69
10SL	2	10660	-97	-133	0.73
10SL	4	17730	-155	-221	0.70
8ST	1	6160	-49	-77	0.64
8ST	2	10660	-99	-133	0.74
8ST	4	17730	-153	-221	0.69
5BL	1	6114	89	69	1.29

Table 3.24. Comparison of Measured and Calculated Strains from February 1993 WSDOT FWD Testing—PACCAR Test Section (Continued)

GAUGE	DROP HEIGHT	AVERAGED LOAD	MICROSTRAIN		RATIO (MEAS/CALC)
			MEASURED	CALCULATED	
5BL	2	10563	114	119	0.96
5BL	4	17853	188	200	0.94
5BT	1	6114	119	69	1.72
5BT	2	10563	156	119	1.31
5BT	4	17853	233	200	1.17
17SL	1	6114	-54	-62	0.87
17SL	2	10563	-120	-107	1.12
17SL	4	17853	-164	-181	0.91
9ST	1	6114	-44	-62	0.71
9ST	2	10563	-98	-107	0.92
9ST	4	17853	-145	-181	0.80
				Mean	0.90
				Standard Dev.	0.26
				n	48

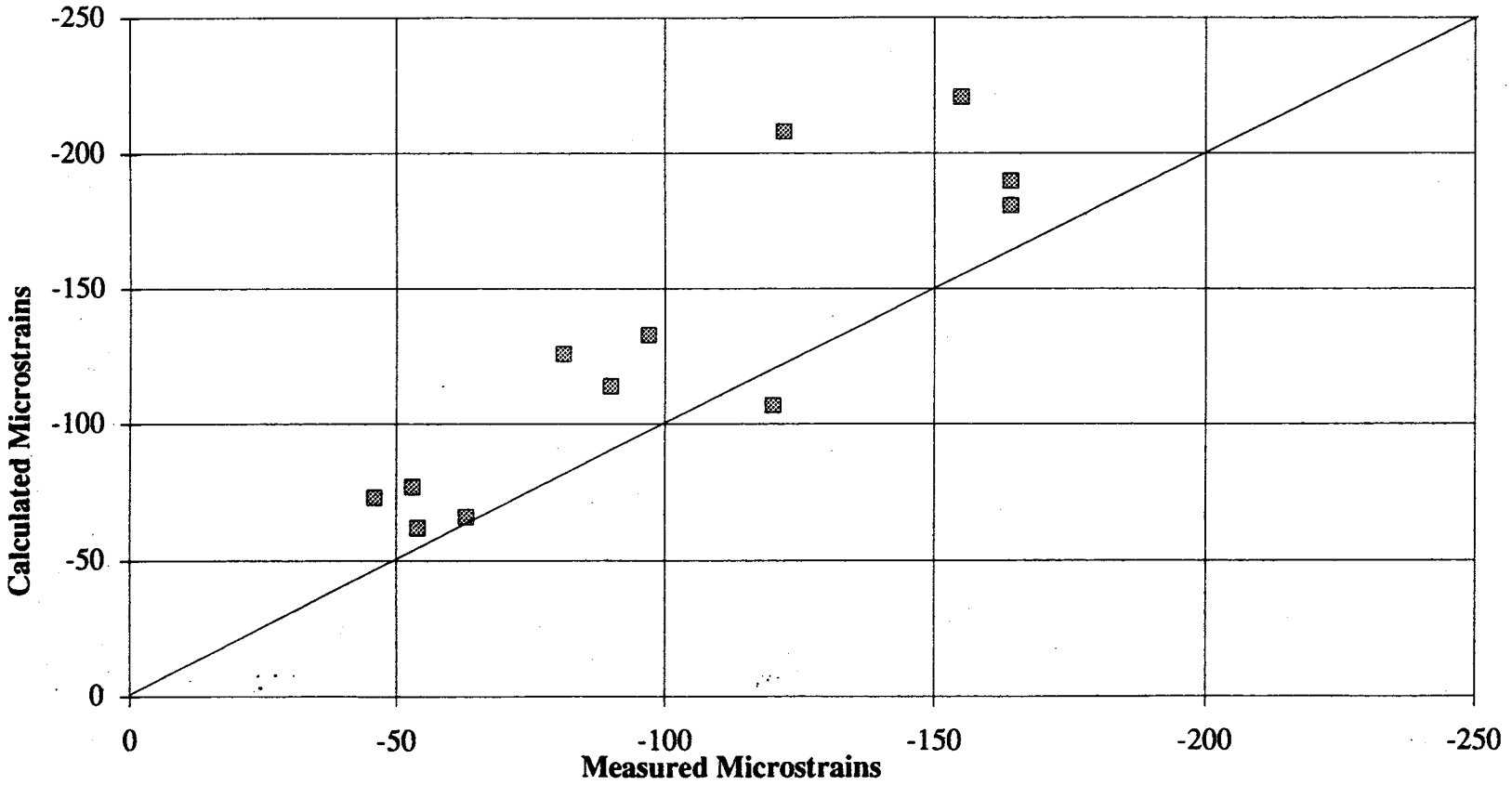

Figure 3.19 Measured vs. Calculated Strain For Axial Core Surface Longitudinal Gauges—February 1993 FWD Testing

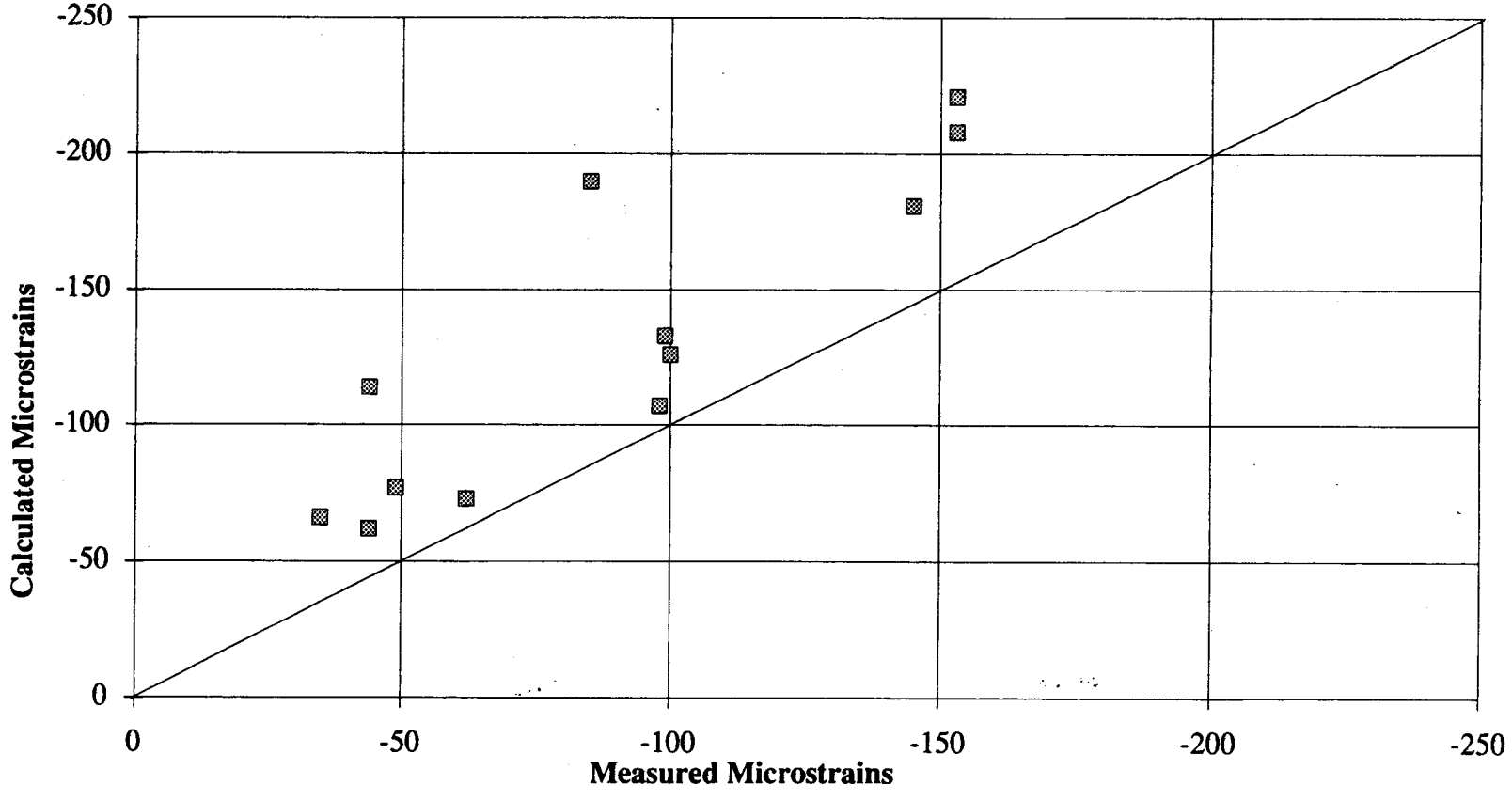

Figure 3.20 Measured vs. Calculated Strain For Axial Core Surface Transverse Gauges—February 1993 FWD Testing

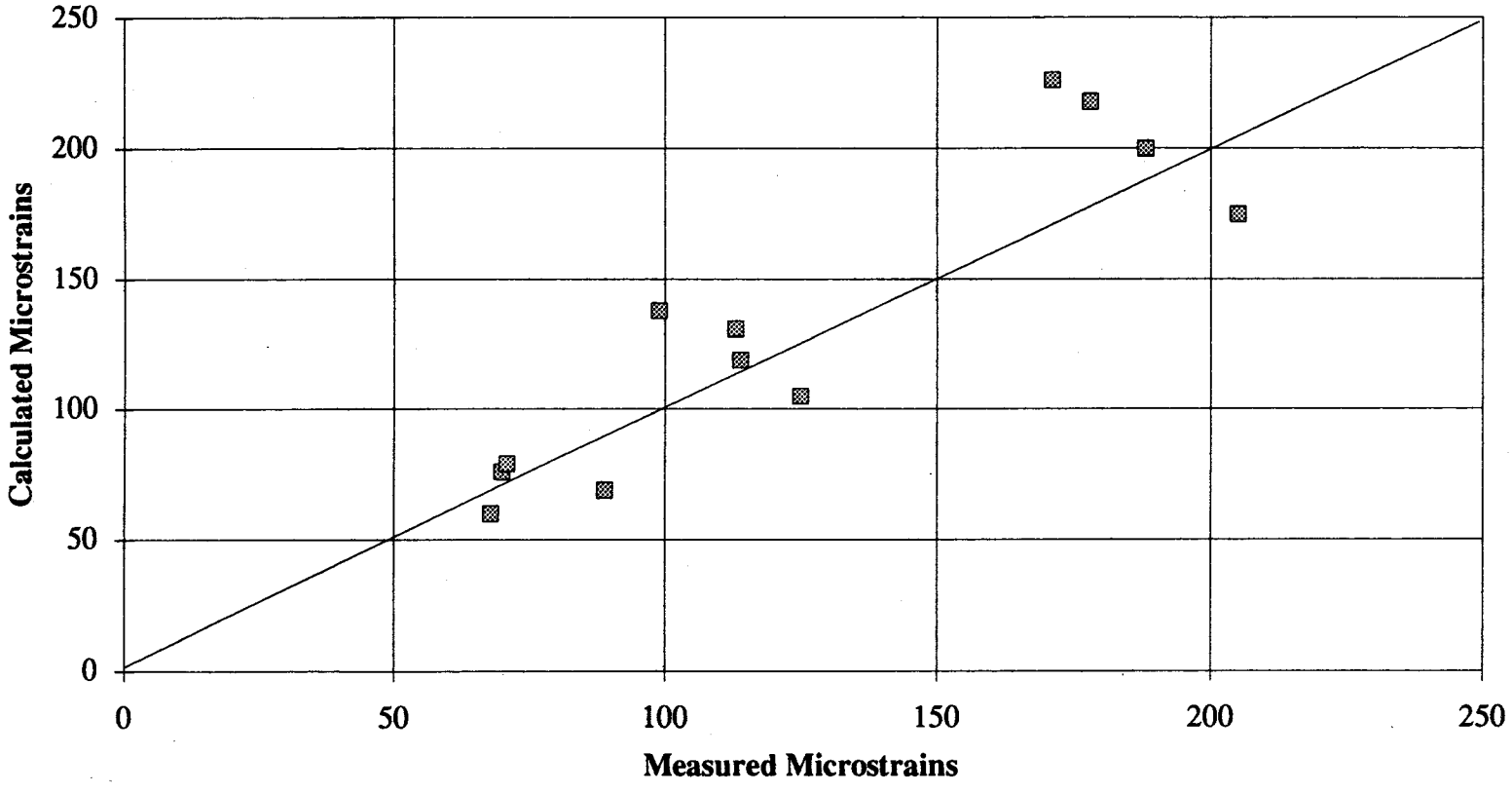

Figure 3.21 Measured vs. Calculated Strain For Axial Core Bottom Longitudinal Gauges—February 1993 FWD Testing

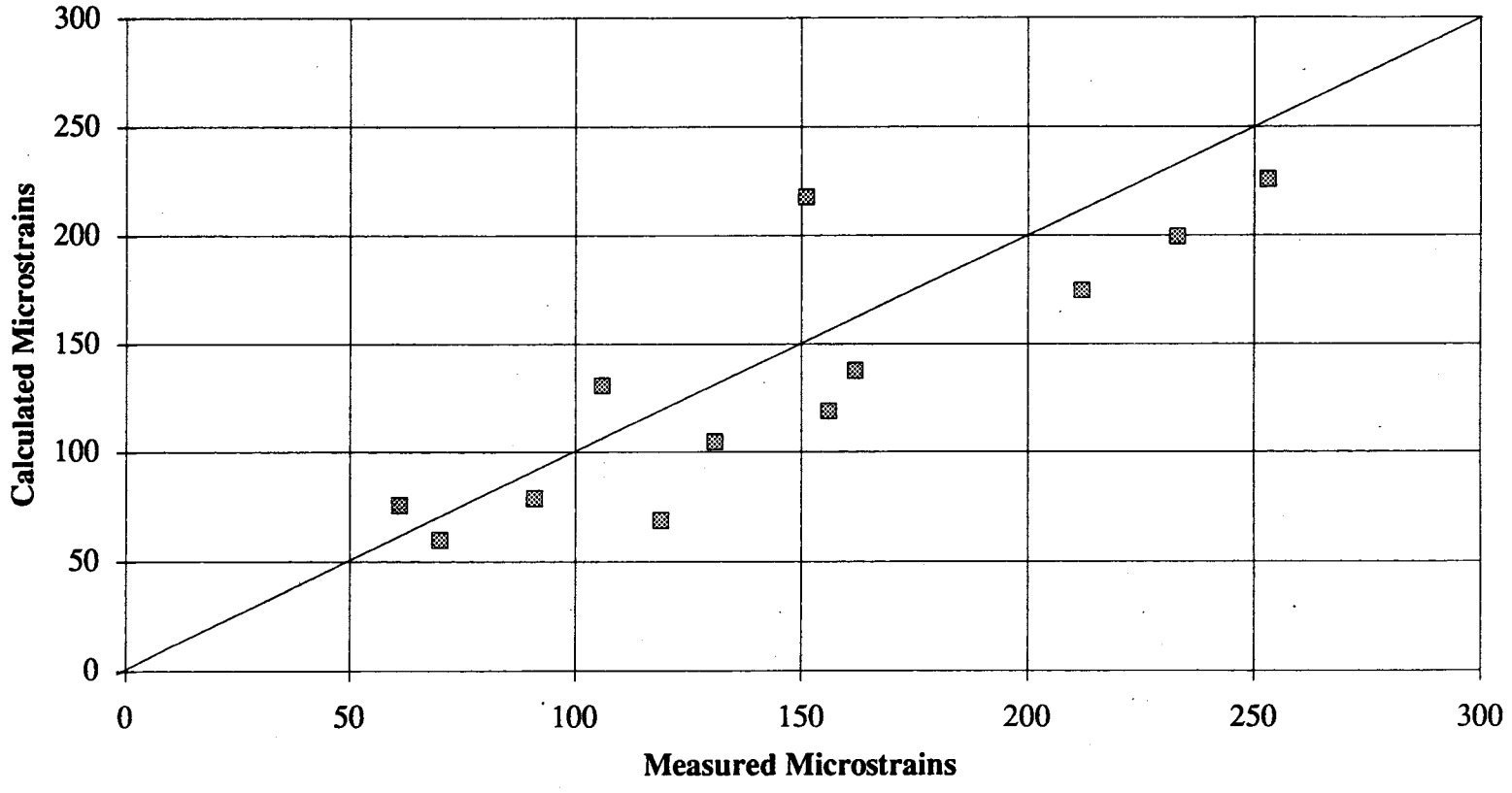

Figure 3.22 Measured vs. Calculated Strain For Axial Core Bottom Transverse Gauges—February 1993 FWD Testing

Table 3.25. Descriptive Statistics for Measured to Calculated Strain Ratios by Gauge Type—February 1993 FWD Testing

MEASURED TO CALCULATED RATIO	GAUGE TYPE			
	SL	ST	BL	BT
Mean	0.79	0.69	0.97	1.13
Standard Deviation	0.16	0.16	0.18	0.27
Minimum	0.59	0.39	0.72	0.69
Maximum	1.12	0.92	1.29	1.72
Sample Size	12	12	12	12

Table 3.26. Descriptive Statistics for Measured to Calculated Strain Ratios by Drop Height—February 1993 FWD Testing

MEASURED TO CALCULATED RATIO	FWD DROP HEIGHT		
	1 (5 ksi)	2 (10 ksi)	4 (17 ksi)
Mean	0.93	0.90	0.85
Standard Deviation	0.30	0.25	0.22
Minimum	0.53	0.39	0.45
Maximum	1.72	1.31	1.21
Sample Size	16	16	16

Table 3.27. Descriptive Statistics for Measured to Calculated Strain Ratios by Core—February 1993 FWD Testing

MEASURED TO CALCULATED RATIO	AXIAL CORE			
	Core 1	Core 3	Core 4	Core 5
Mean	0.84	0.92	0.76	1.06
Standard Deviation	0.21	0.32	0.08	0.28
Minimum	0.59	0.39	0.64	0.71
Maximum	1.17	1.25	0.92	1.72
Sample Size*	12	12	12	12

* Based on 3 drops at 4 gauges.

5.5 Comparison of October 1991 and February 1993 FWD Testing

Given the variability of the testing conditions, it is difficult to perform any definitive comparisons between the two FWD tests. Furthermore, making such comparisons is not the primary purpose of the test section. However, at least two positive observations are appropriate.

First, the BL gauges have shown the best agreement between measured and calculated strains for both test series. Given the importance of this pavement response parameter to mechanistic analyses, the impact of this observation is significant. Second, the strain gauges have shown no sensitivity to load magnitude. Since future testing at this track will examine the effect of varying loads and tire pressures on pavement response, this condition is also critical.

The least satisfactory agreement between measured and calculated strains was observed for the ST gauges. While this is unfortunate, the response measured by these gauges is the least important for this section.

A comparison of the measured to calculated strain ratios for the October 1991 and February 1993 FWD testing is shown in Table 3.28. While there is moderate variability between the two tests, the mean value for the October 1991 to February 1993 ratio is 1.10. The amount of variability is not surprising given the uncertainty in alignment of the FWD load plate over the cores.

In an attempt to evaluate individual gauge performance, the mean value of the measured to calculated ratio was calculated for each gauge that was monitored during both the October and February FWD tests. The results are shown in Table 3.29. All but three gauges show relatively consistent performance. Gauges 10SL and 5BT have a reasonable measured to calculated ratio (mean value) but unusually high standard deviations. Once again, FWD alignment over the core is a potential source of this dispersion. The measured to calculated ratio for 7ST is substantially lower than all other gauges.

Table 3.28. Comparison of Measured to Calculated Strain Ratios from February 1993 and October 1991 FWD Testing—PACCAR Test Section

CORE	GAUGE	DROP HEIGHT	MEAS/CALC RATIO		RATIO (OCT/FEB)
			Oct-91	Feb-93	
1	1BL	1	1.08	0.90	1.20
1	1BL	2	0.95	0.72	1.32
1	1BL	3 or 4	0.97	0.76	1.28
1	1BT	1	1.00	1.15	0.87
1	1BT	2	1.06	1.17	0.90
1	1BT	3 or 4	1.15	1.12	1.03
1	3ST	1	0.99	0.85	1.16
1	3ST	2	0.87	0.79	1.10
1	3ST	3 or 4	0.73	0.74	0.99
3	3BL	1	1.00	1.13	0.88
3	7SL	1	1.17	0.95	1.23
3	7ST	1	0.70	0.53	1.32
4	4BL	1	1.00	0.92	1.09
4	4BL	2	1.00	0.86	1.16
4	4BL	3 or 4	1.14	0.82	1.39
4	4BT	1	0.98	0.80	1.23
4	4BT	2	0.97	0.81	1.20
4	4BT	3 or 4	1.04	0.69	1.51
4	10SL	1	1.04	0.69	1.51
4	10SL	2	1.04	0.73	1.42
4	10SL	3 or 4	1.18	0.70	1.69
5	5BL	1	0.98	1.29	0.76
5	5BL	2	1.04	0.96	1.08
5	5BL	3 or 4	1.01	0.94	1.07
5	5BT	1	0.81	1.72	0.47
5	5BT	2	0.79	1.31	0.60
5	5BT	3 or 4	0.82	1.17	0.70
5	17SL	1	0.86	0.87	0.99
5	17SL	2	0.88	1.12	0.79
5	17SL	3 or 4	0.94	0.91	1.04
				Mean	1.10
				Standard Dev.	0.28
				n	30

Table 3.29. Descriptive Statistics for Measured to Calculated Ratios for Selected Gauges—October 1991 and February 1993 FWD Testing

Gauge Designation	Mean	Standard Deviation	n
1BL	0.90	0.14	6
1BT	1.11	0.07	6
3ST	0.83	0.10	6
3BL	1.12	0.09	4
7SL	0.94	0.17	4
7ST	0.52	0.13	4
4BL	0.96	0.12	6
4BT	0.88	0.14	6
10SL	0.90	0.21	6
5BL	1.04	0.13	6
5BT	1.10	0.37	6
17SL	0.93	0.10	6

SECTION 4

PACCAR TRUCK TESTS

1. INTRODUCTION

Three series of full-scale truck tests were conducted. The first series (May 1 and 4, 1992) was preliminary in nature, and was to provide an initial evaluation of strain gauge performance at different truck speeds and tire pressures. The second series (September 28 and 29, 1993) were used in investigating the effects of truck speed, tire pressure, and pavement temperature on pavement response. Further, these tests were used to evaluate the computer program SAPSI for predicting pavement response under moving loads. The third series (September 30, 1993) was designed to investigate the concept of spatial repeatability on pavement damage by studying the response of different trucks to the roughness of the pavement surface.

2. INSTRUMENTED TEST SECTION

As mentioned in Section 3, the instrumented test section is 40 ft long and is preceded by 116 ft and followed of 98 ft of smooth asphalt concrete pavement. The section is closed to vehicular traffic except during scheduled pavement testing. The axial cores were displaced laterally to allow collection of strain measurements from both wheel paths and the approximate centerline of the wheel base. The longitudinally oriented surface gauges were specifically designed to evaluate the dynamic response of a truck as it travels down the pavement section. The maximum safe speed for testing on this track section was 45 mph so the tests were conducted at creep speed, 20 mph and 40 mph.

3. TEST TRUCKS

Most of the truck testing used one main experimental vehicle: a Peterbilt 359 truck with a load frame and instrumented axles. For the spatial repeatability testing, three more trucks and two trailers were used.

3.1 Primary Test Truck

The only truck used for the smooth track tests (i.e., no induced pavement roughness event) was a fully loaded Peterbilt 359 with a four leaf spring suspension on the drive axle. This truck had been disassembled at the University of Michigan Transportation Research Institute where its physical and dynamic properties were thoroughly documented. The elevation and plan views of the truck are given in Figures 4.1 and 4.2, respectively. The static wheel loads are given in Table 4.1. The test truck was chosen because of this characterization, its instrumentation, and because the majority of trucks use this suspension type. A strain gauge bridge was mounted at each end of each of two controlled axles. Strain measurements were combined with acceleration measurements to calculate the tire forces after the tests.

3.2 Spatial Repeatability Test Vehicles

In addition to the Peterbilt 359 truck, a smaller Peterbilt 330 truck and two larger Kenworth T600 and T800 tractors were used for the spatial repeatability tests; two trailers, a 48-ft van trailer and a 40-ft flatbed trailer, were also used for a total of four tractor-trailer combinations. The Kenworth T600 tractor was equipped with air suspensions on the drive axle whereas the Peterbilt 330 was a single unit truck which had leaf spring suspensions. The Kenworth T800 tractor had a walking beam suspension on the drive axles. Both trailers had leaf spring suspensions. None of the additional trucks and trailers were equipped with instrumented axles. Consequently, it was assumed that the repeatability of the truck response for a given pavement roughness could be indirectly studied by examining the pavement response at closely spaced surface strain gauges along the test track. Figure 4.3 shows the longitudinal dimensions of the various vehicles. Table 4.2 contains various vehicle measurements.

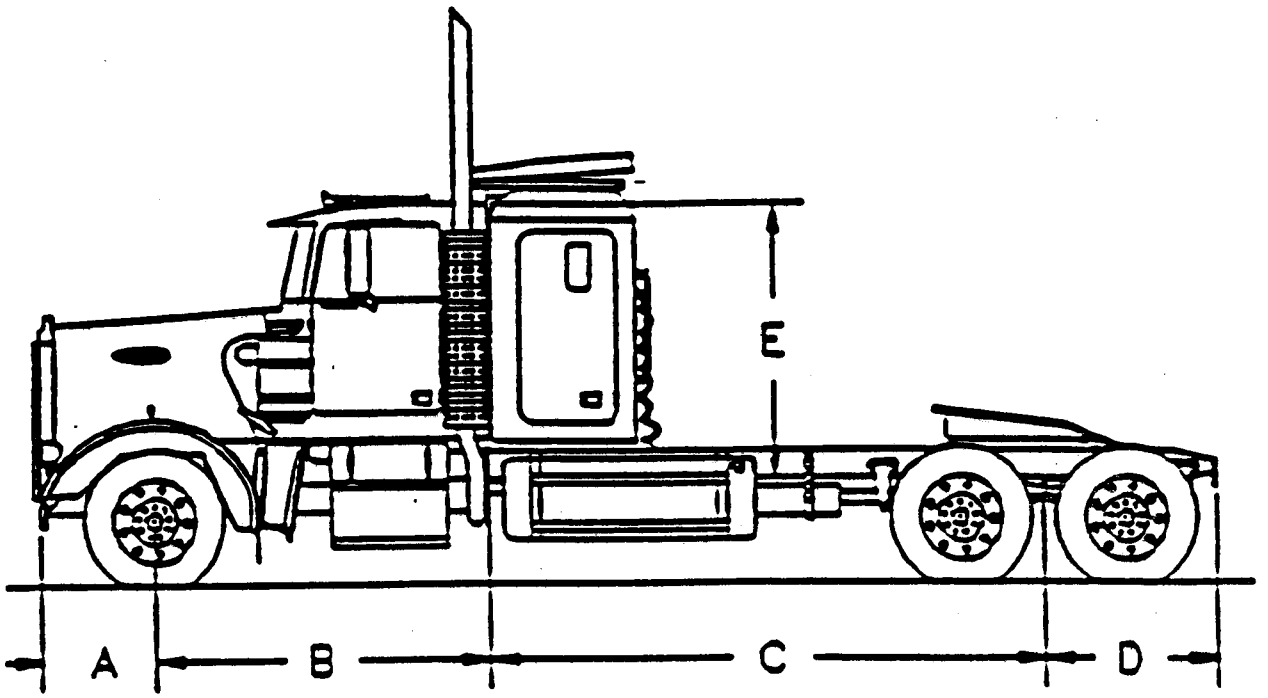

Figure 4.1 Elevation View of Peterbilt B359 Truck

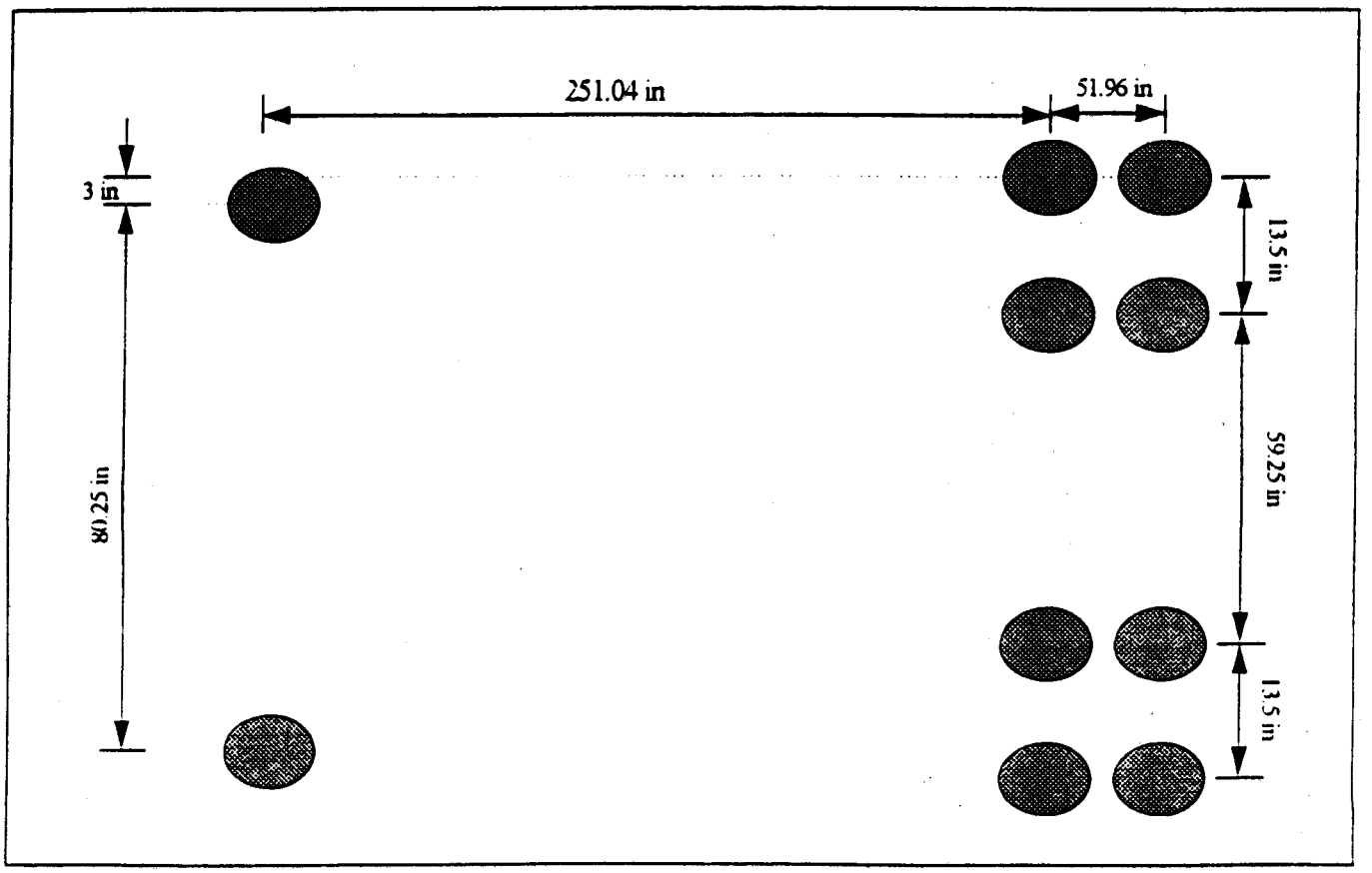

Figure 4.2 Plan View of Peterbilt B359 Truck

Table 4.1 Static Wheel Loads of Test Vehicles

Text Vehicle	Left Steer	Right Steer	Left front Drive	Left Rear Drive	Right Front Drive	Right Rear Drive	Left Front Trailer	Right Front Trailer	Left Rear Trailer	Right Rear Trailer
PB330	6321	6395	11486	N/A	11374	N/A	N/A	N/A	N/A	N/A
PB359	5540	5410	8080	7540	7700	7890	N/A	N/A	N/A	N/A
T600 w/flatbed	5918	5986	16632		17255		7759	6975	7443	8720
T600 w/van	6088	5738	15531		17137		17493		16058	
T800 w/flatbed	5778	6092	15206		17019		7601	6814	7595	8813
T800 w/van	5481	5862	14365		16681		8562	8457	8401	8187

* All dimensions are in inches

Table 4.2 Tire Geometry of Test Vehicles

Vehicle	Truck Width - Steer (outside Tire Edge)	Tire Width - Steer	Truck width - Duals (Outside Tire Edge)	Tire Width - Duals	Gap Between - Duals
PB330	86.5	8.75	94.5	8.75	4.625
PB359	88.75	8.5	94.75	8.5	5
T600	89	9	95	9	4.5
T800	89.25	9.25	95	8.75	4.75
Flatbed	N/A	N/A	93.25	8.75	4.625
	N/A	N/A	99.5	8.75	4.625

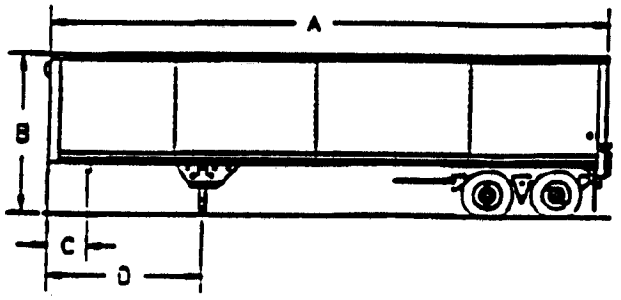

Fruehauf Van

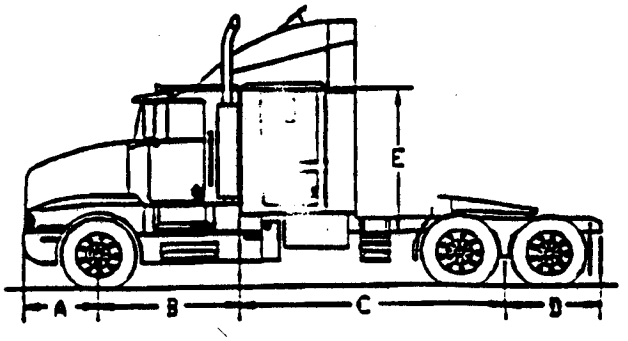

Kenworth T800

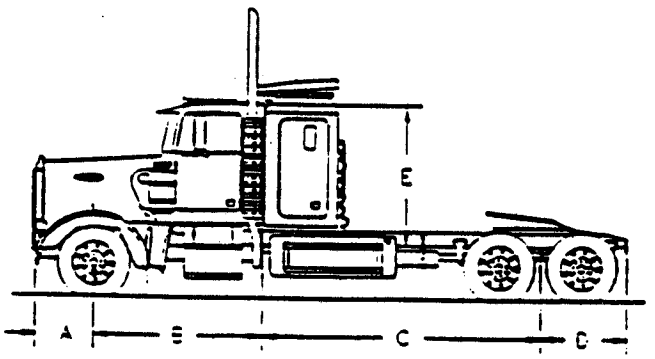

Peterbilt 330

Peterbilt 359

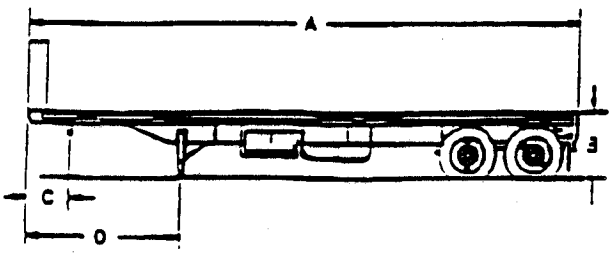

Astec Flatbed

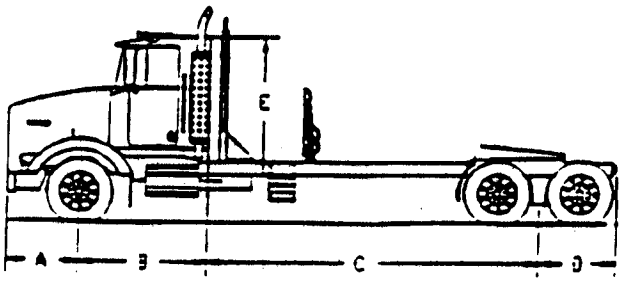

Kenworth T600AII

Figure 4.3 PACCAR Test Vehicles

4. SEPTEMBER 28-29, 1993, TRUCK TEST RESULTS

The formal series of full-scale truck tests were conducted on September 28 and 29, 1993, on PACCAR's test track. The primary goals of these tests were:

- to investigate the effects of vehicle speed and tire pressure (or contact area) on pavement response.
- to investigate the feasibility of using the SAPSI computer program for predicting the dynamic pavement response to moving loads.

4.1 Test Procedure

All tests were done using the Peterbilt 359 truck. Testing was conducted in three blocks: mid-morning of September 28; afternoon of September 28; and mid-morning of September 29. Each test block consisted of three sets of tests corresponding to three different tire pressures: 90 psi, 58 psi and 31 psi. For each tire pressure, three truck speeds were used: Creep speed (1.7 mph,) 20 mph and 40 mph. The tests were conducted in triplicates and according to a random order.

After some trial runs, data acquisition was almost continuous since the data was written to disk, the files renamed, and the input for the next run entered just as the truck made it back around the test section of track. A test was possible every three minutes (when all systems were functional). The tests required at least four people: the driver, one for data acquisition in the truck, one for the pavement computers, and one for marking and reading the offset between the truck tire and the pavement core.

Because of the results in the preliminary tests (May 1992), special care was taken in marking the pavement and reading the tire imprint. Lime dust was used to show the tire imprint. If the offset was greater than four inches the test was repeated.

4.2 Test Results

Test results consisted of strain measurements from the different axial cores and surface gauges as well as tire load measurements from the truck-mounted gauges.

4.2.1 Load Measurements

The load measurements were used to investigate the variability of tire loads with runs of equal truck speed and tire pressure and to study the effects of speed and pressure on tire loads. Figure 4.4 shows typical variability of the load at different truck speeds and tire pressures. The results indicate that the variability is within 5 percent. The figure shows that the average moving loads are somewhat lower than the static load—generally within 10 percent or less. The load differences decrease with decreasing test speed. Some of these observed load differences are likely due to the measurement mechanism mounted on the truck since the average dynamic loads are expected to be a little higher than the static loads. Therefore, the measured static loads were used as the peaks of the load pulses in the portion of the analysis where SAPSI was used to predict pavement response.

4.2.2 Strain Measurements

Strain measurements were used to investigate the effects of truck speed and tire pressure on pavement response. Figure 4.5 shows typical time histories of measured strains in the AC layer. The discussion above indicated that the variability of the load (test run to test run) was quite small in these tests. Other significant variables which should be accounted for in the analysis are the pavement temperature and the offset distance between the truck wheel and the strain gauge. Within a subset of tests with constant tire pressure, the pavement surface temperature did not vary much; this should mean that the temperature at the bottom of the asphalt concrete layer should be very close to a constant within each subset of tests. Accordingly, no temperature correction was used in analyzing the effect of truck speed for a given subset of tests with constant tire pressure. On the other hand, the effect of the offset between the applied loads and the recording strain gauge must be adjusted. These adjustments were made by use of the SAPSI computer program.

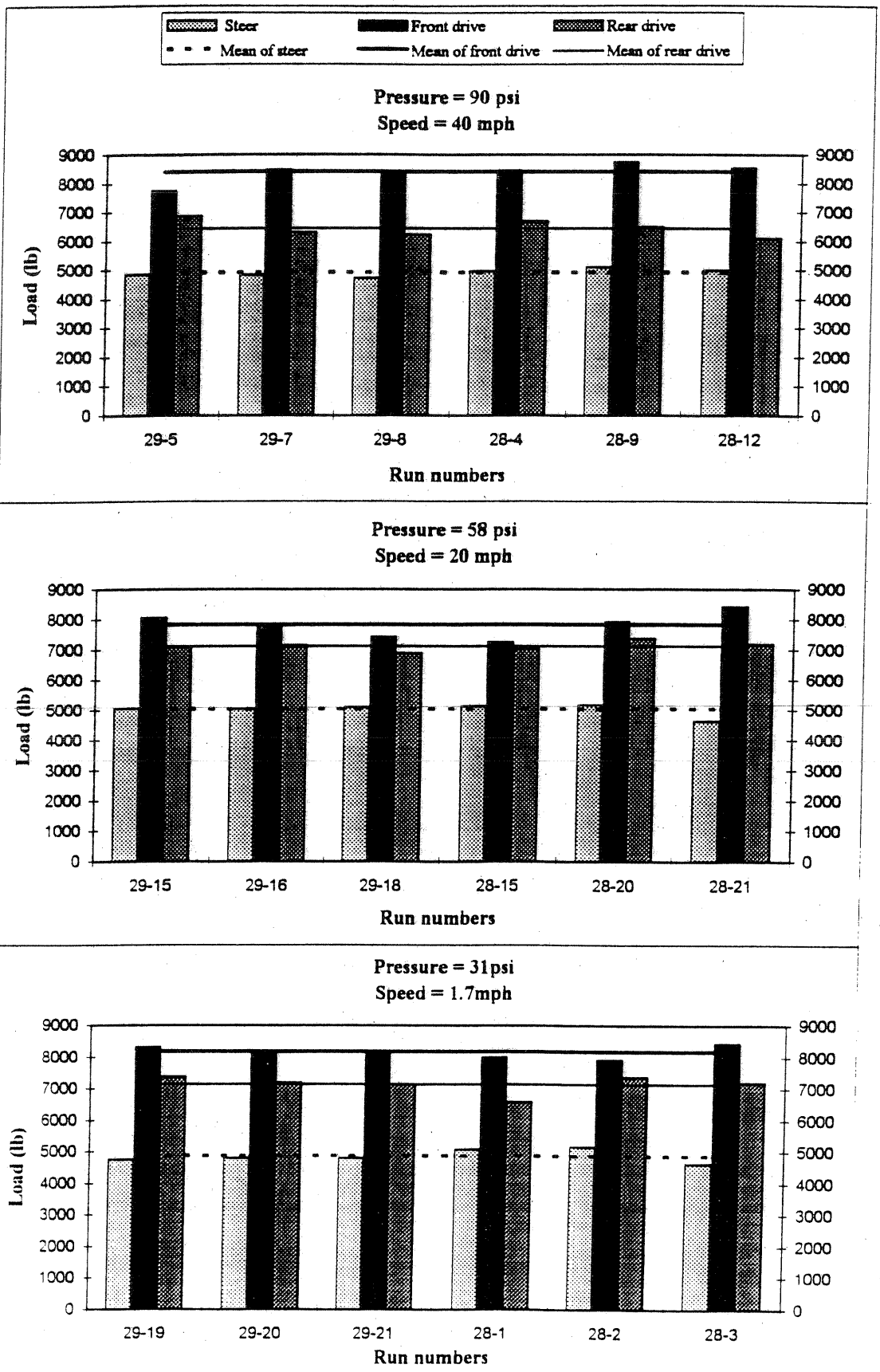

Figure 4.4 Typical Wheel Load Variability with Triplicate Runs (Steer is single tire and drive is dual tires)

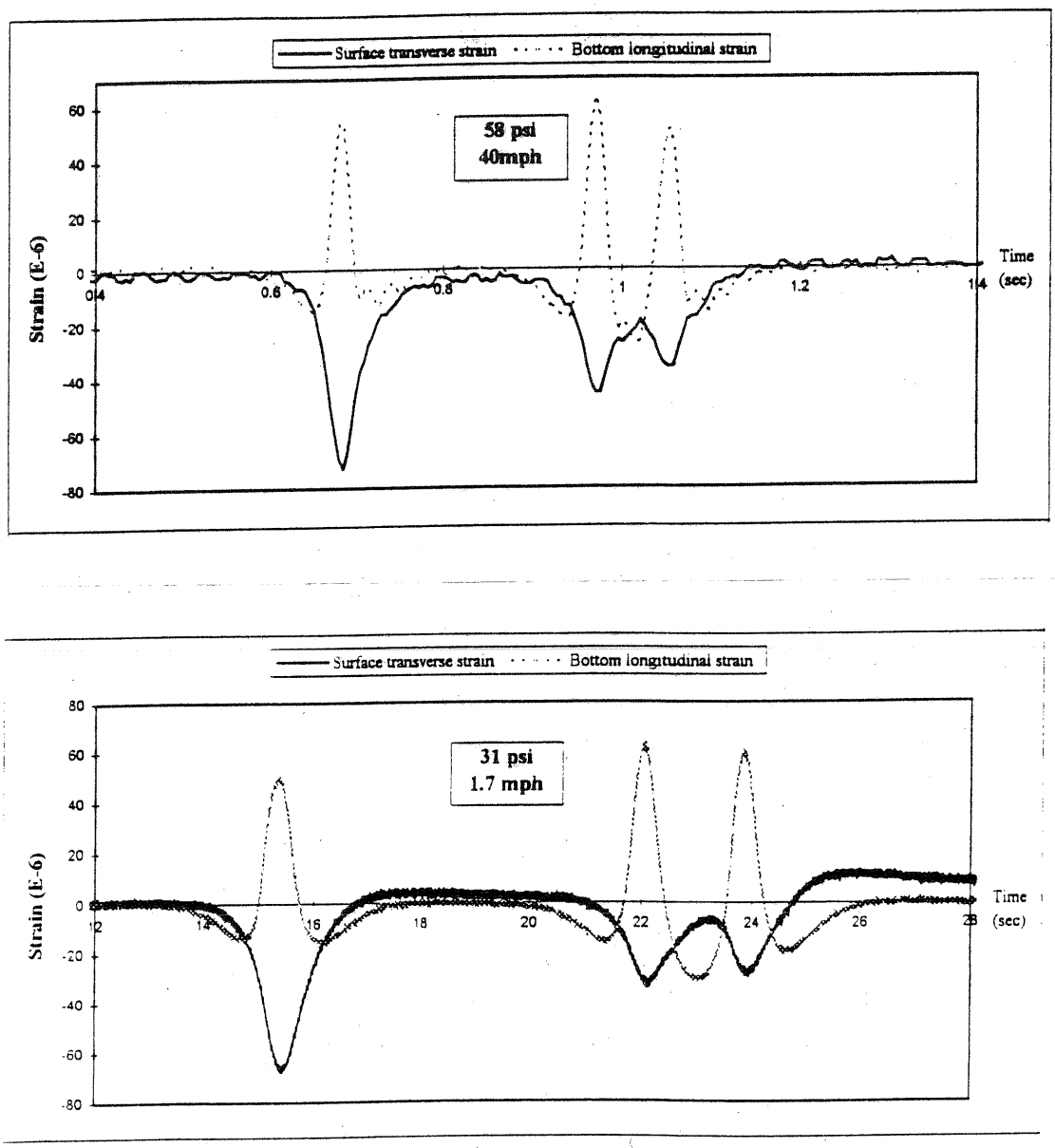

Figure 4.5 Typical Time Histories of Measured Strain in the AC Layer from Peterbilt 359 Truck Tests

4.2.2.1 Effect of Truck Speed on Pavement Response. The effect of speed on longitudinal and transverse strains at the bottom and top of the asphalt concrete layer in the three different cores was investigated at the three different tire pressures. Figures 4.6 through 4.8 show the mean values and the corresponding standard deviations from all tests and all axles for Cores 1, 3 and 4. The speed curves show that:

- Increasing truck speed from 1.7 to 40 mph reduced the longitudinal strain at the bottom of the asphalt concrete layer by about 35 percent, on average.
- The speed effect on longitudinal strain decreases with increasing speed.

Figure 4.9 shows the effect of speed on transverse strains at the bottom of the asphalt concrete layer. The figure indicates that:

- The speed effect for transverse strains is less pronounced than for longitudinal strains.
- The transverse strain due to the drive axles is about half of the longitudinal value. This is due to the dual tires which generate offsetting strains in compression and tension respectively in the transverse direction. SAPSI was used to generate typical strain distributions (longitudinal and transverse) in the transverse direction due to steer and drive axles (duals.) Figure 4.10 clearly shows the transverse strain due to the drive axle to be significantly lower than the longitudinal strain and the strain due to the steer.

Figure 4.11 compares surface to bottom longitudinal strains. The figure shows that:

- The speed effect is more pronounced at the surface than at the bottom of the asphalt concrete pavement layer. For Core 4, increasing truck speed from 1.7 to 40 mph reduced the longitudinal strain a the top of the asphalt concrete layer by about 40 to 60 percent.

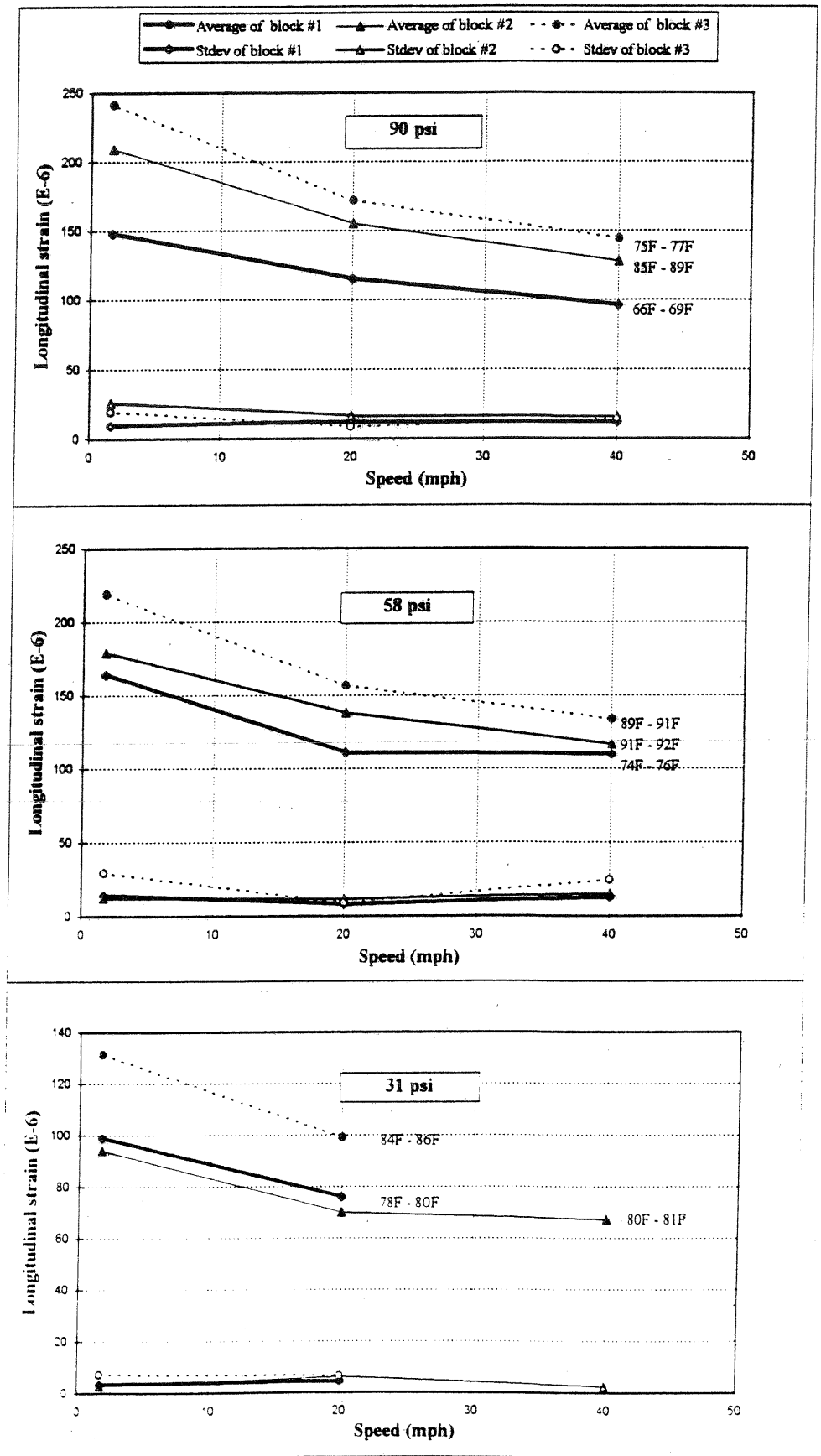

Figure 4.6 Effect of Truck Speed on Longitudinal Strain at the bottom of AC Layer—Core 1

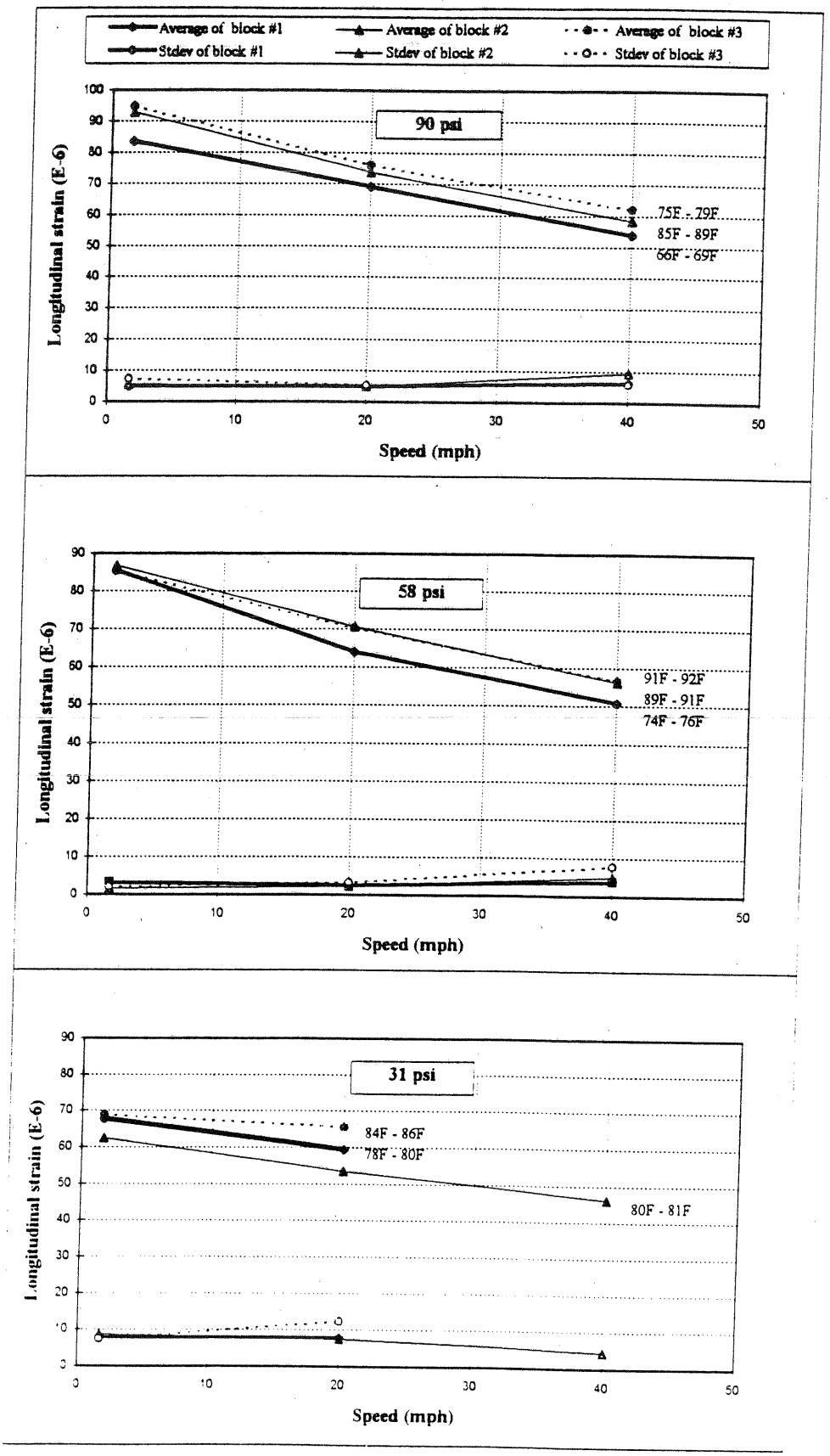

Figure 4.7 Effect of Truck Speed on Longitudinal Strain at the bottom of AC Layer—Core 3

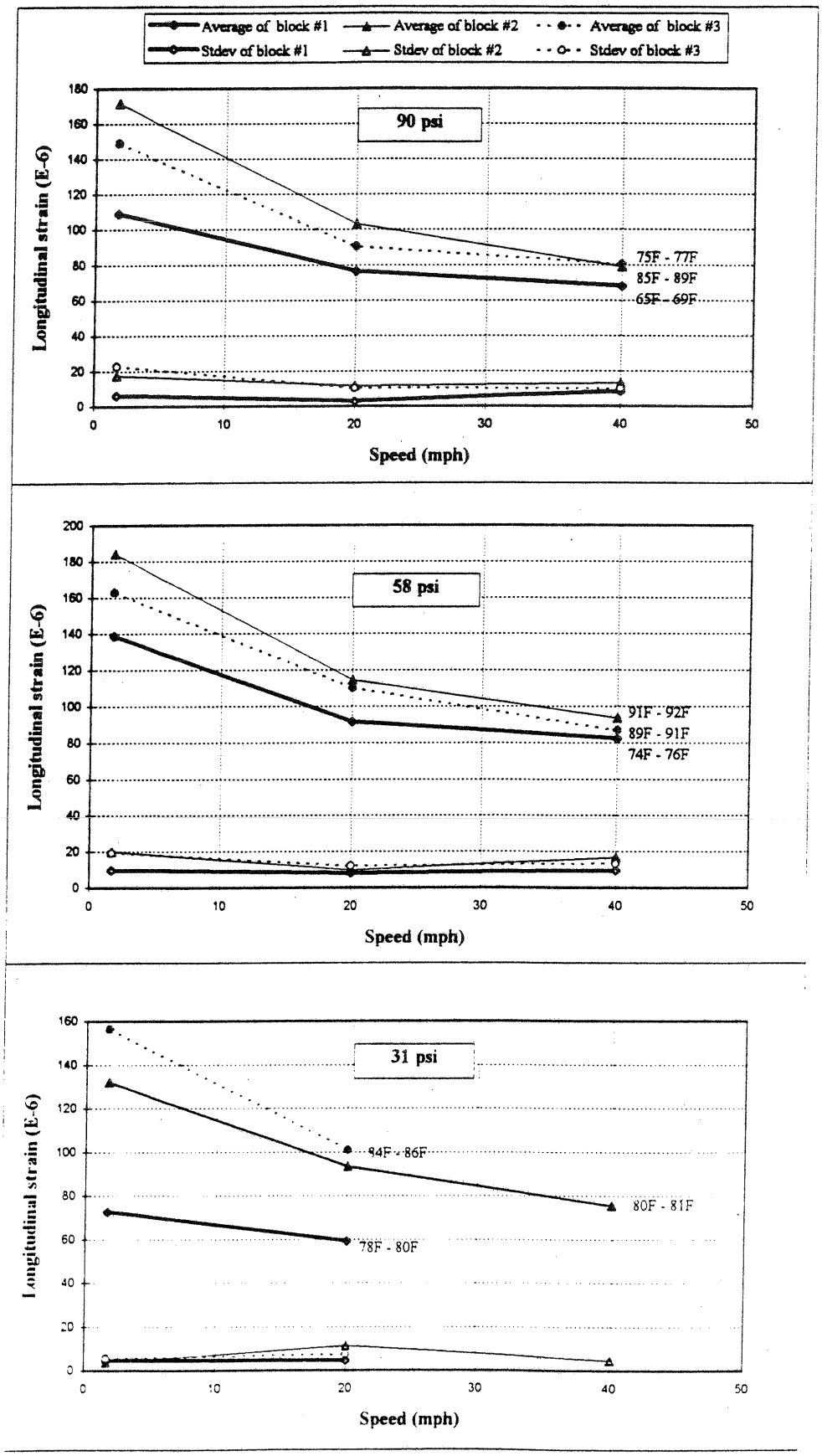

Figure 4.8 Effect of Truck Speed on Longitudinal Strain at the surface of AC Layer—Core 4

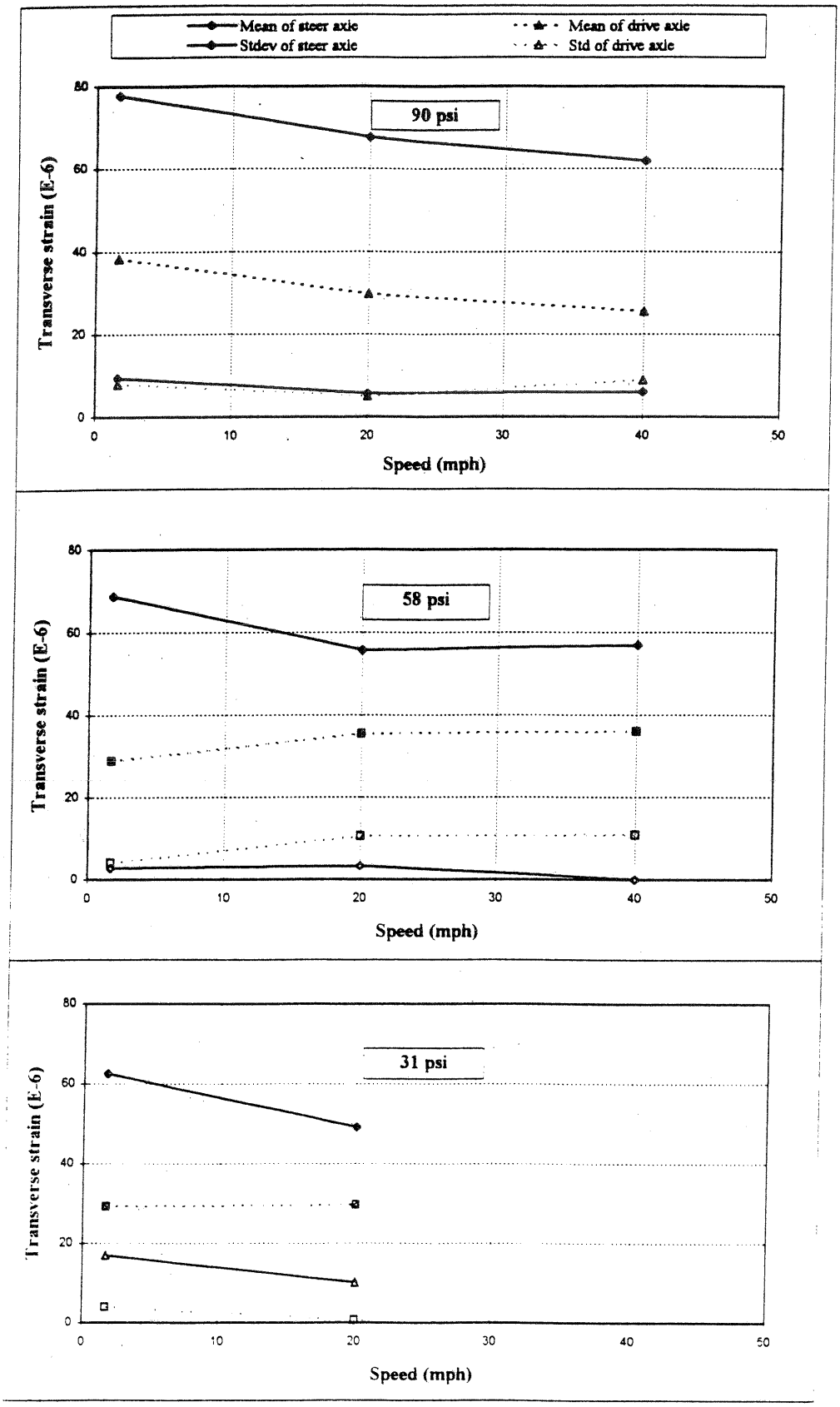

Figure 4.9 Effect of Truck Speed on Transverse Strain at the bottom of AC Layer—Core 4

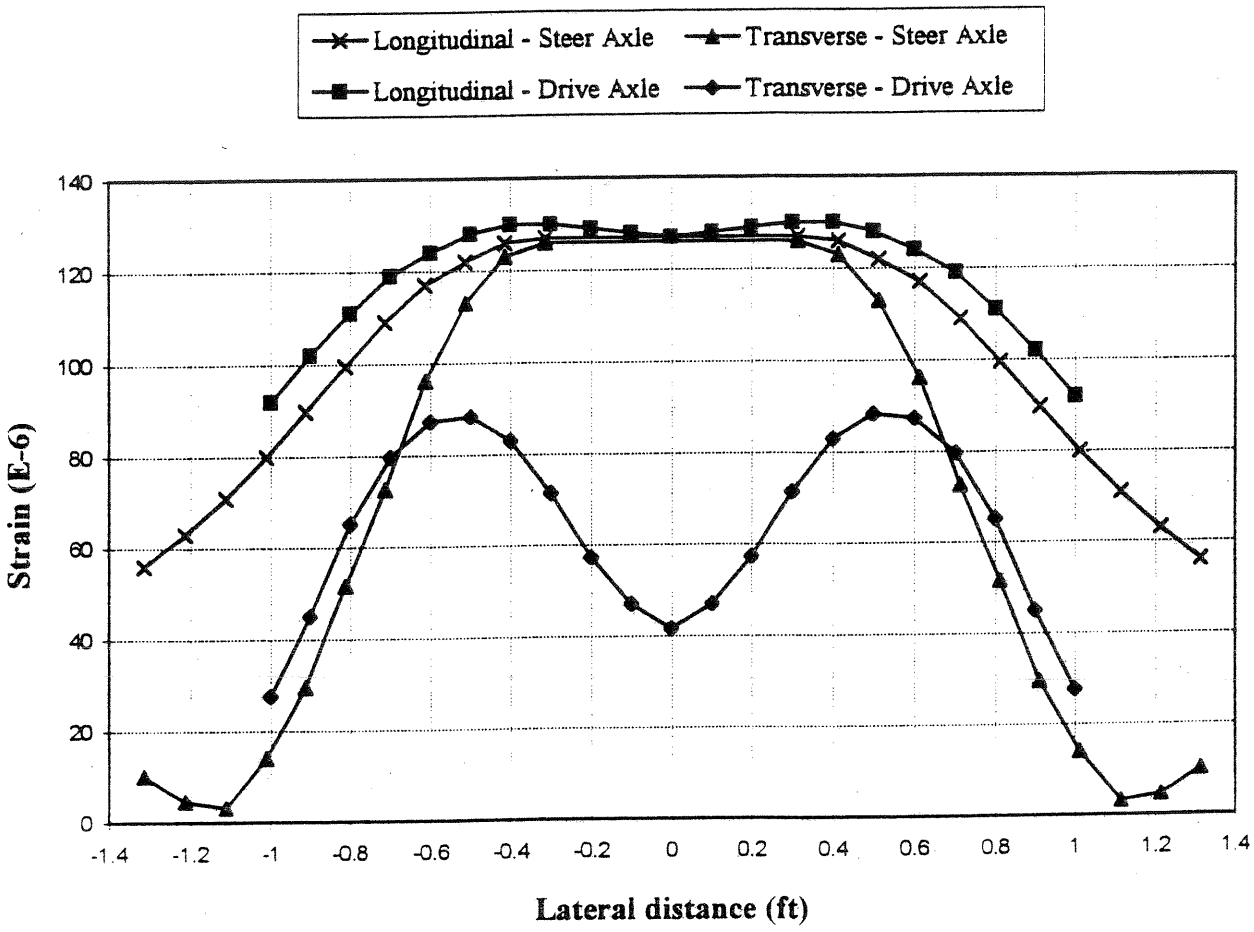

Figure 4.10 Comparison of Longitudinal and Transverse Strain Distributions

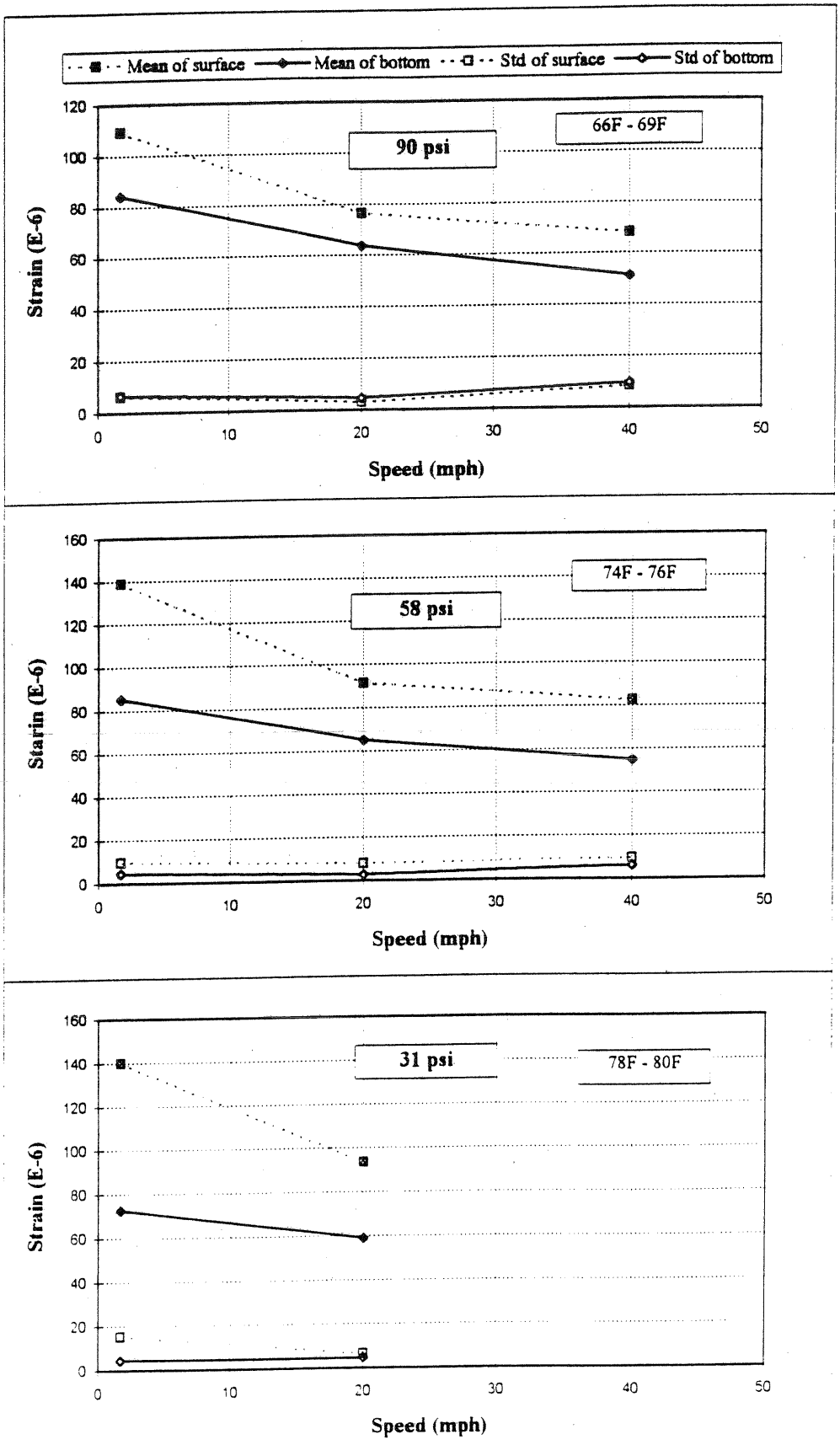

Figure 4.11 Comparison of Surface and Bottom Longitudinal Strain—Core 4 in Block 1

- The surface strain is higher than the bottom strain by 20 to 100 percent with increasing surface temperature. This is thought to be due to the pavement temperature which is higher at the surface than at the bottom.

4.2.2.2 Effect of Tire Pressure on Pavement Strain. Because the time periods between test blocks at different tire pressures were long enough to cause variations in pavement temperature, the effect of temperature on pavement strain needed to be compensated. To do this, the data were lumped into measurements which correspond to a constant truck speed and a constant tire pressure and then plotted as a function of the pavement surface temperature. A linear relationship between the strains at two different temperatures was developed for each case. Using these lines, strains at a constant temperature (T = 80° F), was calculated. For the case of low pressure and low speed (p = 31 psi and v = 1.7 mph) the average of all the strains (corresponding to each axle type) was taken, since the temperature was almost constant. Therefore, for a constant temperature of 80° F the effect of tire pressure was studied at the three truck speeds. Figures 4.12 and 4.13 show the effect of tire pressure on longitudinal strains at the bottom of the asphalt concrete layer for Cores 1 and 3, respectively. Figure 4.14 shows this effect on longitudinal strains at the top of the asphalt concrete layer. Figures 4.12 and 4.13 show that:

- Decreasing tire pressure from 90 psi to 31 psi reduced the longitudinal strain at the bottom of the asphalt concrete layer by about 35 to 40 percent for Core 1 and about 25 to 35 percent for Core 3.
- The pressure effect is somewhat reduced at higher speeds. The effect was a 40 percent reduction in the longitudinal strain at 1.7 mph versus 35 percent at 40 mph for Core 1, and was 35 percent at 1.7 mph versus 25 percent at 40 mph for Core 3.

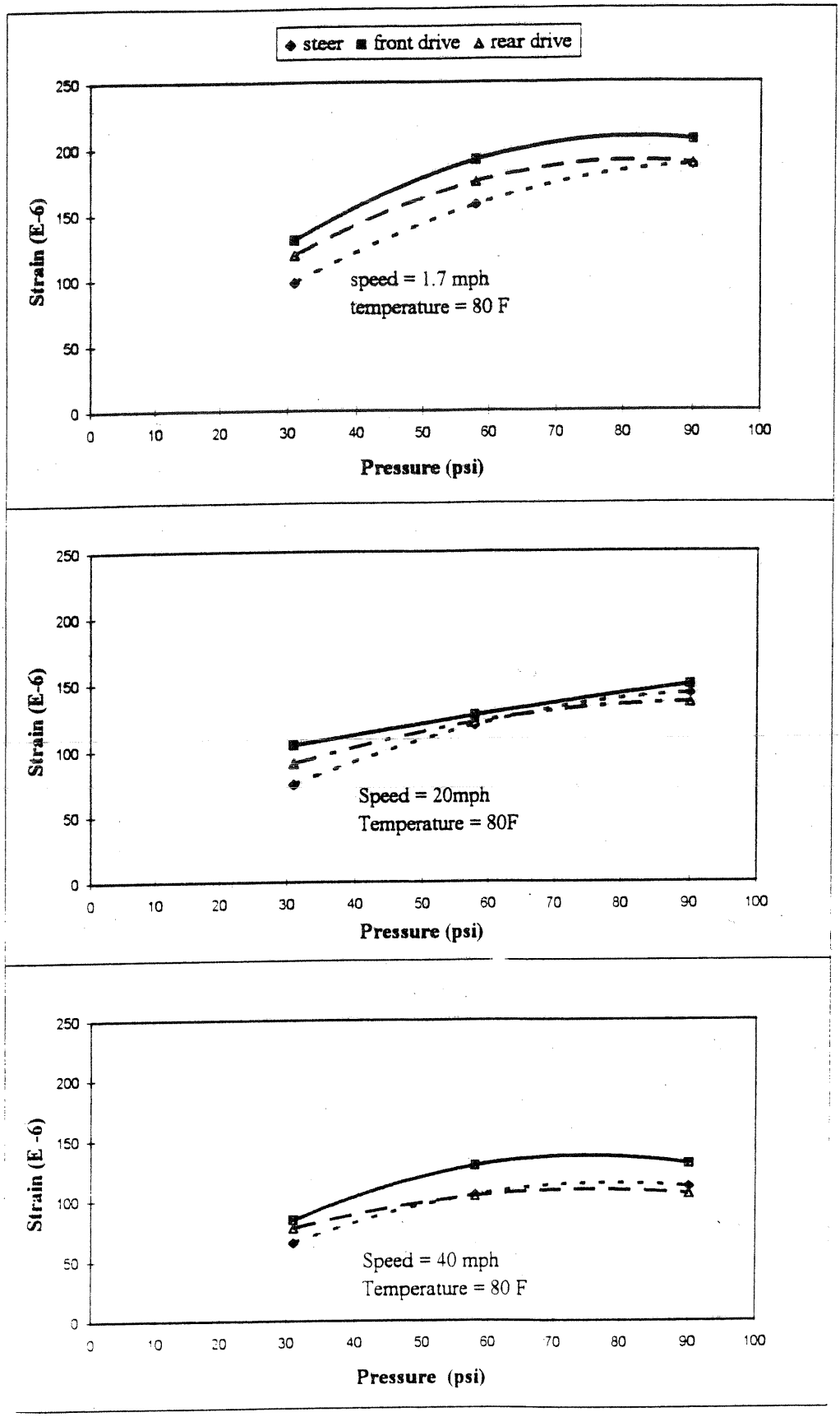

Figure 4.12 Effect of Tire Pressure on Longitudinal Strain at the bottom of AC Layer—Core 1

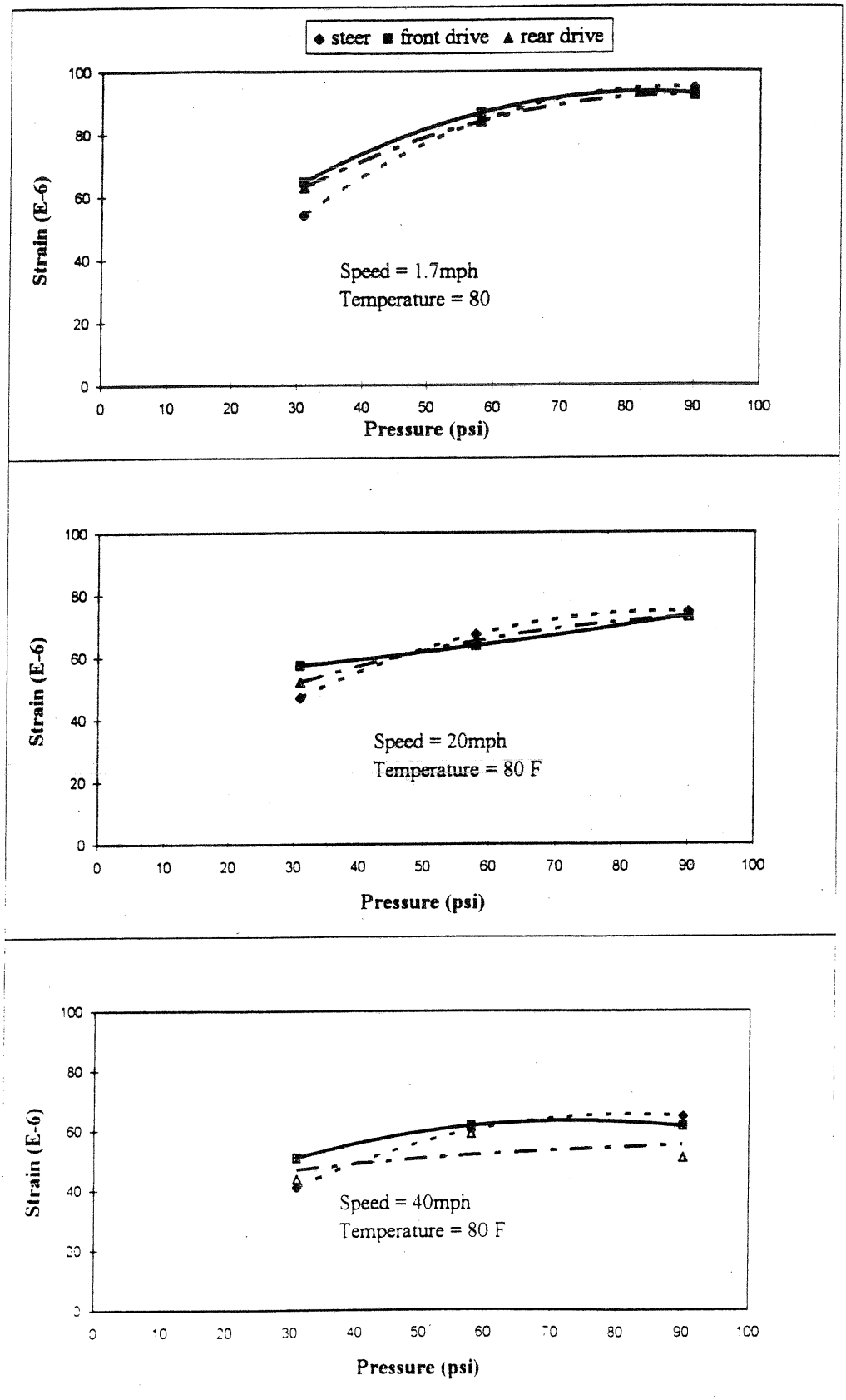

Figure 4.13 Effect of Tire Pressure on Longitudinal Strain at the bottom of AC Layer—Core 3

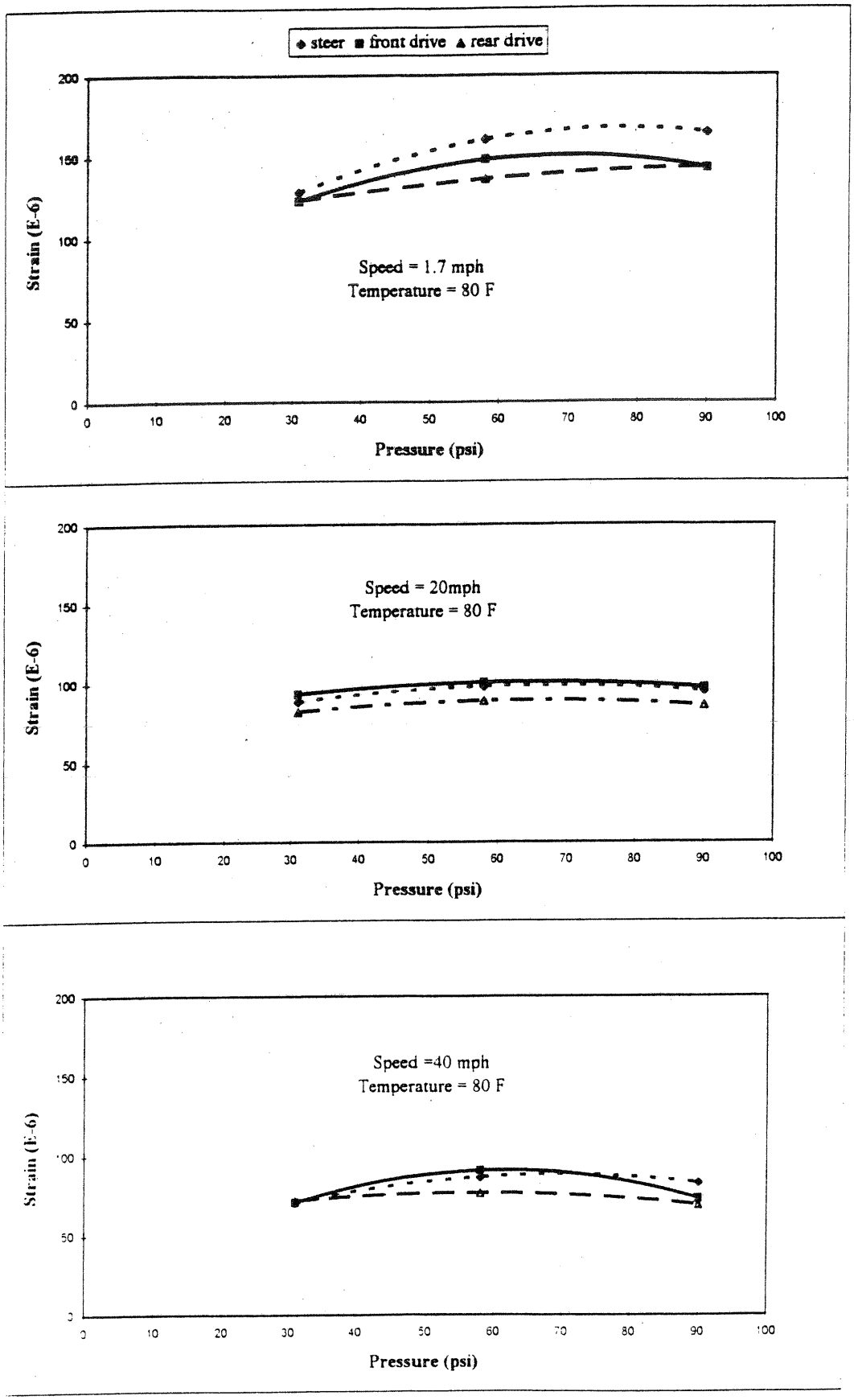

Figure 4.14 Effect of Tire Pressure on Longitudinal Strain at the bottom of AC Layer—Core 4

These tensile strain reductions due to reduced tire pressures are similar to those calculated by Sweet [98]. Sweet examined the effects of reduced tire pressures on frost weakened roads and used layered elastic analysis to make the necessary calculations.

4.3 Spatial Repeatability Tests

The last series of full-scale truck tests at PACCAR's Technical Center was conducted on September 30, 1993. The primary goal of these tests was to investigate the theory of spatial repeatability in pavement damage. This concept states that for any given truck speed, the wheel load time histories generated by a particular heavy vehicle are repeated closely on successive passes over a given length of pavement. Since all heavy commercial vehicles have approximately the same natural frequencies and are driven at approximately the same speed on highways, then for a given pavement the dynamic wheel load peaks would always occur within a relatively narrow band of road sections. Accordingly, the issue of spatial repeatability is central to truck-pavement interaction because some portions of the road may incur much larger damage than other portions. This localized, repetitive phenomenon may not be possible to predict by existing analytical models. Consequently, there is a need to further study the issue analytically as well as with controlled real-scale tests. This series of tests attempted to do just that.

4.3.1 Test Procedure

For these tests, a ramp was used to excite the different trucks. The ramp consisted of three portions: a 4 ft x 2 in section up, a 7 ft flat section and a 4 ft x 2 in section down. Four trucks and two trailers with different suspensions were used: Peterbilt 359 tractor and 330 single unit truck, Kenworth T800 and T600 tractors, and a flat bed and van trailers. The Peterbilt 359 and the trailers were equipped with leaf spring suspensions, as did the Peterbilt 330; the Kenworth T800 and T600 tractors had walking beam and air suspensions, respectively. Testing was conducted in three blocks: mid-morning; mid-afternoon; and late-afternoon of September 30, 1993. Each test block consisted of six sets of tests corresponding to different truck/trailer combinations. For all tests, the truck speed

was 20 mph and the tire pressure was 90 psi. The tests were conducted in triplicates and the order of each set of triplicate tests was random. The three test blocks were identical except for the time-of-the-day and the order of triplicate test sets.

4.3.2 Test Results

The bulk of the test results consisted of strain measurements from the surface gauges. Tire load measurements from the truck-mounted gauges on the Peterbilt 359 were also available. The three other trucks and the trailers were not instrumented.

4.3.2.1 Load Measurements. The load measurements were used to investigate the variability of tire loads with runs, to compare them with those obtained in the "smooth" pavement tests, i.e., tests without a ramp, and to check the match between them and the pavement surface strains. Figure 4.15 shows the measured axle load variations as a function of distance for triplicate runs at different truck speeds and for different axles. The figure clearly shows a repetitive pattern on successive runs over the "smooth" test track. This agrees with the concept of spatial repeatability. Figure 4.16 shows the variations of the different axles loads with distance for both "smooth" and "ramp" tests. The figure clearly shows that the fluctuations in the dynamic loads are higher in the case where the ramp has been added on the pavement surface. The lowest fluctuations are those of the steer axle. The figure also shows different bouncing modes for the three axles with the steer axle exhibiting a bit more than two cycles, the front and rear axles exhibiting about four cycles with the front axle showing the highest damping effect. Note also that the front and rear axles are out of phase.

4.3.2.2 Strain Measurements. Surface strain measurements were used to investigate the concept of spatial repeatability in lieu of wheel loads since only the PB 359 truck was instrumented. This is an indirect way of assessing the repeatability of the loads since load and strain should be directly related. Strain values were corrected for

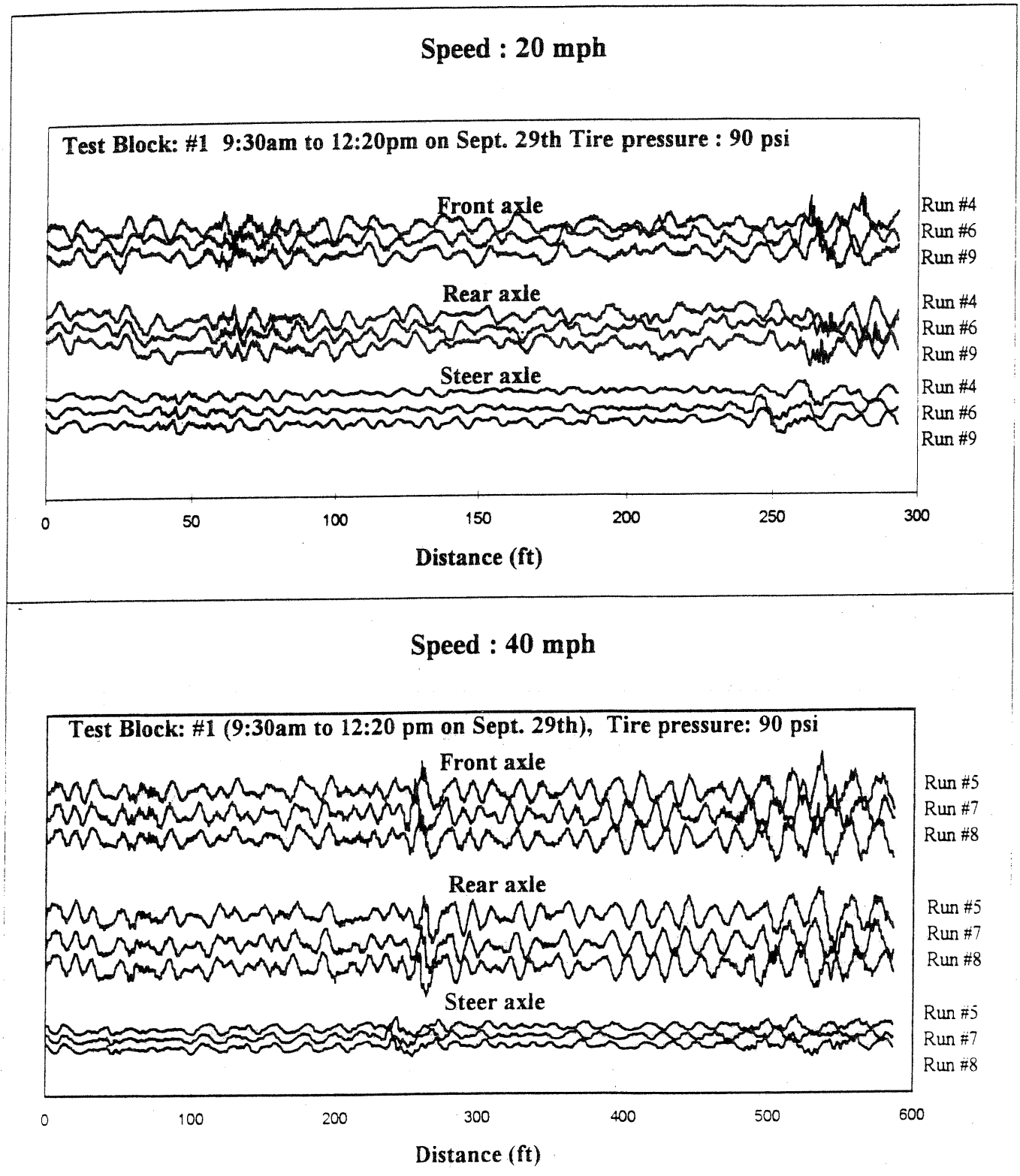

Figure 4.15 Measured Axle Load Variations as a Function of Distance for Triplicate Runs—Peterbilt 359—Smooth Pavement

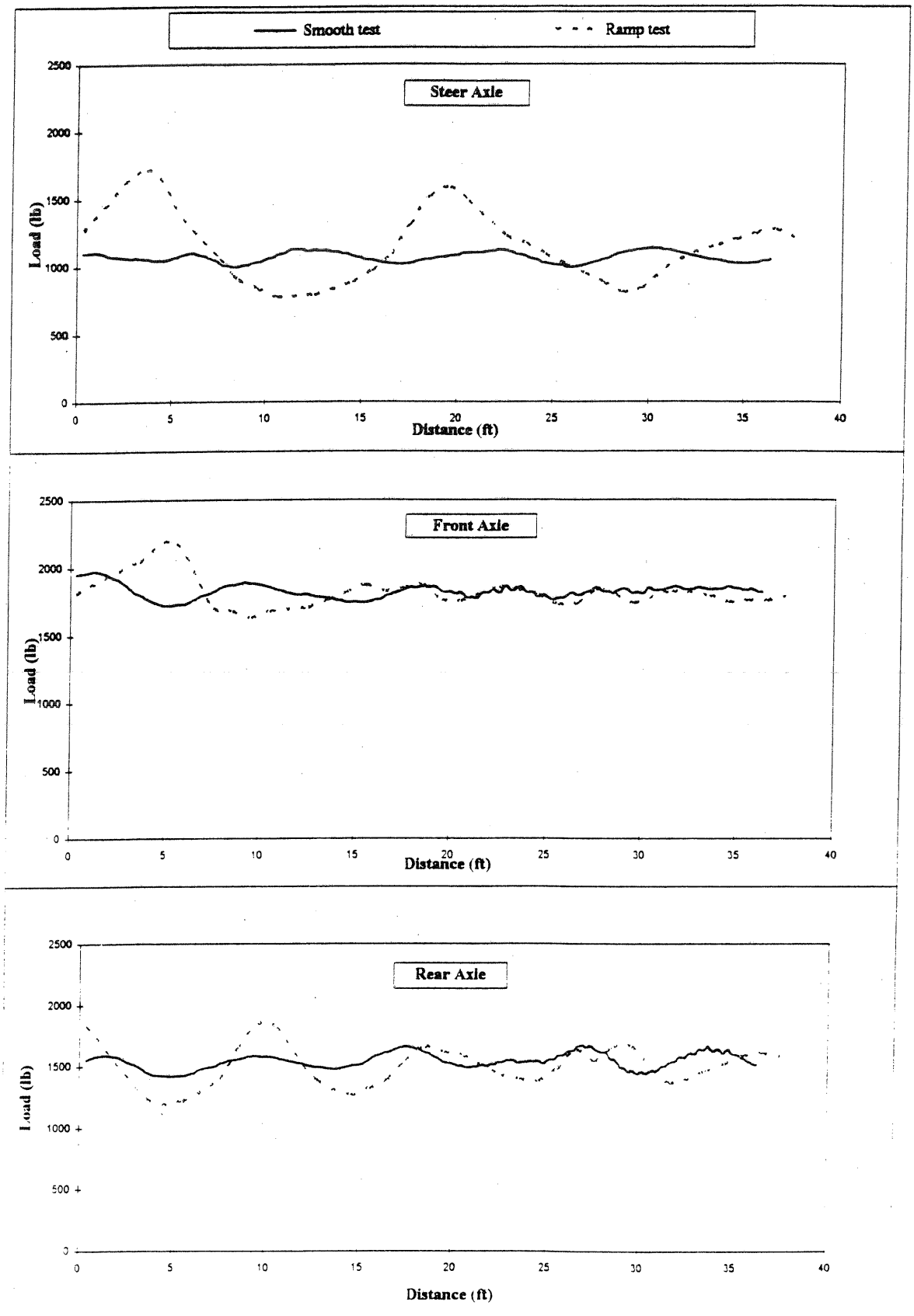

Figure 4.16 Comparison of Axle Loads for the Peterbilt 359 Generated by Pavement Profile with and without Ramp (Distance = 0 at end of roughness event)

offset and temperature effects using equations based on layered elastic theory and laboratory measured AC moduli. Figure 4.17 showed plots of the wheel load and the pavement surface strain as a function of distance for all nine runs of the PB 359 truck. The figure shows that the strain troughs and peaks reasonably match those of the load, thus supporting the use of surface strains in lieu of truck loads. Figure 4.18 shows the variation with distance of the mean and standard deviation of the surface strain for the six vehicles used in the testing. The figure shows very similar variations of high and low strains on the pavement from all trucks with a repetitive trend for all axles. The PB 330 single unit truck can be singled out from the figure as causing the highest pavement surface strains. The figure also indicates that the highest loads are attributed to the steer axle. Figure 4.19 plots the variations of the average pavement strain with distance when the data is grouped by axle and by vehicle, respectively. The figure confirms the observation that the average fluctuations of all axles are similar, with the steer axle exhibiting the highest surface strains, and that all trucks exhibit very similar fluctuations except the PB 330 which showed somewhat higher strains.

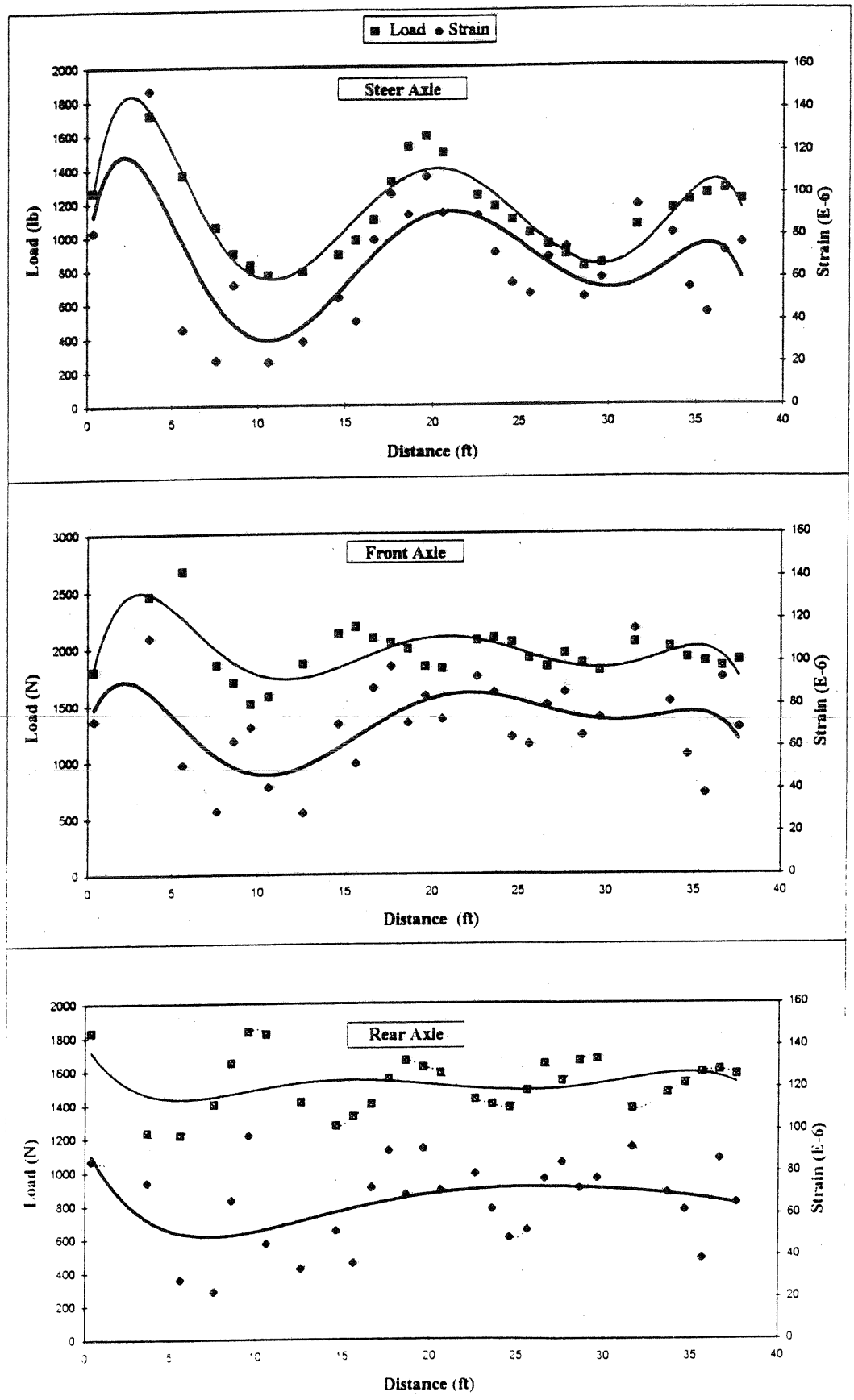

Figure 4.17 Average Load and Surface Strain Variations with Distance for Peterbilt 359 Ramp tests

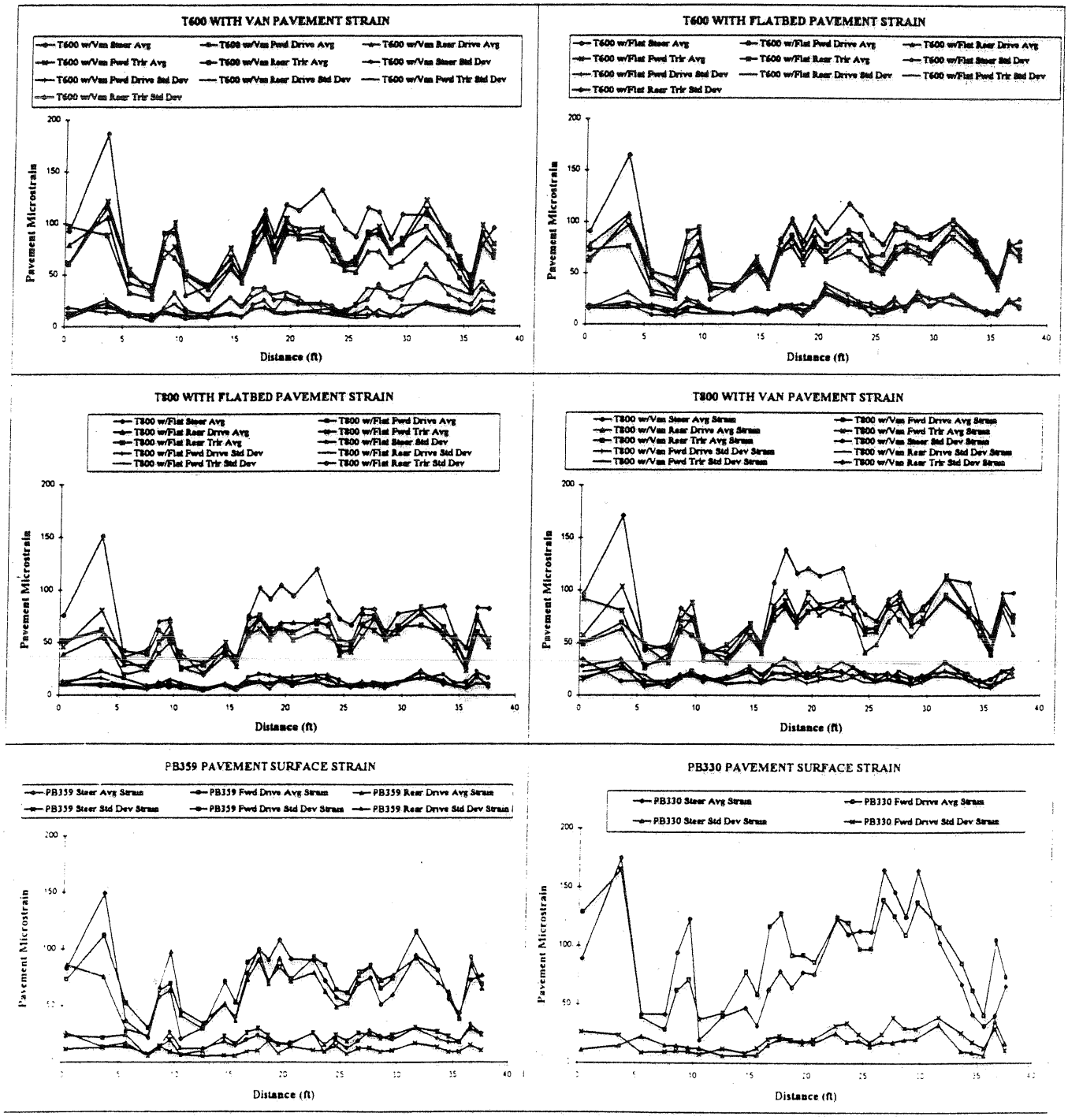

Figure 4.18 Pavement Surface Strain Variation with Distance for All Test Vehicles (Distance = 0 at end of roughness event)

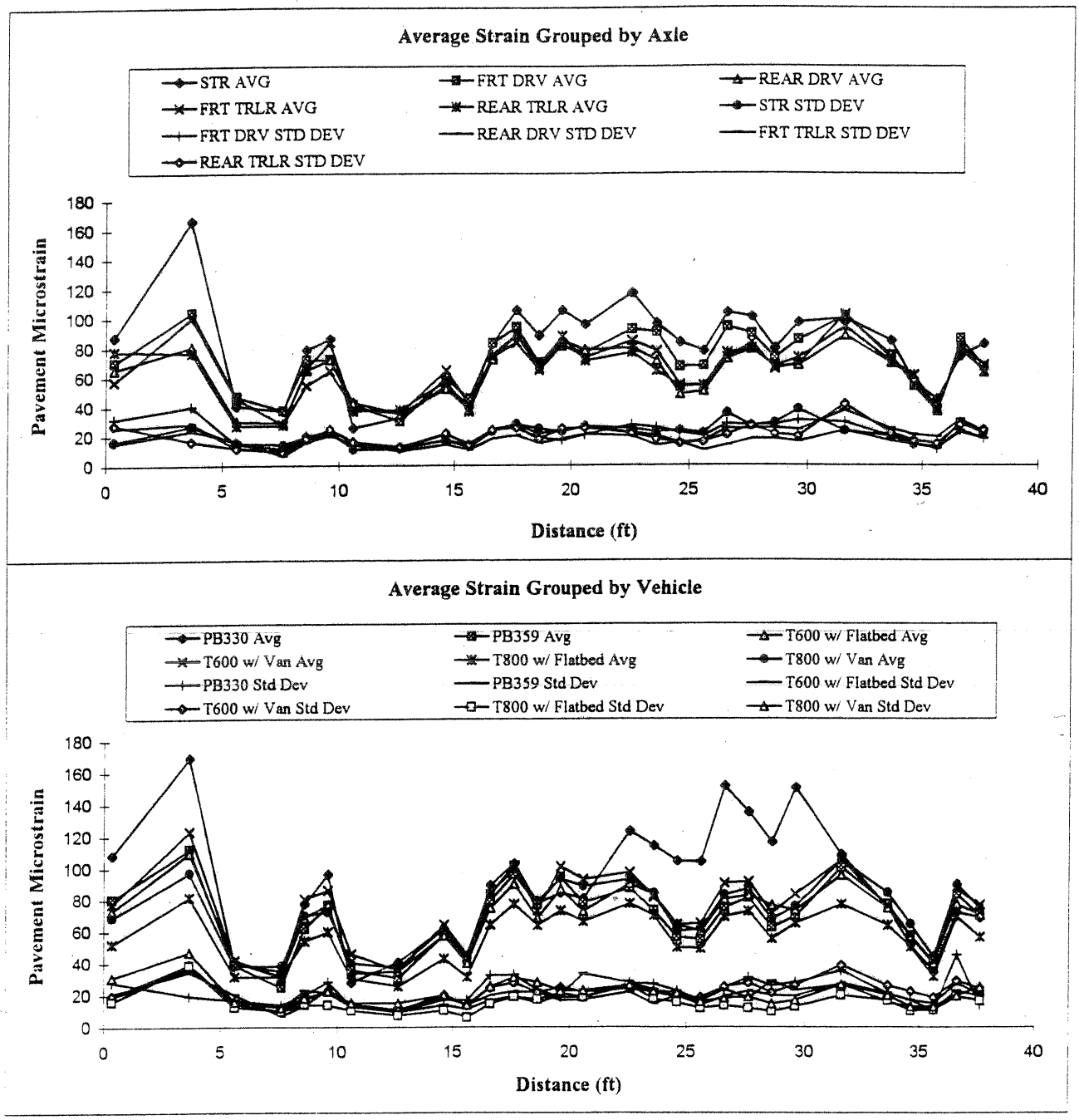

Figure 4.19 Variations of Peak Surface Strain with Distance—Grouped by Axle Type and Vehicle Type (Distance = 0 at end of roughness event)

SECTION 5

SUMMARY AND CONCLUSIONS

1. SUMMARY

A full-scale, instrumented, flexible pavement section was designed and constructed at the PACCAR Technical Center. FWD testing was conducted to characterize the layer properties of the pavement section and compare the strains measured under the FWD load to those calculated using layer elastic analysis.

A review of the available literature has shown that reasonable agreement between measured and calculated strains in AC layers can be expected under a wide variety of experimental conditions. The results of the majority of the previous experiments support the conclusion drawn by Scazziga et al. [35] and the OECD Scientific Expert Group [38] that a range of ± 20 percent represents reasonable agreement between measured and calculated strains.

From backcalculated layer moduli for the PACCAR section, it was found that the saturated condition of the subgrade triggered the stiff layer algorithm in EVERCALC 3.3. Further, a stiff layer modulus of 40 or 50 ksi (instead of the traditional value of 1000 ksi) resulted in more realistic layer moduli for the other pavement layers. This has been true over three series of FWD tests during three seasons (Fall, Summer, and Winter). Standing water year round just 50 feet from the section also supports this observation. Analysis of two locations on SR 525 yielded similar results.

Analysis of the strains under FWD loading conducted on October 10, 1991 has shown that 90 percent of the measured strains are within ± 20 percent of their calculated values. Fifty percent of the strains measured during the FWD testing conducted on February 3, 1993, were within ± 20 percent of calculated. The gauges measuring horizontal tensile strain at the bottom of the AC have shown the best agreement with theoretical strains calculated using CHEVPC.

From the results of the September 28-29, 1993, truck tests the following observations were made:

- The effect of truck speed on the response of asphalt concrete pavements is significant. Increasing truck speed form 0 to 40 mph reduced the peak tensile strain in the asphalt concrete by about 25 to 40 percent.
- The effect of tire pressure on the response of asphalt concrete pavements is significant. Decreasing the tire pressure from 90 to 30 psi reduced the tensile strain in the asphalt concrete layer by about 25 to 40 percent.
- The speed effect is somewhat reduced at lower pressures.
- The pressure effect is somewhat reduced at higher speeds.

From the results of the September 30, 1993, spatial repeatability truck tests the following observations were made:

- The different truck-trailer combinations with different axle suspensions when excited by the same roughness feature applied peak wheel loads to the same localized area in the vicinity of that feature. These results support the spatial repeatability concept of pavement damage.
- The steer axle, among all axles, caused the highest peak strains in the pavement.
- The PB 330 single unit truck with single axles and leaf spring suspensions, among the six different truck-trailer combinations, caused the highest peak strains in the pavement.

Based on work reported by Chatti et al. [96] but not reported here, several observations based on analyses performed with the SAPSI computer program are noteworthy. These include

- Speed has a more pronounced effect on vertical deflection than on tensile strain in the AC layer, as shown by theoretical SAPSI predictions.

- Tire pressure has a less pronounced effect on vertical deflection than on tensile strain in the AC layer. The analytical results show about a 10 to 15 percent increase in vertical deflection when increasing the tire pressure from 30 to 90 psi at creep speed, as compared to 50 percent for the tensile strain. At higher speeds, the effect of increasing tire pressure is to decrease the pavement's vertical deflection by as much as much as 25 percent at 60 mph.
- The analytical results from SAPSI indicate that the tensile strain at the bottom of the asphalt concrete layer is not affected by the depth of the stiff layer for all three speeds (1.7, 20 and 40 mph). The vertical deflection is affected by the depth of the stiff layer only at very low speed, with the deflection decreasing with decreasing depth to stiff layer. The results also show that only the vertical deflection at creep speed is affected by the modulus (stiffness) of the stiff layer.

2. IMPLICATIONS FOR WSDOT

The following conclusions or implications for WSDOT can be drawn.

2.1 Fundamental Pavement Response

The measured and calculated pavement strains (top and bottom of the AC layer) which resulted from the FWD testing further supports the theoretical basis for layered elastic analysis. This is important to WSDOT in that the currently used software for pavement analysis (EVERSTRS), estimation of layer moduli (EVERCALC), and AC overlay design (EVERPAVE) all use this computational approach.

2.2 Truck/Pavement Interaction

2.2.1 Truck Speed

This research further supports the view that low vehicle speeds increase critical pavement response parameters such as the horizontal strain at the bottom of the AC layer. The implication is straightforward: do not slow trucks to lower speeds unnecessarily.

This may be applied to thaw weakened pavements. Unless the pavement is rough, vehicle speeds should not be restricted. Further, the lower truck speeds on climbing lanes often exhibit increased wheelpath rutting. The reported results help to illustrate why such rutting occurs (at least in part).

2.2.2 Tire Pressures

Lower tire pressures clearly resulted in lower pavement horizontal strains. These results support the view that lower tire pressures may partially offset the pavement fatigue cracking damage incurred during spring thaw weakened conditions due to normal truck axle loads. However, fatigue cracking is not the sole pavement distress of concern during such conditions (rutting is the other).

2.2.3 Pavement Temperature

The measured pavement strains generally increased as the AC temperature increased (hence, lower mixture stiffness). This was as expected. This further supports the view that the AC fatigue cracking and rutting largely take place during warm to hot weather.

2.2.4 Spatial Repeatability

These results strongly support the view that a wide variety of vehicles, axles, and suspension types apply their peak dynamic loads at about the same location following a roughness event. This further explains why accelerated pavement damage follows a major pavement distress such as a pothole. The implication is clear: WSDOT needs to continue to maintain relatively smooth pavement surfaces in order to prevent such accelerated pavement distress. These results have implications for bridge structures as well. What is not yet available is a clear statement on the "tolerable" level of roughness.

2.2.5 Axle Loads

The static and dynamic axle loads for the Peterbilt 359 tractor were within about 10 percent of each other for the smooth pavement condition. The percent differences decreased as the test speed decreased. This further supports the view that pavements

should be maintained in a smooth condition to minimize vehicle dynamics. Additionally, the measured steer axle loads were significant when compared to the tandem drive axle loads (Peterbilt 359). This observation, in general, supports WSDOT's concern about single tire loads (versus dual tire loads).

2.2.6 Vehicle Suspensions

In general, the study results do not show significant differences in measured pavement horizontal surface strains for the different suspension systems on the various trucks tested. Based on the analyses performed thus far, these results do not support regulatory measures to encourage or discourage the use of specific suspension systems.

REFERENCES

1. Mahoney, Joe P., Steven L. Kramer, and Newton C. Jackson. "Truck/Pavement Interaction," Research Proposal, Washington State Transportation Center, Seattle, Washington, March 1991.

2. Federal Highway Administration. *Our Nation's Highways: Selected Facts and Figures.* McLean, Virginia: Office of Highway Information Management, Federal Highway Administration, September 1992.

3. Smith, Harry A. "Truck Tire Characteristics and Asphalt Concrete Pavement Rutting." *Transportation Research Record* 1307 (1991): 1-7.

4. Zube, Ernest, and Raymond Foresyth. "An Investigation of the Destructive Effect of Flotation Tires on Flexible Pavement." *Highway Research Record* 71 (1965): 129-150.

5. Winters, Brian C., "The PACCAR Pavement Test Section—Instrumentation and Validation," Thesis, Master of Science, University of Washington, Seattle, Washington, March 1993.

6. Ullidtz, Per. *Pavement Analysis.* Netherlands: Elsevier Science Publishers B.V., 1987.

7. Washington State Department of Transportation. *WSDOT Pavement Guide For Design, Evaluation and Rehabilitation.* Olympia, Washington: Washington State Department of Transportation, 1992.

8. Dorman, G.M., and C.T. Metcalf. "Design Curves for Flexible Pavements Based on Layered System Theory." *Highway Research Record* 71 (1965): 69-84.

9. Mahoney, J.P., R. Gary Hicks, and Newton C. Jackson. *Flexible Pavement Design and Rehabilitation Short Course.* Direct Federal Division, Federal Highway Administration, March 1988.

10. Dynatest. *8000 FWD Test System.* Ojai, California: Dynatest Consulting, Inc.

11. Freeme, Charles R., and Claude P. Marais. "The Structural Behavior of Bituminous Surfacings in an Experimental Asphalt Pavement." In *3rd International Conference on the Structural Design of Asphalt Pavements,* Vol. I. (1972): 812-822.

12. Chou, Y.J., and Robert L. Lytton. "Accuracy and Consistency of Backcalculated Pavement Layer Moduli." *Transportation Research Record* 1293 (1991): 72-85.

13. Hossain, Mustaque, and John Zaniewski. "Variability in Estimation of Structural Capacity of Existing Pavements From FWD Data." A Paper Submitted for Presentation at the 71st Annual Meeting of the Transportation Research Board. Washington, D.C., 1992.

14. Uzan, J., M.W. Witczak, T. Scullion, and R.L. Lytton. "Development and Validation of Realistic Pavement Response Models." In *7th International Conference on Asphalt Pavements,* Vol. I. (1992): 334-350

15. Maser, Kenneth R., and Cheryl Richter. "Ground Penetration Radar Surveys to Characterize Pavement Layer Thickness Variations at GPS Sites." A Paper Submitted for Presentation at the 72nd Annual Meeting of the Transportation Research Board. Washington, D.C., 1993.

16. Washington State Department of Transportation. *WSDOT Design Manual.* Olympia, Washington: Washington State Department of Transportation, 1992.

17. Mahoney, Joe P., Brian C. Winters, Newton C. Jackson, and Linda M. Pierce. "Some Observations About Backcalculation and Use of a Stiff Layer Condition." A Paper Submitted for Presentation at the 72nd Annual Meeting of the Transportation Research Board. Washington, D.C., 1993.

18. Hossain, A.S.M. Mustaque, and John P. Zaniewski. "Detection and Determination of Depth of Rigid Bottom in Backcalculation of Layer Moduli from Falling Weight Deflectometer Data." *Transportation Research Record* 1293 (1991): 124-135.

19. Uddin, Waheed, A.H. Meyer, and W. Ronald Hudson. "Rigid Bottom Considerations for Nondestructive Evaluation of Pavements." *Transportation Research Record* 1070 (1986): 21-29.

20. Rohde, G.T., and T. Scullion. *MODULUS 4.0: Expansion and Validation of the MODULUS Backcalculation System.* Research Report No. 1123-3. College Station, Texas: Texas Transportation Institute, Texas A&M University System, 1990.

21. Bush, A.J. *Nondestructive Testing for Light Aircraft Pavements, Phase II.* Report FAA-RD-80-9-11. Washington, D.C.: U.S. Department of Transportation, 1980.

22. Mahoney, J., D. Newcomb, N. Jackson, L. Pierce, and B. Mårtensson. *Pavement NDT Data Applications Course Notes.* Seattle, Washington: Washington State Transportation Center, January 1992.

23. "Accuracy in FWD/HWD Measurements." *Dynatest Newsletter,* Spring/Summer 1992, pp. 1-3.

24. Lenngren, Carl A. "Relating Deflection Data to Pavement Strain." *Transportation Research Record* 1293 (1991): 103-111.

25. Wester, K. "Moderators' Summary Report of Papers Prepared for Discussion at Session V." In *2nd International Conference on the Structural Design of Asphalt Pavements,* Vol. I. (1967): 638-647.

26. Nijboer, Ir L.W. "Testing Flexible Pavements Under Normal Traffic Loadings By Means of Measuring Some Physical Quantities Related to Design Theories." In *2nd International Conference on the Structural Design of Asphalt Pavements,* Vol. I. (1967): 689-705.

27. Sebaaly, Peter, Nader Tabatabaee, and Tom Scullion. *Instrumentation For Flexible Pavements.* Report FHWA-RD-89-084. McLean, Virginia: Federal Highway Administration, 1989.

28. Dempwolff, R., and P. Sommer. "Comparisons Between Measured and Calculated Stresses and Strains in Flexible Road Structures." In *3rd International Conference on the Structural Design of Asphalt Pavements,* Vol. I. (1972): 786-794.

29. Gusfeldt, K.H. and D.R. Dempwolff. "Stress and Strain Measurements in Experimental Road Sections Under Controlled Loading Conditions." In *2nd International Conference on the Structural Design of Asphalt Pavements,* Vol. I. (1967): 663-669.

30. Klomp, A.J.G. and Th. W. Niesman. "Observed and Calculated Strains at Various Depths in Asphalt Pavements." In *2nd International Conference on the Structural Design of Asphalt Pavements,* Vol. I. (1967): 671-685.

31. Miura, Yuji. "A Study of Stress and Strain in the Asphalt Pavement of Tomei-Highway." In *3rd International Conference on the Structural Design of Asphalt Pavements,* Vol. I. (1972): 476-489.

32. Valkering, C.P. "Effects of Multiple Wheel Systems and Horizontal Surface Loads on Pavement Structures." In *3rd International Conference on the Structural Design of Asphalt Pavements,* Vol. I. (1972): 542-549.

33. Halim, A.O. Abdel, Ralph Haas, and William A. Phang. "Geogrid Reinforcement of Asphalt Pavements and Verification of Elastic Theory." *Transportation Research Record* 949 (1983): 55-65.

34. Autret, P., A. Baucheron de Boissoudy, and J.C. Gramsammer. "The Circular Test Track of the "LABORATOIRE CENTRAL DES PONTS ET CHAUSSÉES" (L.C.P.C.) Nantes - First Results." In *6th International Conference on the Structural Design of Asphalt Pavements,* Vol. I. (1987): 550-561.

35. Scazziga, I.F., A.G. Dumont, and W. Knobel. "Strain Measurements in Bituminous Layers." In *6th International Conference on the Structural Design of Asphalt Pavements,* Vol. I. (1987): 574-589.

36. Bonaquist, Ramon F., Charles J. Churilla, and Deborah M. Freund. "Effect of Load, Tire Pressure, and Tire Type on Flexible Pavement Response." *Transportation Research Record* 1207 (1988): 207-216.

37. Dohmen, L.J.M., and A.A.A. Molenaar. "Full Scale Pavement Testing in the Netherlands." In *7th International Conference on Asphalt Pavements,* Vol. II. (1992): 64-82.

38. OECD Scientific Expert Group. *OECD Full-Scale Pavement Test.* France: Organization for Economic Cooperation and Development, 1991.

39. Sebaaly, P., N. Tabatabaee, B. Kulakowski, and T. Scullion. *Instrumentation For Flexible Pavements--Field Performance of Selected Sensors.* Report FHWA-RD-91-094. McLean, Virginia: Federal Highway Administration, 1992.

40. Hardy, M.S.A. and D. Cebon. "The Effects of Dynamic Axle Loads on the Response and Life of Flexible Pavements." In *7th International Conference on Asphalt Pavements,* Vol. III. (1992): 148-162.

41. Yap, Pedro. "A Comparative Study of the Effect of Truck Tire Types on Road Contact Pressure." In *Vehicle/Pavement Interaction: Where The Truck Meets The Road*, SP-765. Society of Automotive Engineers. (1988): 53-59.

42. Bu-bushait, A.A. "Development of a Flexible Pavement Fatigue Model for Washington State," Ph.D. dissertation, University of Washington, 1985.

43. Dally, James W. and William F. Riley. *Experimental Stress Analysis.* 2nd ed. New York: McGraw-Hill, 1978.

44. Johnson-Clarke, Jim. May 28, 1991. Australian Road Research Board. Facsimile Transmission.

45. Yazdani, J.I. and T. Scullion. "Comparing Measured and Theoretical Depth Deflections Under a Falling Weight Deflectometer Using a Multidepth Deflectometer." *Transportation Research Record* 1260 (1990): 216-225.

46. Measurements Group, Inc. *M-Line Accessories Instruction Bulletin B-137-15.* Raleigh, NC. 1979.

47. Rummage, Tom. Atlas Supply Co. Seattle, WA: February 3, 1993. Phone Conversation.

47. Rummage, Tom. Atlas Supply Co. Seattle, WA: February 3, 1993. Phone Conversation.

48. Sika Corporation. Technical Data Sheet, 32 Hi-Mod Epoxy. Lyndhurst, NJ. July 1990.

49. Russo, Ray. Sika Corporation. Los Angeles, California, February 4, 1993. Phone Conversation.

50. National Oceanic and Atmospheric Administration. Seattle, Washington, February 4, 1993. Phone Conversation.

51. Abbo, E. "The Influence of Heavy Vehicle Dynamics on Rigid Pavement Response," M.Sc. Thesis, Massachusetts Institute of Technology; 1987.

52. Achenback J. D., S.P. Keshava, and G. Hermann. " Moving Load on a Plate Resting on an Elastic Halfspace." Trans. ASME J. Applied Mechanics, December 1967, pp. 910-914.

53. Ahlborn, G. ELSYM5: Computer Program for Determining Stresses and Deformations in Five Layer Elastic System. University of California, Berkeley.

54. Barenberg, E. J. "Role of Instrumented Pavements in Establishing Load Equivalencies. " FHWA Load Equivalence Workshop, Washington D.C., September 1988, 27p.

55. Boquenet, D., and D. Le Houedec. "Comportement d'une chaussée reposant sur un matelas antivibratile et soumise ‡ des charges roulantes vibratoires se déplaáant ‡ vitesse constante." Annales de l'Institut Technique du B-,timent et des Travaux Publics, Paris, série: Essais et Mesures, Mar. 1979, pp.33-56.

56. Burmister, D. M. "The Theory of Stresses and Displacements in Layered Systems." Journal of Applied Physics, Vol.16, Nos. 2, 3, and 5, 1945.

57. Cebon, D. "An Investigation of the Dynamic Interaction Between Wheeled Vehicles and Road Surfaces." Ph.D. dissertation, University of Cambridge, 1985.

58. Cebon, D. "Road Damaging Effects of Dynamic Axle Loads." Proc. Int. Symp. on Heavy Vehicle Weights and Dimensions, Kelowna, British Columbia, 1986, pp. 37-53.

59. Cebon, D. "Vehicle-Generated Road Damage: A Review." Vehicle System Dynamics, 18(1-3), 1989, pp. 107-150.

60. Chatti, K. Dynamic Analysis of Jointed Concrete Pavements Subjected to Moving Transient Loads. Ph.D. Dissertation, the University of California-Berkeley, 1992.

61. Chen, S.S. The Response of Multi-layered Systems to Dynamic Surface Loads. Ph.D. Dissertation, University of California-Berkeley, 1987.

62. Chen, S. S.; "The Response of Multi-layered Systems to Dynamic Surface Loads." Ph.D. thesis, University of California-Berkeley; 1987.

63. Chou, Y. T. "Structural analysis computer programs for rigid multi-component pavements with discontinuities—WESLIQUID and WESLAYER." Tech. Reports 1, 2, and 3, U.S. Army Engineer Waterways Station, Vicksburg, Miss., May 1981.

64. DeJong, D. L.; M. G. F. Peutz, A. R. and Korswagen. Computer Program BISAR. Layered Systems under Normal and Tangential Loads. Koninklijke Shell-Laboratorium, Amsterdam, External Report AMSR.0006.73, 1973.

65. Gillespie, T.D. and C. C. MacAdam. Constant Velocity Yaw/Roll Program: User's Manual. University of Michigan Transportation Research Institute, UMTRI-82-39 (1982) 119p.

66. Gillespie, T.D., et al. Effects of Heavy-Vehicle Characteristics on Pavement Response and Performance. NCHRP Report 353, 1993.

67. Hanazato, T.; K. Ugai, M. Mori, and R. Sakaguchi. "Three-Dimensional Analysis of Traffic-Induced Ground Vibrations." ASCE Journal of Geotechnical Engineering, Vol. 117, No.8, August, 1991.

68. Hedrick, J. K., M. J. Markow, and B. Brademeyer. The Simulation of Vehicle Dynamic Effects on Road Pavements. Final Report to USDOT - Office of University Research — under Contract DTRS5684-C-0001, December 1988.

69. Holder, B. W., and C. D. Michalopoulos. "Response of a Beam on an Inertial Foundation to a Traveling Load." AIAA Journal, Vol.15, No.8, August 1977, pp. 1111-1115.

70. Huang, Y. H. "Finite element analysis of slabs on elastic solids." J. Trans. Engineering., ASCE, Vol. 100, No. 2, 1974, pp. 403-416.

71. Huang, Y. H., and S. T. Wang. "Finite element analysis of concrete slabs and its implications for rigid pavement design." Highway Res. Rec., Vol. 466, 1973, pp. 55-69.

72. Huang, Y. H., and S. T. Wang. "Finite-element analysis of rigid pavements with partial subgrade contact." Highway Research Record No. 485; 1974.

73. Huang T. C., and V. N. Shah V. N. "Elastic System Moving on an Elastically Supported Beam." J. Vibration, Acoustics, Stress and Reliability in Design, (ASME Trans.) Vol.106, April 1984, pp. 292-297.

74. Ioannides, A. M., M. R. Thompson, and E. J. Barenberg. "Finite Element Analysis of Slab-on-Grade Using a Variety of Support Models." Proceedings, 3rd International Conference on Concrete Pavement Design and Rehabilitation, Purdue University, West Lafayette, Indiana, April 1985; pp. 309-324.

75. Kenis, W. J. Predictive Design Procedures, VESYS User's Manual: An Interim Design Method for Flexible Pavements Using the VESYS Structural Subsystem. FHWA, Final Report FHWA-RD-77-154, Washington, D. C., January 1978.

76. Kukreti, A. R., M. R. Taheri, and R. H. Ledesma. "Dynamic Analysis of Rigid Airport Pavements with Discontinuities." J. Transp. Engrg., ASCE, Vol. 118, No. 3, 1992, pp. 341-360.

77. Larralde, J. Structural Analysis of Rigid Pavements with Pumping; Final Informational Report. Joint Highway Research Project JHRP-85-4, January 1985.

78. Le Houedec D. "Response of a Roadway Lying on an Elastic Foundation to Random Traffic Loads." J. Applied Mechanics, (ASME Trans.) Vol.47, March 1980, pp. 145-149.

79. Majidzadeh, K.; G. J. Ilves, and H. Sklyut. Mechanistic Design of Rigid Pavements, Volume I — Development of the Design Procedure. Final Report to FHWA Contract No. DTFH-11-9568, 1983.

80. Majidzadeh, K.; G. J. Ilves, and H. Sklyut. "RISC — A Mechanistic Method of Rigid Pavement Design." Proceedings, 3rd International Conference on Concrete Pavement Design and Rehabilitation, Purdue University, West Lafayette, Indiana, April 1985; pp. 325-339.

81. Nasim, M. A., et al. "The Behavior of Rigid Pavement under Moving Dynamic Loads." Transportation Research Board, 1990.

82. Nishizawa, T., S. Matsuno, S., and T. Fukuda. "A Mechanical Model for the Rational Design of CRCP;" Proceedings, 3rd International Conference on Concrete Pavement Design and Rehabilitation, Purdue University, West Lafayette, Indiana, April 1985; pp.341-350.

83. Rauhut, J. B., Roberts, F. L., Kennedy, T. W.; "Response and Distress Models for Pavement Studies;" Transportation Research Record 715 TRB, 1979, pp 7-14.

84. Richart, F. E. Jr.; Hall, J. R.; Woods, R. D.; Vibrations of Soils and Foundations; Prentice-Hall; 1970.

85. Roberts, F. L.; "Flexible Pavement Strains Caused by Auto Tyres;" ASCE J. Transportation Engineering, Vol.113, No.5, Sept. 1987.

86. Sebaaly, P.; Tabatabaee, N. and Scullion, T. Instrumentation for Flexible Pavements. Report FHWA-RD-89-084. McLean, Virginia: Federal Highway Administration, 1989.

87. Shah, V. N., Cook, R. D., Huang, T. C.; "Loads Moving on a Beam Supported by a Layered Elastic Foundation;" J. Mechanical Design, (ASME Trans.) Vol.102, April 1980, pp.295-302.

88. Siddharthan, R., P. Sebaaly, and Z. Zafir. Pavement Strains Induced by Spent Fuel Transportation Trucks. Preprint Paper No. 940125, TRB, National Research Council, Washington, D.C., 1994.

89. Sousa, J. M. B.. Dynamic Properties of Pavement Materials. Ph.D. Dissertation, University of California-Berkeley, 1986.

90. Sousa, J. B.; Lysmer, J.; Chen, S. S.; and Monismith, C. L.; "Effects of Dynamic Loads on Performance of Asphalt Concrete Pavements;" Trans. Res. Record 1207; 1988, pp. 145-168.

91. Tabatabaie, A. M.; Barenberg, E. J.; "Finite-Element Analysis of Jointed or Cracked Concrete Pavements", Transportation Research Record, No.671, 1978, pp. 11-19.

92. Tabatabaie, A. M.; "Dynamic Analysis of Pavement Systems-Model Evaluations"; paper presented at the 70th Annual TRB Meeting; Washington, D. C.; 1991.

93. Tayabji, S. D.; Colley, B. E.; Analysis of Jointed Concrete Pavements; Interim Report to FHWA, Report No. FHWA/RD-86/041, February 1986.

94. Winkler, E.; Study of Elasticity and Strength; H. Dominikus, Prague, 1867.

95. Winters, B. C.. The PACCAR Pavement Test Section - Instrumentation and Validation. M.S. Thesis, University of Washington-Seattle; 1993.

96. Yoshida, D. M. and Weaver, W.; "Finite-Element Analysis of Beams and Plates with Moving Loads;" Inl. Assoc. Bridge Struc. Engr. Vol. 31 (l); pp. 179-195; 1971.

97. Chatti, K., K.K. Yun, H.B. Kim, and R. Utamsingh, "PACCAR Full-Scale Pavement Tests," Report for the University of California—Berkeley and the California Department of Transportation, Prepared at Michingan State University, East Lansing, Michingan, April 1995.

98. Sweet, Brian R., "Effects of Lower Tire Pressure on Frost Weakened Roads," Research Report, Master of Science in Civil Engineering, University of Washington, Seattle, Washington, 1994.

APPENDIX A

SUMMARY OF MEASURED AND CALCULATED STRAINS FROM VARIOUS FLEXIBLE PAVEMENT EXPERIMENTS

APPENDIX A

SUMMARY OF MEASURED AND CALCULATED STRAINS FROM VARIOUS FLEXIBLE PAVEMENT EXPERIMENTS

1. INTRODUCTION

This appendix contains an overview of prior flexible pavement experiments which attempted to measure and calculate pavement strains due to an imposed load. This information was significant in this study to help assess the degree of agreement the study team might expect at the PACCAR test section.

2. NIJBOER

In 1967, Nijboer [A1] compared the strains measured under a single wheel load (2804 to 4847 lbs) on State Highway 1 in the Netherlands to those calculated using Burmister's two layer solution (partial results are summarized in Tables A.1 and A.2). Radial strain at the surface and bottom of a 7.5 inch layer of AC was measured using strain gauges attached to a thin layer of "sand asphalt" and installed during paving. The average ratio of measured to calculated strains was 0.94 at the surface and 1.01 at the bottom of the AC layer.

3. DEMPWOLFF AND SOMMER

Dempwolff and Sommer [A2] conducted a two year testing program (1967-1969) at the Shell Laboratory test track in Hamburg, Germany. The test track was constructed in two sections. Section 1 was dense graded AC and Section 2 was an open graded hot mix. The AC layer was 8.7 in. thick in both sections. The load (ranging from 1100 to 4400 lbs) was applied by way of a single tire, linear accelerated loading device. Strain responses were measured through wire strain gauges that were glued into asphalt carrier blocks. As can be seen from Table A.3, the ratio of measured to calculated strain at the

Table A.1 Comparison of Measured and Calculated Surface Radial Strains—State Highway 1, The Netherlands (after Nijboer [A1])

Test Run	Wheel Load (pounds)	AC Modulus (ksi)	Microstrains		Ratio Measured/Calculated
			Measured	Calculated	
1	2804	292	62	109	0.57
2	2804	398	65	88	0.74
3	2804	526	58	68	0.85
4	2804	384	78	74	1.05
5	4847	213	137	165	0.83
6	4847	185	213	189	1.13
7	4827	313	108	126	0.86
8	4827	228	121	164	0.74
11	4827	292	107	131	0.82
18	4827	555	84	82	1.02
19	4827	384	101	112	0.90
20	4430	1920	41	31	1.32
21	4430	1706	35	34	1.03
22	4467	1920	39	32	1.22
23	4467	1706	36	35	1.03
Mean					0.94

Calculated strains according to Burmister.

Table A.2 Comparison of Measured and Calculated Radial Strains at the Bottom of the AC Layer—State Highway 1, The Netherlands (after Nijboer [A1])

Test Run	Wheel Load (pounds)	AC Modulus (ksi)	Microstrains		Ratio Measured/Calculated
			Measured	Calculated	
1	2804	292	86	85	1.01
2	2804	398	92	68	1.35
3	2804	526	73	53	1.38
4	2804	384	84	67	1.25
5	4847	213	112	145	0.77
6	4847	185	155	136	1.14
7	4827	313	123	112	1.10
11	4827	292	100	118	0.85
18	4827	555	83	80	1.04
19	4827	384	100	110	0.91
20	4430	1920	28	30.5	0.92
21	4430	1706	27	33.5	0.81
22	4467	1920	28	31.5	0.89
23	4467	1706	25	34.5	0.72
Mean					1.01

Calculated strains according to Burmister.

Table A.3 Comparison of Measured and Calculated Strains at the Bottom of the AC Layer—Shell Laboratory Test Track, Hamburg (after Dempwolff and Sommer [A2])

	Section I Depth in AC Layer (in.)				Section II Depth in AC Layer (in.)			
	0	2.6	5.5	8.7	0	2.6	5.5	8.7
Measured / Calculated	1.7-2.2	1.8-2.2*	1.4-1.8	0.9-1.0	1.7-2.0	1.8-2.0*	0.8-1.6	0.9-1.2

* Maximum tensile strain measured at temperatures above 25°C.
All strains calculated using BISTRO.

bottom of the AC layer for both sections is quite good (0.9-1.0 for Section 1 and 0.9-1.2 for Section 2). The strains measured at the surface were always larger (35-100 microstrains) than the theoretical values, and as such, the measured to calculated ratios are less than satisfactory. An interesting observation made by Dempwolff and Sommer [A2] was that, contradictory to theory, the longitudinal and transverse strains were not equivalent. The transverse strains were larger (5-50 percent) than the longitudinal strains. The authors provided no explanation for this observation. Given the extensive research into contact pressure distribution of loaded truck tires conducted in recent years, such results should be expected. The maximum contact pressures can be as high as two times the inflation pressure. Also, at a constant tire inflation pressure, the contact pressure in the shoulder region of a bias ply tire can increase substantially for a modest increase in tire load. [A3]

4. HALIM

In 1983, Halim et al. [A4] compared measured and theoretical strains in flexible pavements using a test site at the Royal Military College in Kingston, Canada. The main objective of the research was to evaluate the effectiveness of flexible pavements reinforced with a plastic mesh (geogrid). A secondary benefit was the ability to verify or modify elastic layer theory. To conduct this analysis, two foil type strain gauges were embedded in a mastic strain carrier and placed at the bottom of the AC layer. Loads were applied to the test sections through a hydraulic actuator on a 12 inch diameter rigid circular plate. For a load of 9000 pounds the measured and calculated strains at the bottom of the AC compared quite well; a difference of only 3 to 5 percent (Table A.4). However, the comparison at lower load levels using a constant layer modulus (calculated at a 9000 pound load) was progressively worse. To compensate for this effect the authors applied a calibration factor to the layer modulus (the calculation of the calibration factor is discussed in detail in Halim [A4]). The calibration factor (F_p) is the ratio of the elastic

Table A.4 Comparison of Measured and Calculated Strains at the Bottom of the AC Layer—RMC Test Pit (after Halim et al. [A4])

Load pounds	Calibration Factor F_p	AC Modulus (ksi) $E_p = F_p \times E_{4c}$	Subgrade Modulus (ksi) $E_p = F_p \times E_{40}$	AC Thickness (inches)	Microstrains				
					Measured	Calculated		Error %	
						E_{4c}	E_p	E_{40}	E_p
2250	0.905	184	3.1	6.5	243	179	200	26%	18%
4500	1.000	203	3.4	6.5	358	358	358	0%	0%
6750	1.034	210	3.5	6.5	475	536	518	-13%	-9%
9000	1.000	203	3.4	6.5	680	715	715	-5%	-5%
2250	0.905	127	2.3	7.9	282	191	215	32%	24%
4500	1.000	140	2.6	7.9	475	382	382	20%	20%
6750	1.034	145	2.6	7.9	622	573	555	8%	11%
9000	1.000	140	2.6	7.9	805	765	765	5%	5%
2250	0.905	162	2.0	9.8	122	110	125	10%	-2%
4500	1.000	179	2.2	9.8	217	226	226	-4%	-4%
6750	1.034	185	2.3	9.8	315	330	328	-5%	-4%
9000	1.000	179	2.2	9.8	440	452	452	-3%	-3%

Table A.5 Composition of OECD Group RTR 12 "Full Scale Pavement Tests" (after Scazziga [A5])

Country Name	**Participated In Nardò Experiments**
Australia	Yes
Belgium	No
Canada	Yes
Denmark	Yes
Finland	Yes
France	Yes
Germany	Yes
Italy	Yes
Japan	No
Switzerland	Yes
United Kingdom	No
United States of America	No

modulus of the asphalt or subgrade layer under the load (p) to the elastic modulus at a load of 9000 pounds. The modulus (E_p) for the asphalt or subgrade is then determined by multiplying the modulus at 9000 pounds by the calibration factor. As can be seen in Table A.4, this decreased the error in measured and calculated strains by as much as 8 percent.

5. OECD/NARDÒ TEST

One of the largest instrumented pavement studies was conducted by the Organization for Economic Cooperation and Development (OECD) Group RTR I2 "Full Scale Pavement Tests." The membership of the group represented 12 countries (Table A.5) and was established in March of 1983. The group had three basic objectives for instrumented pavement testing [A5]:

- develop and perpetuate a common technical language for pavement testing
- provide a framework for direct comparison of research results across differing nations
- conduct some common pavement tests under the same testing conditions.

In April of 1984, Group RTR I2 conducted a landmark instrumented pavement test. The test was important for two major reasons:

- The number and variety of participating organizations (see Table A.5). Nine teams from eight member countries installed their own gauges using their own techniques.
- The variety of strain gauges employed. Seven different gauges representing three gauge groups were installed in the test section (Figure A.1).

The purpose of the test was to compare the instruments and techniques used by member countries to measure the horizontal tensile strain at the bottom of the AC layer generated by the rear axle of a loaded truck.

For ease in comparing measured responses, three of the test conditions were controlled to the extent possible given the nature of such testing.

GROUP	SCHEMATIC CONSTRUCTION	GAUGE MODEL	ACTIVE LENGTH OF WIRE/ ANCHOR	RESIST-ANCE (Ω)	COST US $	TEAM	ASSEMBLY
1.1	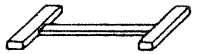	KYOWA KM-120-H2-11L 100-3	70mm/104mm	120 ± 1%	40	3	- FIXATION OF ANCHOR BARS IN THE LABORATORY
		KYOWA KM-120-H2-11L 100-3	70mm/106mm	120 ± 1%	35	5	
		KYOWA KM-120-H2-11L 100-3	70mm/100mm	120 ± 1%	75	7	
1.2	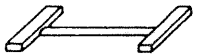	KYOWA KC-70-A1-11	67mm/130mm	120	35	2	- GAUGE GLUED TO SUPPORT AND FIXATION OF ANCHOR BARS IN THE LABORATORY
		PL 30 ou KYOWA KFC-30-C1-11	30mm/100mm	120	23	6	
1.3	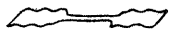	HBM DA 3	88mm/140mm	350	180	1	
2.1		HBM LP 21 60-120	60mm/60mm	120	12	1	- GLUED ON MARSHALL SPECIMEN CUT TO 1/3 HEIGHT
		BLH FAE 2-300-35 PL	76mm/76mm	350	35	8	- GLUED ON LABORATORY SPECIMEN
2.2	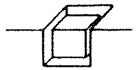	HBM 20/600 XA21	20mm/20mm	600±0.25	10	9	- GLUED IN THE CENTER OF A LABORATORY SPECIMEN
2.3	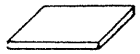	METAL FOIL GAUGE	13mm/25mm	120	15	4	- GLUED ON A BLOC OF SHEET ASPHALT
3.1		HBM LP 21 60-120	60mm/60mm	120	12	1	- GLUED ON CORE TAKEN FROM THE PAVEMENT
		HBM 60/600 LP 21		600±0.25	15	3	

Figure A.1. Classification of Gauges Installed at the Nardò Test Facility [A5]

- Pavement Structure — The test was conducted on a 131 foot section of an experimental road at the Nardò test facility in southern France. The section consisted of a 5.1 inch AC layer on top of a 6.7 inch crushed stone base. Each team was given about 9.8 linear feet of the section in which to install their instruments.

- Applied Load — There were three almost identical trucks used throughout the testing cycle. These 2 axle trucks had a single tire steer axle and a dual tire drive axle. The axle loads, tire types, and tire pressures were the same for all three trucks and held constant throughout the testing.

- Loading Time — Truck speed was held reasonably close to 19 mph.

As is common in most field experiments, there were some variables of the testing environment that were either uncontrollable or lacking sufficient control for meaningful comparisons.

- Pavement Structure — Even though the experiment was performed over a relatively short pavement section, there were still significant differences in the pavement structure across the teams' sites (see Figure A.2). The AC thickness varied from 4.6 inches to 5.4 inches. The void content was as low as 11 percent and as high as 19 percent. The high void content was due to the special procedures used during paving operations to prevent damage to the gauges.

  To account for this variability several actions were taken. First, BISAR was used to determine the effect (theoretically) of the differing AC layer thicknesses on strain at the bottom of the AC. An 18 percent difference (4.6 to 5.4 inches) equated to only a 5 percent decrease in strain. Additionally, cores were taken from each team's area at the conclusion of testing to accurately determine the layer thicknesses. The difference in the material properties was accounted for by using backcalculated layer moduli from FWD tests conducted at each team's site.

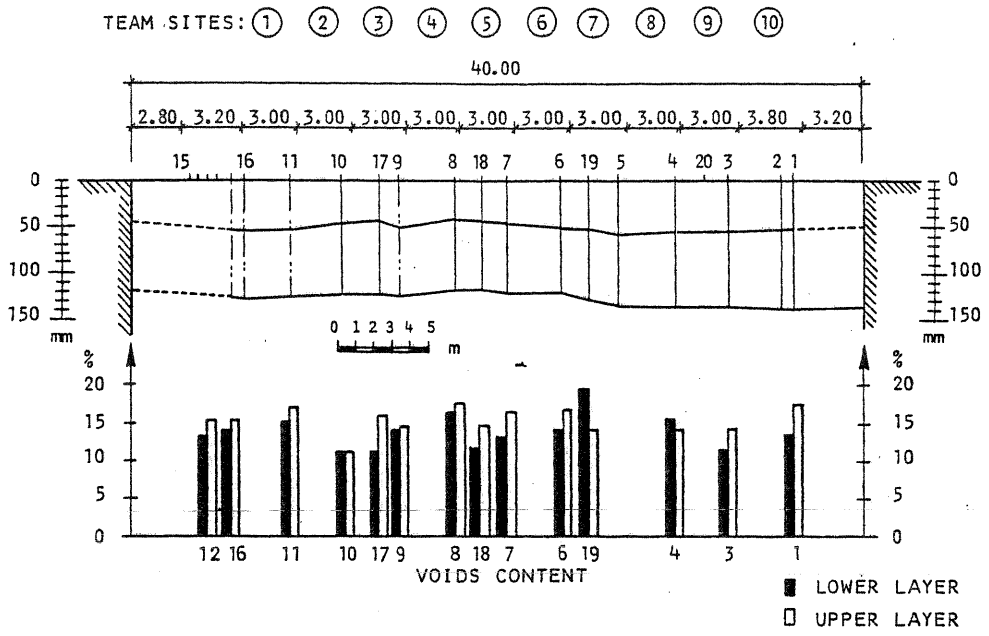

Figure A.2 Thickness and Voids Content of the AC Layer—Nardò Test Facility [A5]

- Pavement Temperature — The pavement temperature as measured by three teams varied by as much as 18° F. Theoretical analysis using BISAR demonstrated that only a 9° F difference in temperature equaled a 50 percent difference in calculated strain. To account for this, all responses were standardized to 75° F.

- Actual Gauge Location in Reference to the Bottom of the AC — Once again using BISAR, it was determined that a difference of only 0.2 of an inch could cause a 10 percent difference in measured strain. A 0.8 inch difference equaled a 30 percent error. To solve this potential source of error, the exact position of the gauge in the AC layer was determined.

- Transverse Vehicle Position — It became obvious during testing that it was virtually impossible to drive the test vehicle over the exact gauge location over repeated test runs (due to driver variability). Calculations with BISAR showed that the maximum strain at the bottom of the AC under the dual wheel load was 50 percent less at a distance of only 2 inches outside the outer wheel. There was no practical solution to account for this potential variability and as such, must be kept in mind when reviewing the results of the experiment.

The results of the experiment are summarized in Figures A.3 to A.6. Figure A.3 shows the mean and standard deviation of all the strain measurements standardized at 75° F. It appears that some gauges (1.1, 2.2, and 2.3) performed better than others. The variability in the results is attributed to gauge repeatability and truck alignment. In an attempt to reduce the effect of truck alignment the mean and standard deviation of the maximum strains were presented in the same format (Figure A.4). The mean of the strain maxima from Figure A.4 gives a range of 181 to 357 microstrains. Taking into account varying layer thicknesses and gauge locations, BISAR calculated values ranged from 168 to 263 microstrains. While the range of the measured values is somewhat larger than the theoretical, the mean of all the strain maxima (about 260 microstrains) falls within that theoretical range rather nicely.

The moduli backcalculated from the FWD deflection data were used in the Method of Equivalent Thickness (MET) to calculate the theoretical horizontal tensile

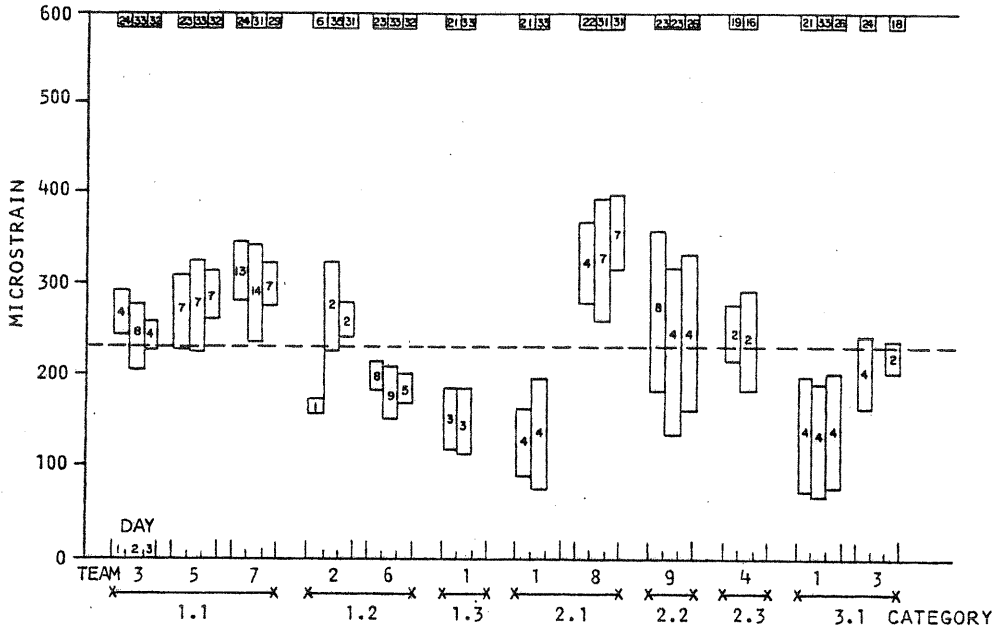

Figure A.3 Mean and Standard Deviation of Strain Measurement Results at 75° F, All Gauges, By Day of Measurement, Team and Gauge Category—Nardò Test Facility [A5]

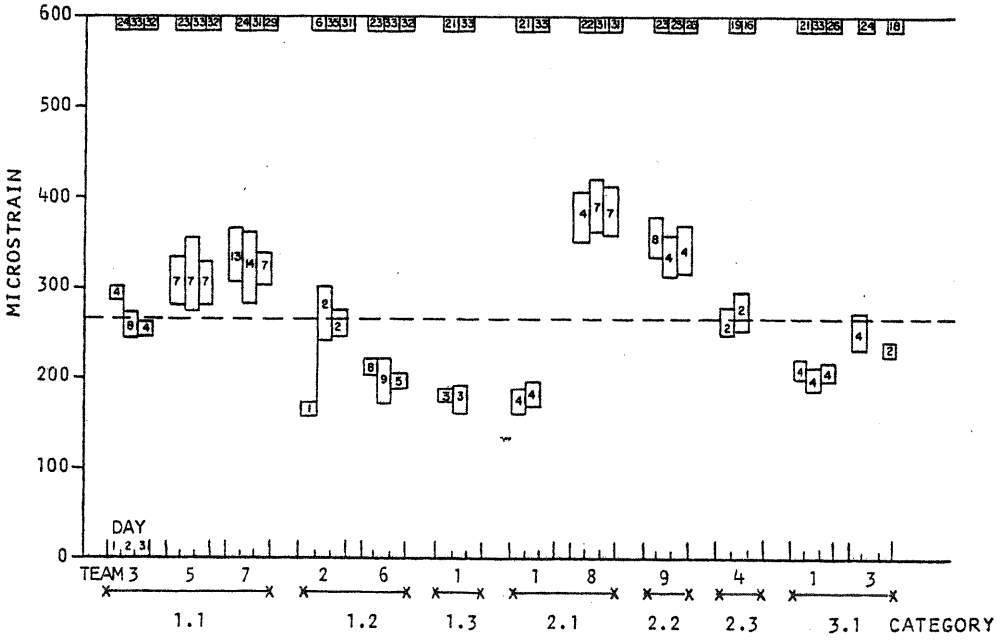

Figure A.4 Mean and Standard Deviation of Maximum Strains at 75° F, All Gauges, By Day of Measurement, Team and Gauge Category—Nardò Test Facility [A5]

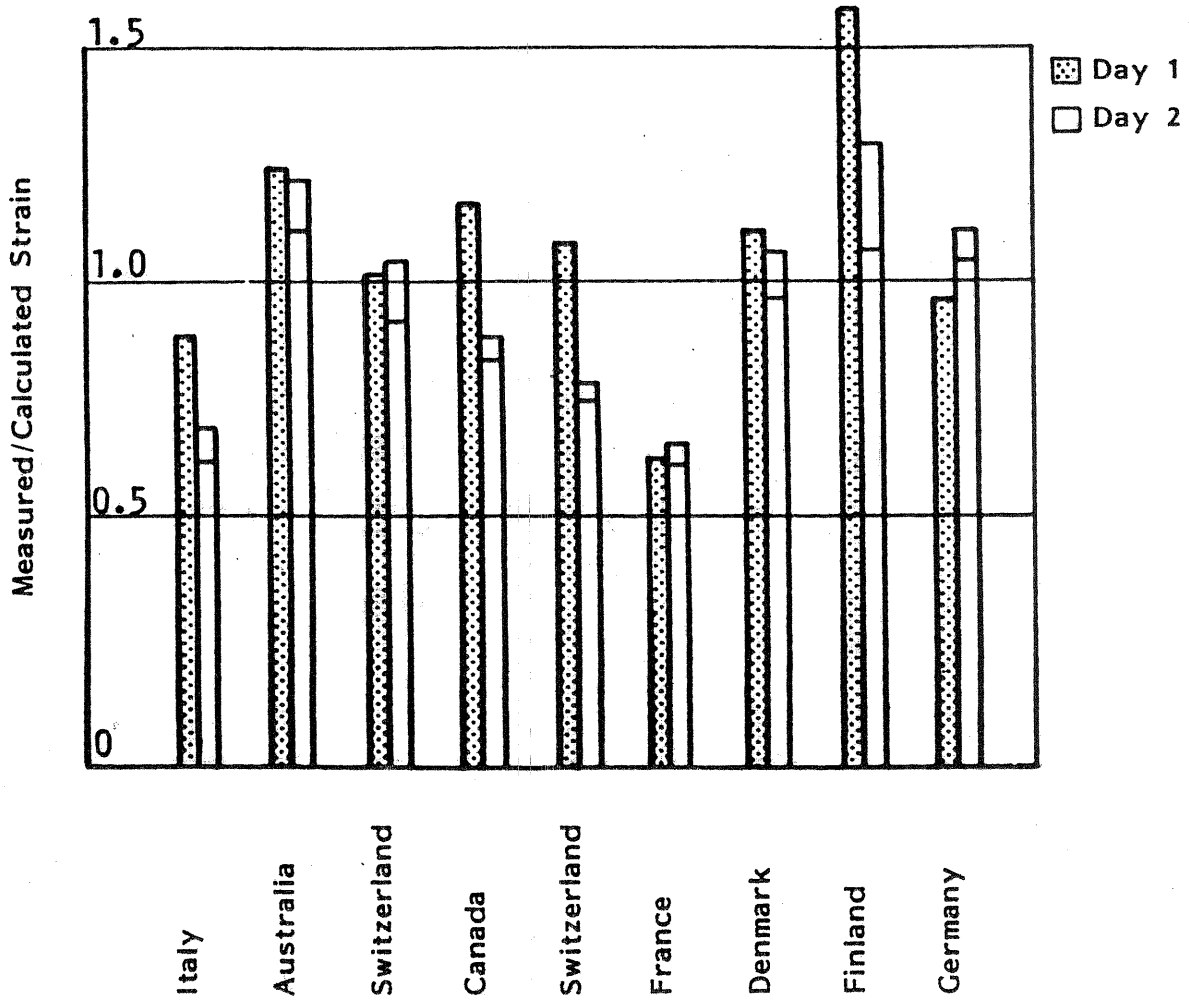

Figure A.5 Ratio of Measured to Calculated Strain from FWD Testing—Nardò Test Facility [A5]

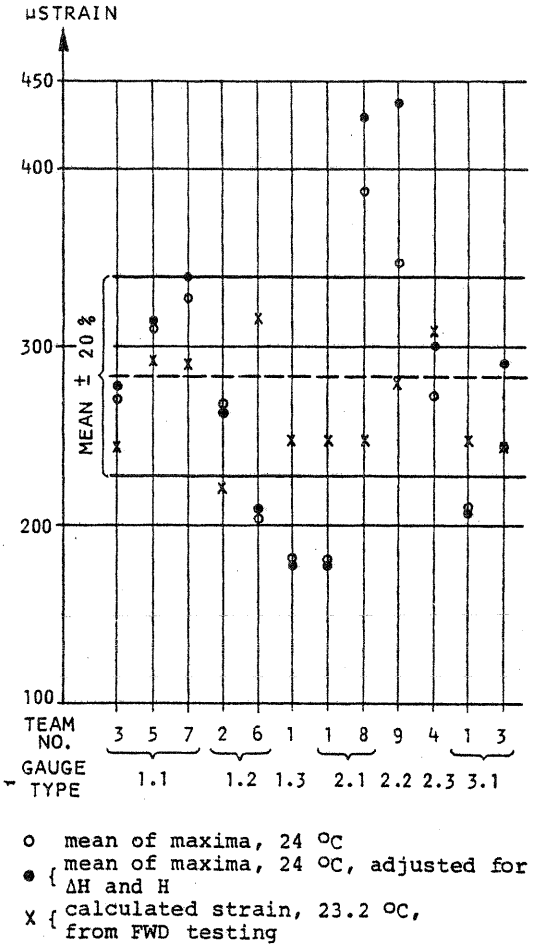

Figure A.6 Comparison of Measured and Calculated Strains Adjusted for AC Temperature, AC Thickness, and Gauge Location—Nardò Test Facility [A5]

strain under a dual wheel load. A comparison of these calculated strains to strains measured during truck testing at a similar pavement temperature is presented in Figure A.5. Most of the ratios are within ± 20 percent of equality.

A final comparison is presented in Figure A.6. The mean of all maximum strains (adjusted only for temperature) is shown with a range of ± 20 percent. Three sets of data for each team and gauge combination are compared to this range: strain calculated based on FWD moduli, mean of measured strain maximums, and mean of measured strain adjusted for layer thickness and gauge position. Most of the strains fall within the 20 percent range. Given the number of groups and techniques, the agreement was "astonishingly good." [A5]

6. DOHMEN AND MOLENAAR

Dohmen and Molenaar [A6] provided a review of three full scale pavement tests conducted by Dutch pavement engineers. All three tests showed reasonable agreement between measured and calculated strains.

The first test was performed on test pavements at the Delft University test facilities. These pavements were subjected to 1,000,000 repeated plate loads. Before each application of 100,000 loads, strains generated by the load of a FWD were analyzed at a point 0.3 inches above the bottom of the AC layer. For the first series of tests, the thickness of the AC surface was 9.4 inches. The AC layer thickness was reduced by milling before each subsequent application of loads. The AC thickness for the second and third test series was 7.1 inches and 4.7 inches respectively. The agreement between measured and calculated strains for each series was extraordinary (Table A.6).

The second test was conducted at the Laboratoire Central des Ponts et Chaussées (LCPC) facility in Nantes, France during the First OECD Road Common Experiment (FORCE). Once again, the measured and calculated strains (using BISAR) at the bottom

Table A.6. Comparison of Measured and Calculated Strains — Delft University Test Facility (after Dohmen and Molenaar [37])

Surface Thickness	Microstrain		Ratio
	Measured	Calculated	Measured/Calculated
9.4 in.	50	50	1.00
7.1 in.	79	78	1.01
4.7 in.	191	190	1.01

Strains calculated using BISAR.

of the AC layer under a FWD load were compared. The Dutch team conducted testing in two sections of the test pavement. Section 01 had a 4.8 inch (123 mm) AC surface and Section 02 had a 5.5 inch (139 mm) AC surface. Figures A.7 and A.8 show the results for sections 01 and 02 respectively. Dohmen and Molenaar proposed that the scatter in the data for both sections was caused by variability in the alignment of the FWD over the strain gauges. For Section 01, Dohmen and Molenaar suspect that difficulty in backcalculating the layer moduli and possible cracking at the bottom of the AC layer also contributed to the disagreement.

The third study was performed at the Road and Railroad Lab (RRRL) of the Delft University of Technology. In this analysis, the strains at the bottom of the AC layer were measured in both the longitudinal and transverse directions. Comparisons of these measured and calculated strains due to a FWD load are shown in Figures A.9 and A.10. The variation in the measured strains is attributed to the gauge installation procedure and the uncertainty of FWD placement over the gauges. The relationship between transverse and longitudinal strains observed by Dohmen and Molenaar was opposite of that observed by Dempwolff and Sommer. [A2] In their study (Dohmen and Molenaar [A6]), the transverse strains were smaller than longitudinal strains for which no explanation was offered. The difference seen between the two tests (FWD and truck tire) could be attributed to the source of load and its potential effect based on placement over the exact

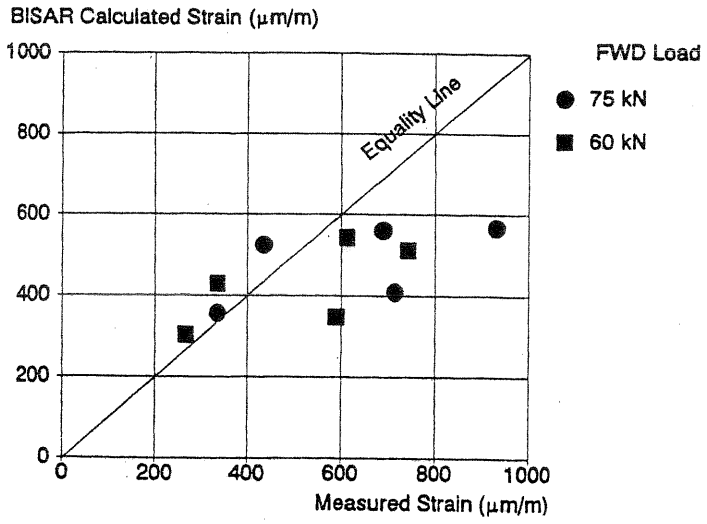

Figure A.7 Comparison of Measured and Calculated Strains Due to a FWD Load—Section 01, FORCE Project [A6]

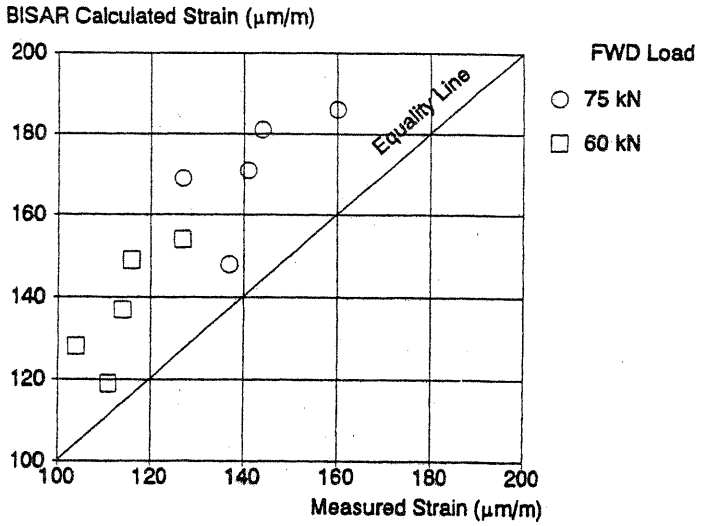

Figure A.8 Comparison of Measured and Calculated Strains Due to a FWD Load—Section 02, FORCE Project [A6]

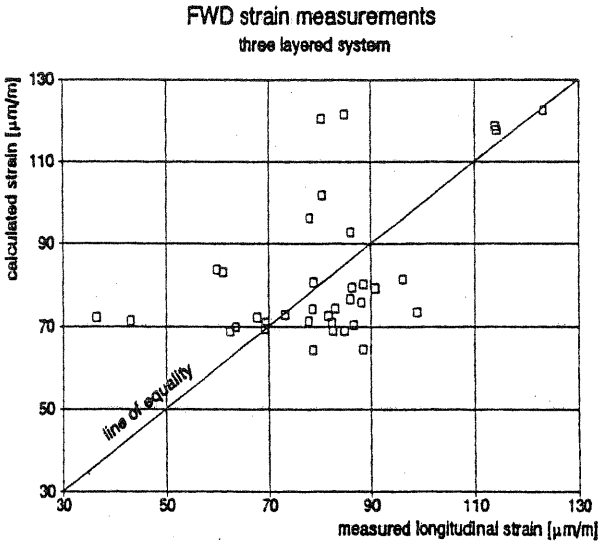

Figure A.9 Comparison of Measured and Calculated Longitudinal Strains Due to a FWD Load—RRRL, Delft University of Technology [A6]

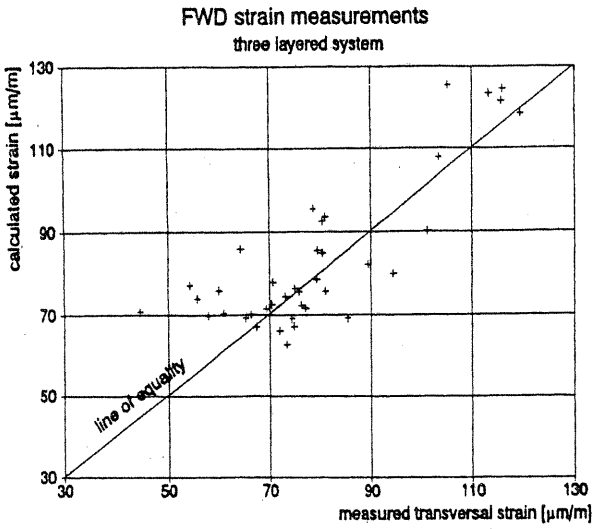

Figure A.10 Comparison of Measured and Calculated Transverse Strains Due to a FWD Load—RRRL, Delft University of Technology [A6]

gauge location. By examining the response of only one gauge in one of the pavement sections, Dohmen and Molenaar have shown good agreement (see Figure A.11).

Following the FWD testing, further testing was performed on the same test section using LINTRACK. LINTRACK is the linear ALD of the Delft University. Dohmen and Molenaar compared both longitudinal and transverse strains at the bottom of the AC layer as calculated by BISAR and those measured under dual tires and super singles. They did find that the transverse strain under the center of the load was less than the longitudinal strain, as seen with a FWD load. The difference was approximately 15-20 microstrains under the super singles and 30-40 microstrains in the dual wheel configuration. Dohmen and Molenaar suspect that the difference between the actual and modeled contact pressure distribution could possibly have affected this difference.

7. SEBAALY

One of the more recent instrumented flexible pavement studies was conducted by Sebaaly et al. [A7] in 1989. One of the three main objectives of the study was to compare measured strains to calculated strains generated by mechanistic models. The test pavement consisted of two sections. The thick section had a 10 inch AC layer and the thin section had a 6 inch AC layer. The test vehicle was a single drive axle tractor pulling a tandem axle semi-trailer. One unique aspect of the testing program was a comparison of the performance of four different types of strain gauges as listed below.

- Dynatest H - gauge
- Kyowa H - gauge
- Alberta Research Council (ARC) gauge
- Core gauge

The first three gauge types were installed during construction (after construction of the base course but before paving operations). The core gauges were retrofitted after construction. This provided the ability to compare the performance of gauges installed during construction to those installed in pavement cores. The results of this comparison

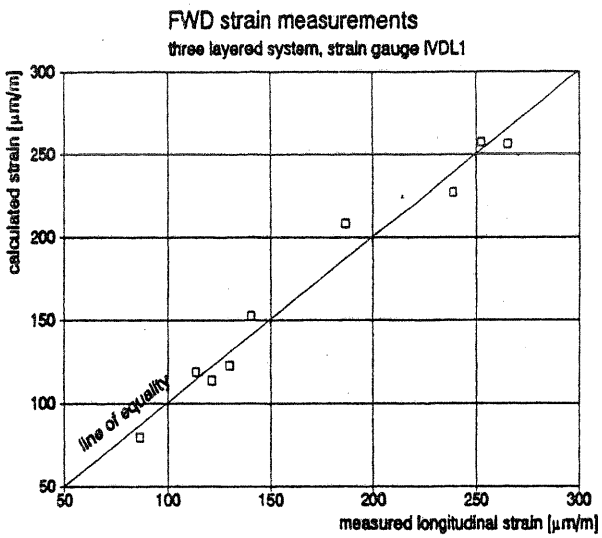

Figure A.11 Comparison of Measured and Calculated Longitudinal Strains Due to a FWD Load for Gauge IVDL1—RRRL, Delft University of Technology [A6]

would help address the uncertainties in instrumenting in-service pavements. The results from both sections at two loads are shown in Figures A.12 to A.15 which contain two sets of data points. The data points forming the band represent the upper and lower limit for the calculated strain based on a known deviation in AC layer thickness of ± 0.5 inch. The second set of points represent the mean and ± one standard deviation of the measured strain responses. For the thin section, the difference between measured and calculated response is small for all gauges except the ARC gauge. The thick section shows more variability but good agreement is evident for some of the gauges. The fact that the measured strains are greater than calculated at some stations and less than calculated at other stations is attributed to the dynamic load profile. It is interesting to note that the core gauge performed as well as, if not better than, the other gauge types.

8. LENNGREN

At about the same time Sebaaly et al. [A7] were conducting their work in the U.S., Lenngren [A8] was comparing measured to calculated strains at the instrumented pavement test section at The Road and Traffic Laboratory in Finland. The test section contained two pavement structures. The thin structure had a 3.1 inch AC layer on top of a base and subbase totaling 24.4 inches. The 5.9 inch AC layer of the thick structure was above a base and subbase of 21.7 inches. The base and subbase of both structures were composed of sand and gravel; the only difference being in maximum aggregate size (1 in. in the base, 2 in. in the subbase). The instrumentation in this section consisted of strain gauges glued to 6 inch diameter cores retrofitted to the pavement. Horizontal tensile strains at the bottom of the AC layer were measured under the load generated by a KUAB 50 FWD. Three load levels were used: 2000, 5000, and 11,000 pounds. Layer moduli were backcalculated from the FWD deflection data using CLEVERCALC (a metric modification of EVERCALC). A comparison of the strains measured under the FWD load and calculated by CLEVERCALC for both structures is shown in Tables A.7 and

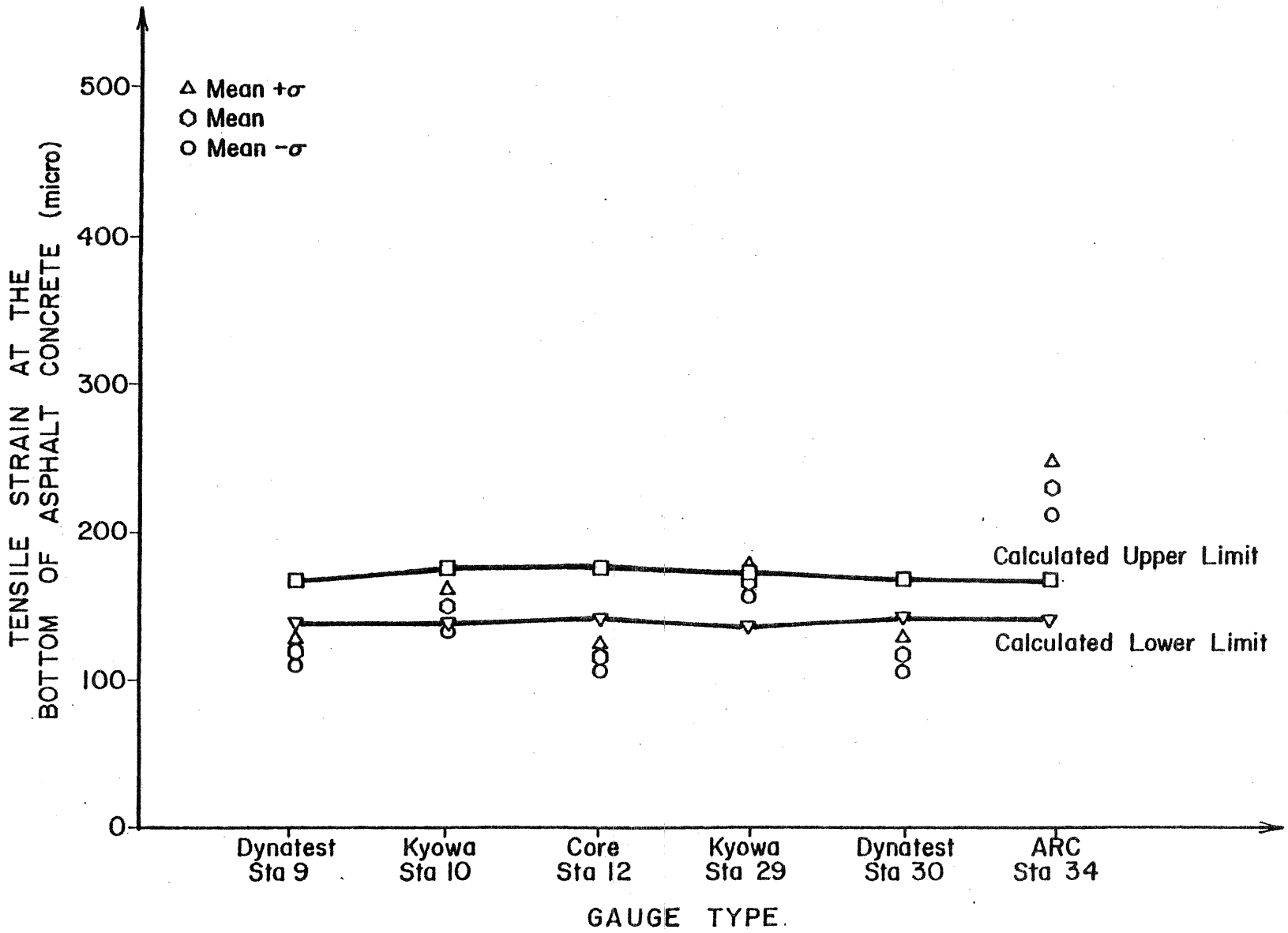

Figure A.12 Comparison of Measured and Calculated Strains under a Drive Single Axle Load of 12,000 Pounds—Thin Section [A7]

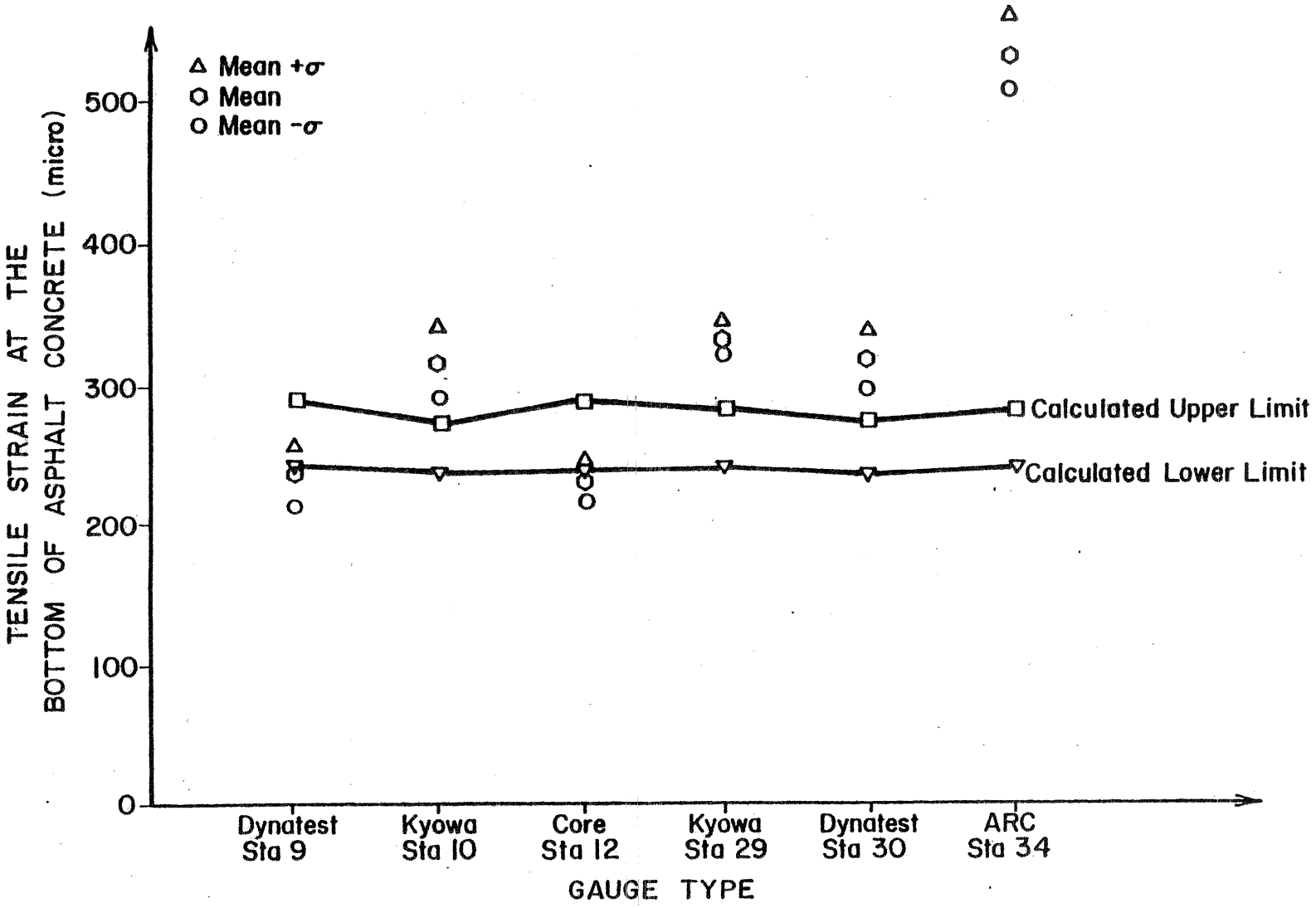

Figure A.13 Comparison of Measured and Calculated Strains under a Drive Single Axle Load of 20,000 pounds—Thin Section [A7]

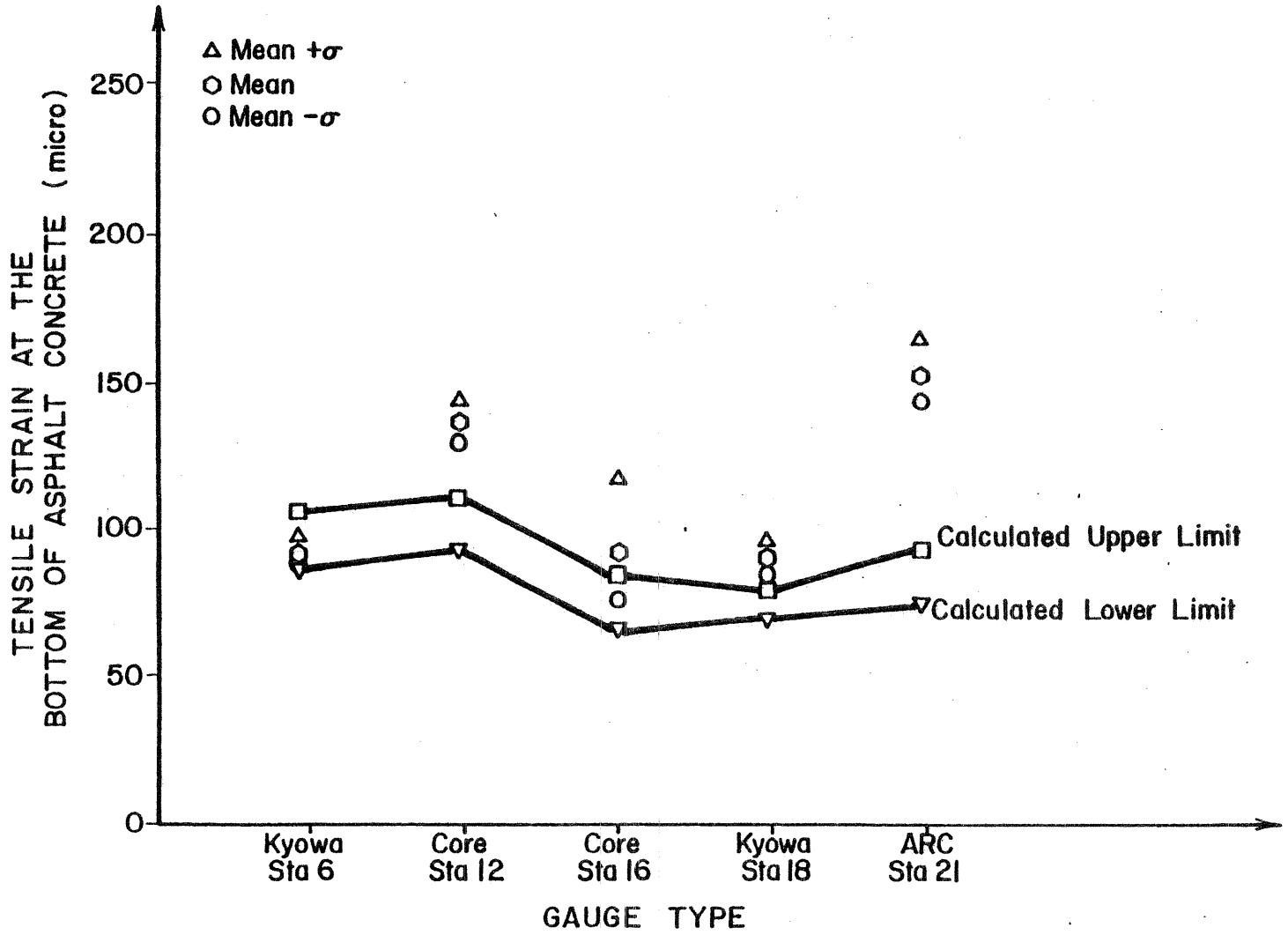

Figure A.14 Comparison of Measured and Calculated Strains under a Drive Single Axle Load of 12,000 pounds—Thick Section [A7]

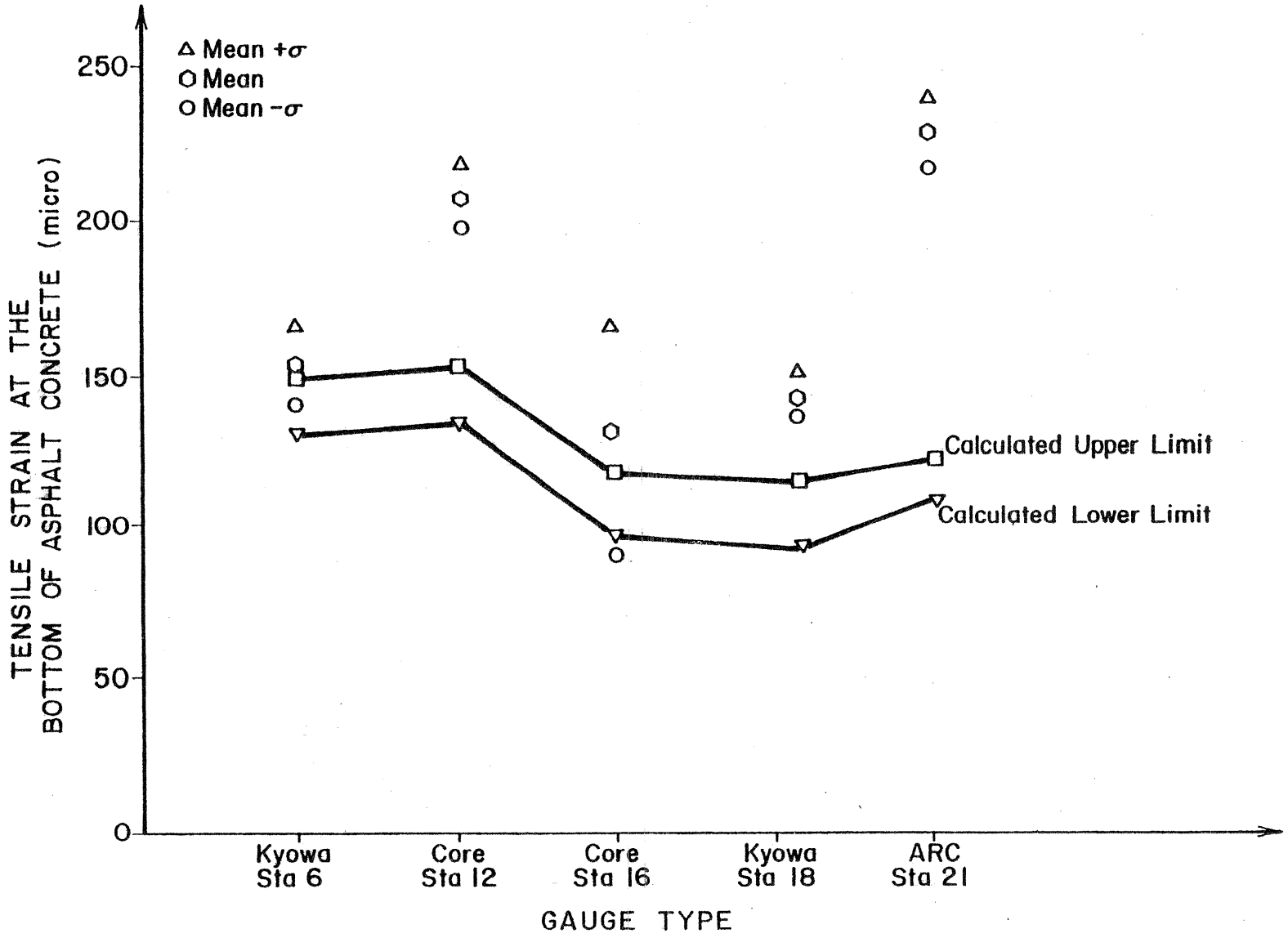

Figure A.15 Comparison of Measured and Calculated Strains under a Drive Single Axle Load of 20,000 pounds—Thick Section [A7]

Table A.7 Comparison of Measured and Calculated Strains at the Bottom AC Layer—3.1 inch Section: Road and Traffic Laboratory, Finland (after Lenngren [A8])

Time	Load (pounds)	Microstrains		% Difference
		Measured	Calculated	
pm	11723	283	295	-4%
pm	11723	283	284	0%
pm	5715	159	174	-9%
pm	5715	159	167	-5%
pm	5715	158	176	-11%
pm	5715	158	167	-6%
pm	2880	84.8	95	-12%
pm	2880	84.8	87	-3%
pm	2880	84.2	82	3%
pm	2880	84.2	81	4%

Absolute Average 6%
Arithmetic Average -4%

Strains calculated using CLEVERCALC.

Table A.8 Comparison of Measured and Calculated Strains at the Bottom of the AC Layer—5.9 inch Section: Road and Traffic Laboratory, Finland (after Lenngren [A8])

Time	Load (pounds)	Microstrains		% Difference
		Measured	Calculated	
pm	11273	185	189	-2%
pm	11273	185	178	4%
pm	11318	183	186	-2%
pm	11318	183	182	1%
pm	5715	95.9	103	-7%
pm	5715	95.9	104	-8%
pm	2880	48	57	-19%
pm	2880	48	51	-6%
pm	2880	48.5	58	-20%
pm	2880	48.5	56	-15%

Absolute Average 8%
Arithmetic Average -5%

Strains calculated using CLEVERCALC.

A.8. The backcalculated layer moduli were used as input to BISAR to provide a comparison of the calculated strain at the bottom of the AC layer. The strain differences calculated by the two computer programs were negligible (1 microstrain). The majority of the measured strains were within ± 10 percent of calculated. The maximum difference was 20 percent.

9. COMPARISON OF STRAIN GAUGE TYPES

Sebaaly et al. [A7, A9] have conducted an in-depth literature review and field performance testing of various strain gauges. In their literature review (Sebaaly et al. [A9]), the strain gauges used in bonded layers fall into four categories:

- H-gauges and strip gauges
- foil gauges glued to or embedded in carrier blocks prepared in the laboratory
- foil gauges glued to cores extracted from the pavement section
- strain coils.

The H-gauge is made of a strip of material upon which a strain gauge is attached. Metallic bars are attached to both ends of the strip to serve as anchors. These gauges are called H-gauges because the resulting shape of the assembly resembles the letter "H". As the pavement strains under a load, the anchor moves with the pavement causing the strip to elongate and hence a strain measurement. For the gauge to experience (and measure) the same strain as the pavement the stiffness of the strip material must be approximately equal to or slightly less than that of the AC layer. Additionally, the anchors must remain firm so as not to introduce artificial elongation. Many models and varieties of these gauges have been built using different materials and slightly differing designs to attempt to overcome these challenges.

The use of carrier blocks prepared in a lab has also been common. In this application, a foil type gauge is either glued to a lab specimen, glued between two pieces

of a lab specimen or embedded in a lab specimen. The theory behind this application is that the lab specimen will melt somewhat when the hot mix is placed around it. As a result, the carrier block will become a contiguous part of the AC layer.

Mounting foil gauges to pavement cores is very similar to that of carrier blocks. The obvious difference being that the strain gauge "carrier" is actual in-situ material versus laboratory prepared material. The major concern with this technique is the epoxy used to bond the core back to the pavement structure. The stiffness of the epoxy should match that of the AC as closely as possible. Epoxy that is too soft could cause the bond to fail. Epoxy that is too stiff could cause cracking around the core.

Strain coils work on an electromagnetic output and are usually installed in carrier blocks. Their output can be affected by metallic wheels and vehicular ignition systems. Their use is virtually nonexistent in the literature. See Sebaaly [A9] for a more detailed discussion of the characteristics of all these gauge types.

As previously mentioned, Sebaaly et al. [A7] conducted a field performance evaluation of a selected group of strain gauges (Table A.9) and established four performance related criteria. The four criteria and their definitions are as follows.

1. Survivability — "...the number of gauges that remain operational after construction and testing relative to the number of gauges that were initially installed."

2. Repeatability — "...a measure of dispersion of measuring results obtained from a specific gauge for specific test conditions."

3. Effect of Test Variables — "...the sensitivity of each type of gauge to various combinations of load, speed, tire pressure, and axle configuration."

4. Uncertainty — "...the difference between the measured response and the theoretically calculated values."

This discussion will only highlight the performance of the gauges installed to measure one of the primary pavement responses for mechanistic-design -- strain at the bottom of the AC layer.

Table A.9 Strain Gauges Evaluated During Field Performance Testing (after Sebaaly [A7])

Gauge Type	Number of Gauges/Section	Orientation	Location
Dynatest (H)	2/thin and thick	Longitudinal	Bottom of AC Layer
Kyowa (H)	4/thin and thick	Longitudinal	Bottom of AC Layer
Asphalt Carrier Block (ARC)	1/thin and thick	Longitudinal	Bottom of AC Layer
Core	4 thick	Longitudinal	Bottom of AC Layer
Core	1 thin	Transverse	Bottom of AC Layer

Table A.10 Survivability of Gauges Installed in the Thin Section (after Sebaaly [A7])

Gauge Type	Number Installed	After Construction/Installation		After Testing	
		Number Surviving	Percent Operational	Number Surviving	Percent Operational
Dynatest	2	2	100%	2	100%
Kyowa	4	3	75%	2	50%
ARC	1	1	100%	1	100%
Core (Transverse)	1	1	100%	1	100%
Totals	8	7	88%	6	75%

The survivability data for the gauges installed in the thin and thick sections is contained in Tables A.10 and A.11, respectively. Survivability varied across gauge types and pavement sections. The two ARC gauges were the only gauges with perfect survivability in both sections. The core gauges (transverse and longitudinal) had the next best survival rate at 60 percent after installation and testing. All the failures occurred in the thick section after testing. All four of the Dynatest gauges survived construction but only half survived testing. Like the core gauges, all the failures were in the thick section. The Kyowa gauges demonstrated the least favorable survivability with just over 60 percent of the gauges surviving construction and only 50 percent remaining operational after testing. These results are summarized in Table A.12. It is noteworthy that the worst overall survivability rate by section was found in the thick section. Sebaaly et al. did not make this observation and as such provide no explanation. Also, the original authors did not address the pavement condition at the conclusion of testing. Therefore, it is unknown if excessive pavement deterioration contributed to any of the gauge failures. Given that each section received approximately 125 truck passes with a maximum axle load of 20,820 pounds, this is unlikely.

In the area of repeatability, Sebaaly et al. [A7] performed two sets of analyses. First, an evaluation was made "...of the means, standard deviations, and coefficients of variation for the four replicate measurements for each combination of the test variables." To "...increase the number of observations and reduce the effect of potential random error in the collected data" the data was pooled by test variable combinations. The standard deviation of the measured strains in each pooling was also evaluated. From their data analysis, Sebaaly et al. concluded that the repeatability of all the gauges was "...very good even under the conditions that created relatively high standard deviations."

Table A.11 Survivability of Gauges Installed in the Thick Section (after Sebaaly [A7])

Gauge Type	Number Installed	After Construction/Installation		After Testing	
		Number Surviving	Percent Operational	Number Surviving	Percent Operational
Dynatest	2	2	100%	0	0%
Kyowa	4	2	50%	2	50%
ARC	1	1	100%	1	100%
Core (Longitudinal)	4	2	50%	2	50%
Totals	11	7	64%	5	45%

Table A.12 Survivability of Gauges—Both Pavement Sections (after Sebaaly [A7])

Gauge Type	Number Installed	After Construction/Installation		After Testing	
		Number Surviving	Percent Operational	Number Surviving	Percent Operational
Dynatest	4	4	100%	2	50%
Kyowa	8	5	63%	4	50%
ARC	2	2	100%	2	100%
Core	5	3	60%	3	60%
Totals	19	14	74%	11	58%

In studying the effects of the test variables (axle load, tire pressure, and truck speed) on gauge performance Sebaaly et al. drew the following conclusions.

- "[T]he effect of tire pressure on strain at the bottom of the asphalt concrete layer is insignificant compared to the effects of axle load and truck speed for all types of strain gauges."
- "[T]he effect of increasing load level from the intermediate to the fully loaded level on the measured strains was consistent among all types of gauges under both the single and tandem-axle configurations. However, the effect of increasing the load level from empty to the intermediate level on the measured strain was less consistent."
- "[I]t [was] impossible to correlate the speed effect to specific gauge types."

The final form of analysis conducted by Sebaaly et al. [A7] was a regression analysis using the response from each gauge type as the dependent variable and the overall mean of all gauge types as the independent variable. The ARC gauges were excluded from this analysis because of the high uncertainty in their measured responses. The results of the regression analysis are contained in Table A.13. The performance of the Dynatest and Kyowa gauges is essentially equal. Compared to the H-type gauges (Dynatest and Kyowa) the core gauges performed less consistently. However, one must realize that the installation procedures and strain measurement concepts between the two gauge types are very different. Sebaaly et al. [A7] present two possible explanations for the difference in performance between the two gauge types.

1. Use of epoxy to glue the gauges to the cores.
2. The ability of the core to become an integral part of the pavement section.

Table A.13 Statistical Summary of the Regression Analysis of All Measured Strain Responses (after Sebaaly et al. [A7])

Dependent Variable	Intercept (a)	Slope (b)	Sample Size	R-squared %	Std. Error of Est.	Mean	Minimum	Maximum
Dynatest	-5.58	1.017	399	98.70	13.32	139.2	2	622
Kyowa	-3.18	1.108	480	97.94	17.33	141.3	5	632
Core	12.59	0.768	478	93.15	22.31	112.2	11	462

Independent Variable: Average value of all the gauges.

Another important consideration is the type of application in which the two gauge types are used. Core gauges can be retrofitted to new and existing pavements. H-type gauges must be installed before paving operations. Because of their exclusive ability to be retrofitted to in-service pavements further study should be conducted to establish an effective calibration procedure to account for the effect of the epoxy used to mount the gauges to the pavement core.

REFERENCES

A1. Nijboer, Ir L.W. "Testing Flexible Pavements Under Normal Traffic Loadings By Means of Measuring Some Physical Quantities Related to Design Theories." In *2nd International Conference on the Structural Design of Asphalt Pavements,* Vol. I. (1967): 689-705.

A2. Dempwolff, R., and P. Sommer. "Comparisons Between Measured and Calculated Stresses and Strains in Flexible Road Structures." In *3rd International Conference on the Structural Design of Asphalt Pavements,* Vol. I. (1972): 786-794.

A3. Yap, Pedro. "A Comparative Study of the Effect of Truck Tire Types on Road Contact Pressure." In *Vehicle/Pavement Interaction: Where The Truck Meets The Road*, SP-765. Society of Automotive Engineers. (1988): 53-59.

A4. Halim, A.O. Abdel, Ralph Haas, and William A. Phang. "Geogrid Reinforcement of Asphalt Pavements and Verification of Elastic Theory." *Transportation Research Record* 949 (1983): 55-65.

A5. Scazziga, I.F., A.G. Dumont, and W. Knobel. "Strain Measurements in Bituminous Layers." In *6th International Conference on the Structural Design of Asphalt Pavements,* Vol. I. (1987): 574-589.

A6. Dohmen, L.J.M., and A.A.A. Molenaar. "Full Scale Pavement Testing in the Netherlands." In *7th International Conference on Asphalt Pavements,* Vol. II. (1992): 64-82.

A7. Sebaaly, P., N. Tabatabaee, B. Kulakowski, and T. Scullion. *Instrumentation For Flexible Pavements--Field Performance of Selected Sensors.* Report FHWA-RD-91-094. McLean, Virginia: Federal Highway Administration, 1992.

A8. Lenngren, Carl A. "Relating Deflection Data to Pavement Strain." *Transportation Research Record* 1293 (1991): 103-111.

A9. Sebaaly, Peter, Nader Tabatabaee, and Tom Scullion. *Instrumentation For Flexible Pavements.* Report FHWA-RD-89-084. McLean, Virginia: Federal Highway Administration, 1989.